May 2019

Reducing Uncertainties in Conservation Decision-Making for American Alligators

Abigail Lawson
Clemson University, abbylawson@gmail.com

REDUCING UNCERTAINTIES IN CONSERVATION DECISION-MAKING FOR AMERICAN ALLIGATORS

A Dissertation
Presented to
the Graduate School of
Clemson University

In Partial Fulfillment
of the Requirements for the Degree
Doctor of Philosophy
Wildlife and Fisheries Biology

---

by
Abigail J. Lawson
May 2019

Accepted by:
Patrick Jodice, Committee Co-Chair
Clinton Moore, Committee Co-Chair
Robert Baldwin
Thomas Rainwater
Beth Ross

ABSTRACT

Effective conservation decision-making necessitates monitoring programs that are designed to collect unbiased and precise measurements of relevant attributes deemed to reduce structural uncertainty of the managed resource state. American alligators (*Alligator mississippiensis*; hereafter alligator) are a keystone species within the southeastern United States that have cascading effects on ecosystem structure and function, and are managed under consumptive use management programs throughout their range. Management of alligator populations in South Carolina is challenging due to pervasive uncertainties regarding the size class distribution, which is only partially observable using the primary monitoring tool (nightlight surveys), a lack of demographic parameter estimates, and identification of measurable attributes that could pose conservation threats (e.g., drought, contaminants). My objective was to develop analytical tools to reduce partial observability in alligator monitoring and identify potential drivers of alligator population dynamics to reduce structural uncertainty. I developed a Bayesian integrated population model (IPM) that produced among the first demographic parameter estimates for alligators in South Carolina and determined that survival probabilities increased greatly among immature size classes, but are relatively similar among adults (>0.90); a pattern that has been previously reported for American crocodiles (*Crocodylus acutus*). The IPM produced size-class specific abundance estimates for alligators from count data with prolific state uncertainty (>60% unknown size observations). In general, alligator abundance trends were uncertain and appeared to

vary spatially, though the mean population growth (λ) estimates for all sites, IPM versions, and the Lefkovtich matrix were <1, indicating a population decline. However, the 95% Bayesian credible intervals for λ at one survey site included 1, indicating some uncertainty. I then used the demographic parameter estimates to simulate virtual alligator populations under varying gradations of initial population density, harvest rate to determine an optimal level of spatiotemporal replication for a monitoring programs. To evaluate the need to obtain size class-specific abundance estimates, the simulated count data from the underlying virtual population was total individuals (of all size classes). Based on fundamental objectives to maximize financial effectiveness and minimize management and ecological uncertainty, all of the harvest and density scenarios (except low density and maximum harvest) selected a monitoring program with six temporal replicates (the maximum) and 320 spatial replicates (1 spatial replicate = 0.5 km river segment). In general, data reliability (precision and accuracy) was more sensitive to increasing temporal, compared to spatial, replication, which has been previously reported in other simulation based studies in which detection probabilities are low ($p< 0.10$). Moreover, all scenarios and monitoring programs induced changes in alligator size class structure, though the effects were minimized with reduced harvest rate, increase survey effort and population density. In synthesis, the demographic parameter estimates produced by the IPM can and are being used to improve monitoring methodology for alligators in South Carolina, and provide a mechanism to increase the demographic resolution of monitoring data, inform optimal monitoring decisions, and explore further uncertainties associate with harvest decisions. Finally, to better elucidate potential drivers

of alligator population status, I evaluated total mercury (THg) concentrations in adult alligator whole blood from a longitudinal mark-recapture study. I determined that THg in whole blood was best described by an interactive effect of sex and predicted age, as calculated by predicted age at first capture using a recently developed growth model for alligators in South Carolina. THg concentrations averaged 0.16 ± 0.05 mg kg^{-1} *ww* and were slightly higher in males than female, though the overall average is significantly lower than other estimates reported in the Florida Everglades and the Savannah River Site in South Carolina. The quadratic effect of THg with predicted age, in which older individuals had lower levels than younger individuals is novel, and contrasts with previous assumptions that THg bioaccumulates with age (i.e., does not decrease). We posit that determinate (asymptotic) growth, which could accompany age-related changes in foraging patters and metabolism, could potentially explain the lower THg we detected in the oldest individuals. The results from our study could highlight the need for long-term longitudinal monitoring of sentinel species to further evaluate our hypotheses.

DEDICATION

This work is dedicated to the lasting memory of Dr. Katherine Walton McFadden, a cherished mentor, colleague, and friend. In December 2012, I moved across the country to South Carolina (sight unseen) to pursue my PhD, under the advisement of Kate in the South Carolina Cooperative Fish and Wildlife Unit. I was impressed by Kate's accomplishments as an international conservation biologist, and her interdisciplinary approach to research. Despite the many uncertainties associated with starting a PhD, the first time I met Kate and tossed around research ideas, I knew that I made the right decision. Kate taught me many important lessons about professional development (including navigating the scientific profession as a woman), work/life balance, and personal accountability. Often the wisdom I gleaned from Kate was not when we were nodding our heads in agreement, rather, it was when Kate had challenged my thinking and made me carefully evaluate my assumptions, beliefs, and process. I am grateful for the personal and professional standards that Kate expected of those in her life, and am confident that many others would say the same. Though our tenure together was brief, knowing Kate has had a profound influence on my life that was both challenging, and positive. I've thought about Kate nearly every day since her passing, and imagine that I will continue to for some time. My coadvisors, and I hope that the research contained both here and future manuscripts will honor her legacy of integrated thinking and collaboration. I'm forever grateful to Kate for taking a chance on me, and to have had the opportunity to work with her— it's a chance that I would take again.

ACKNOWLEDGEMENTS

Primary funds for the research in this dissertation were provided by the South Carolina Department of Natural Resources (SCDNR), U.S. Geological Survey, and the Yawkey Foundation I. I also thank the Clemson College of Agriculture, Forestry, and Life Sciences (Wade Stackhouse Fellowship and the Marion Bailey Assistantship), Clemson Department of Forestry and Environmental Conservation, Clemson Graduate School, Clemson Natural Resources Graduate Student Association, Hobcaw Barony Foundation, Wildlife Society Biometrics Working Group, Greenville Zoo, South Carolina Wildlife Federation for additional research, assistantship, and travel funds.

Chapters 2–4 of this manuscript represent stand-alone publications intended for submission to peer-reviewed journals, and multiple collaborators participated as co-authors on the manuscripts. Patrick Jodice, Clinton Moore, and Kate McFadden co-authored all three data chapters, Beth Ross co-authored Chapters 2 and 3, Thomas Rainwater and Philip Wilkinson co-authored Chapters 2 and 4, and Louis Guillette Jr., Russell Lowers, and Frannie Nilsen co-authored Chapter 4. Their contributions included project conceptualization and management (PJ, KM), field data collection assistance (RL, TR, PW), auxiliary data and sample access (LG, RL, FN, PW), laboratory analysis guidance (FN), data analysis (CM, BR), and manuscript preparation (PJ, CM, FN, BR, TR). Additional collaborators are included in the acknowledgements sections of each chapter.

As the title of my dissertation implies, a primary motivator of my research was to inform management decisions for alligators in South Carolina. Derrell Shipes, Jay

Butfiloski, Emily Cope, and Brad Taylor of SCDNR were instrumental in the development of my dissertation's structure, and helping me identify the key uncertainties that needed further scrutiny. I thank them for their input and guidance, and willingness to patiently answer my many alligator questions as I was learning the lay of the lowcountry. I further thank Jay and Brad for their extensive assistance with nightlight surveys— your expertise and guidance were essential in study design, determining what would be logistically feasible, and troubleshooting boat (aka: "bring out another thousand") issues.

I was incredibly fortunate to have the help of many talented and motivated field technicians, student interns, and volunteers for the field component of my dissertation. In particular, I thank Chris Boyce, Catherine May, Tanner West, Maddy Feiste, and Parker Johnson for their invaluable assistance with nightlight surveys. Nocturnal field work is grueling, exhausting, socially-isolating (at times), and often unforgiving; requiring a commitment to safety, problem-solving, and tolerance for things that go bump (or sting, or bite) in the night. Supervising remotely is a tricky business; I am thankful that I could leave data collection in the hands of a capable, safety-conscious crew, and for their prompt responses to (sometimes-frantic) emails and texts. If our paths cross in the future, I will gladly buy you coffee.

Conducting annual nightlight surveys across the midlands and lowcountry of South Carolina for two–four months from 2013–2016 required a brigade of assistance, beyond those already mentioned. I thank Forrest Sessions, Nick Wallover, Al Segars, Daniel Barrineau, Joachim Treptow, Mark Purcell, Mike Prevost, Dean Harrigal, as well as other staff of the SCDNR Dennis Center, Santee Coastal Reserve Wildlife Management Area

(WMA), Bear Island WMA, Tom Yawkey Wildlife Center, McKenzie Field Station, USFWS ACE Basin National Wildlife Refuge, as well as Rochelle and Annandale Plantations. Thank you for helping me and my crew with lodging arrangements, property access, boat and truck lending and repair, and sometimes pulling the survey crew out of the ditch/impoundment/mud at all hours of the day or night.

I thank the many individuals (easily in the high hundreds) who assisted with alligator captures and sample collection on the Yawkey alligator study, many of whom I only know from their names on scanned datasheets. To that end, I thank Maggie Wilkinson who was essential in digitizing nearly 40 years of alligator mark-recapture data, which is no small feat! Similarly, I thank Jamie Dozier for his continued support of the Yawkey alligator study as well as my project. Jamie's knowledge and expertise with moist soil management was incredibly useful for study design and data interpretation. It is no exaggeration to state that this dissertation, in its current form, would not have been possible without the persistence and dedication of Phil Wilkinson to the study of alligators in South Carolina. I have immense appreciation towards Phil for welcoming me into the local alligator research community, field assistance, allowing me to use the mark-recapture dataset for my dissertation, and for his friendship. I thank Phil and Libby Bernardin for their kindness and hospitality on so many occasions over the years— I'll always cherish my memories of the "garage-mahal", evenings at the Big Tuna, and the many "alligator summits" BBQs/boils you hosted. Similarly, I owe thanks to my other alligator mentors whose brains I picked mercilessly, including Allan Woodward, Tom Murphy, Arnold Brunell, Walt Rhodes, and Cameron Carter.

Joining the “Yawkey alligator collaboration” was unquestionably one of the highlights of my dissertation research. Stacey Lance, Ben Parrott, Matthew Hale, Josh Zajdel, Lou Guillette Jr., and Frannie Nilsen all helped me view my research through interdisciplinary lenses, which improved both the quality of my dissertation and my development as a scientist. It has been such a privilege to work with a talented group of scientists, who I have also immensely enjoyed getting to know through field work (I consider the 2016 “capture frenzy” a great success!) and conference travel, to places near and far. I thank this group, as well as Angela Lindell and John Bowden for their instrumental role in my mercury chapter, and for hosting during my trips to Aiken. I am indebted to Lou for allowing me to use archived samples from the Yawkey study, and hope that the eventual manuscripts can honor his legacy of rigorous, interdisciplinary collaboration.

Much of the data that I collected is not contained in this volume, and is in manuscripts of varying stages of completion. Despite the omission, the many people who contributed to these projects deserve recognition here. I deployed 30 GPS transmitters from 2015–2017 which would not have been possible without invaluable assistance from Matthew Guillette, Terry Norton, Russ Lowers, Lindsay Bittner, Thomas Galligan, Jacob Scott, Ernie Wiggers, and many others. For the stable isotope component of my research, I thank Adam Rosenblatt, Tom Maddox, and the University of Georgia Stable Isotope Ecology Lab for their valuable input on study design and analysis, Stephen Czwartacki, Paul Kenny, Pearse Webster, and the SCDNR SEAMAP crew for prey sample collection. In the summer of 2017, I conducted nightlight surveys within Congaree National Park,

which is undoubtedly among the most challenging and rugged landscapes I've ever had the pleasure of working— the "Alaska of South Carolina" as David Shelly aptly described it! That said, I owe great thanks to David Shelly, Jake Beechler, Trey Kelly, Bradley Wilkinson, and Hannah Plumpton. Remember: zeroes are data too.

Administering a wide-ranging field-intensive study is a harrowing task, and I owe special thanks Carolyn Wakefield, Brenna Byler, Andrea Kessler, Jennifer Hooper, and Vickie Byko of Clemson University for their help navigating these matters. Your attentiveness, kindness, and patience did not go unnoticed and is greatly appreciated. While pursuing my PhD, I had the freedom to pursue additional professional development activities, including coordinating the weekly seminar series, serving on a faculty search committee and as instructor of record. I thank our FEC department chair, Greg Yarrow, for his willingness to offer these opportunities to graduate students, as they undoubtedly benefitted my career trajectory. I also thank Kyle Barrett, Shari Rodriguez, and Brandon Peoples for their mentorship and friendship over the years. Similarly, I thank my labmates of the McFadden and Jodice Labs at Clemson University, and Moore Lab at the University of Georgia for helpful input on presentations and manuscripts, field support, quantitative assistance, and camaraderie.

I am extremely grateful to the members of my doctoral advisory committee (past and present) at Clemson University— Drs. Rob Baldwin, Thomas Rainwater, Beth Ross, and Yoichiro Kanno— for their flexibility, insightful comments, helping me sort through ideas (conceptual and analytical), and challenging me as a scientist to think broadly about my research. I worked alongside Thomas in the field for nearly every single alligator

capture over the last six years ($n \geq 200$). Thomas went above and beyond what is typically expected of a committee member through his field work contributions alone, while also helping me navigate numerous (countless?) challenges— always with a positive attitude and infectious sense of humor. I thank Thomas for encouragement to pursue big (but realistic!) ideas and opportunities; your mentorship is both appreciate and inspiring.

Six years is a very long time to be in a PhD program and I owe much of my perseverance to my incredibly supportive friends— including those who are not named here— you all have made me a stronger, better version of myself in your own way. I thank you all for your patience and understanding, especially as I dropped off the communication radar for extended periods. I'm grateful to friends from my M.S. days— Drs. (!!!) Erik Blomberg, Dan Gibson, Sabrina Morano, and Amanda van Dellen, Thank you for the never-ending peanut gallery commentary from our group text thread, life advice, and help with code. I'm also grateful to my M.S. advisor, Jim Sedinger, for his continued mentorship, particularly on navigating decisions after the PhD.

I owe thanks to two friends who I have known for over ten years now (how'd that happen?). Dr. Erin Hestir, you have always been an inspiration to me and I am so grateful to you for helping me through difficult life events, and support over the years, it means more than you know. Caitie Kroeger recently helped me persevere one of the darkest periods of my life; I deeply appreciate and admire your seemingly endless capacity for compassion and empathy. Caitie, there is nobody else who I would rather go hiking on a foggy on a mountaintop with, or kayak with through Nile crocodile-infested waters.

I was incredibly lucky to overlap in both time and topic (is topical-temporal replication a 'thing'?) with Tara Gancos Crawford in the Moore Lab. I have many fond memories from the harvest decision-support group, conferences, and am so grateful to you and Daniel (+Juno and Woodrow) for giving me a place to stay on my trips to Athens. To Katie Hooker, my McFadden labmate, thank you for your (often) brutal honesty and making me laugh, particularly when quoting Mean Girls. Likewise, I am grateful to Christie Sampson for being a calm source of reason in my life, and her kindness, and support.

I thank Brett Frye for her humor and much-needed perspective, especially during our many dog walks (thanks to Anna and Dale too). You have inspired me with your own grit and determination, whether we were in the midst of taco and beer catharsis or somewhere along our trajectory of physical fitness— from 6 AM cardio HIIT classes in year 1 to noon "breathe and relax" yoga in year 4+. Pallavi Sirajuddin is a wonderful reminder that important people can enter your life through mere chance. I thank you Pallavi, for your compassion, willingness to listen, and for our much-needed walks in the "Botan" as well as sparkling wine and enchilada nights— let's be neighbors again soon. Somehow, despite moving across the country, the first friend I made at Clemson was another U.C. Davis WFCB alumni, Nikki Roach. I can't adequately express the powerful experience of having a trusted friend with a shared background to navigate the unfamiliar southern landscape of college football tailgating, blue laws, and meat-n-threes. Watching you make the leap from the Lehotsky tornado shelter to international conservation

biology has been such a joy to witness. Thank you for bringing out the best in me, and not accepting anything less.

My dissertation was initially conceptualized by my original PhD advisor, Dr. Kate McFadden, to whom my dissertation is dedicated. Following Kate's passing in October 2014, Drs. Patrick Jodice and Clinton Moore became my coadvisors and graciously welcomed me into their labs— an action for which I am deeply humbled by and grateful for with every passing day. You both contributed immeasurably to my growth and development as a scientist and decision-maker; often in complementary ways, no less. Pat's mentoring taught me to remove my "quantitative blinders" and think about the bigger picture, which has made me a more broadly trained ecologist. Clint's mentoring provided me with a great depth of understanding for our shared area of specialization. I thank Pat for giving me room to grow in both my scientific and professional development (and learn the hard lessons of where and how to focus effort on my own), and his consistent efforts to provide a source of stability my life, and those of his other students, amidst professional upheavals, changing graduation timelines, and government shutdowns. I thank Clint for both his patience and fortitude in helping me master a subject matter (that strikes fear in the hearts of many graduate students) and teaching me how to troubleshoot problem-solve the seemingly unsolvable problems in quantitative wildlife ecology. I thank Clint for fostering my growing interests in structured decision-making, and being so generous with his time during my trips to Athens. Though I could easily fill another Acknowledgements section of similar length, but in short, I am very lucky to have had such an effective and generous team of mentors.

Pursuing a PhD four time zones away from family has been challenging to say the least. I owe thanks to my family, Tom, Kim, and Andy Lawson and Taylor Baker for their understanding, love, and support over the years as I pursued my dream. Lastly, I thank my dear goofball of a dog (but potentially part dolphin and kangaroo), Minnie, for her companionship, carrying my shoes outside for no apparent reason, and unbridled enthusiasm for walks (and food) that made me smile every day.

TABLE OF CONTENTS

Page

Table of Contents (Continued)

Page

LIST OF TABLES

LIST OF FIGURES

List of figures (continued)

Figure Page

CHAPTER ONE

SUMMARY OF DISSERTATION CONTENT

American alligators (*Alligator mississippiensis*, hereafter alligator) are a species of ecological, cultural, and economic importance in the southeastern United States. The fundamental objective of this dissertation is to develop tools to reduce the uncertainty in the outcomes of management decisions for alligators in South Carolina, USA and to identify important measureable attributes for effective monitoring programs.

Chapter 2 synthesizes multiple alligator demographic datasets within an integrated population model framework to produce size class-specific abundance and survival probability estimates. Chapter 3 uses the demographic parameter estimates produced in Chapter 2 to simulate a virtual alligator population that is subject to differing gradations of initial population density, harvest rate, and monitoring program designs. The realized outcomes of the simulation were then placed in a decision analytic framework to identify the optimal monitoring plan based on fundamental objectives that maximize financial efficiency and minimize management and ecological uncertainty. Chapter 4 evaluated total mercury concentrations in whole blood of American alligators and related them to individual and ecological variables.

CHAPTER TWO

HIDDEN IN PLAIN SIGHT: INTEGRATED POPULATION MODELS AS A TOOL TO DESCRIBE PARTIALLY OBSERVABLE LATENT DEMOGRAPHIC STRUCTURE

Abstract

State uncertainty of individuals within sampled populations is a ubiquitous problem in applied conservation, and it is particularly problematic for stage- or size-structured species subject to consumptive use. We constructed a Bayesian integrated population model (IPM) for American alligators (*Alligator mississippiensis*) in Georgetown County, South Carolina, USA using a combination of mark-recapture records (1979–2017), harvest data and nightlight survey counts (2011–2016), and auxiliary information on fecundity, sex ratio, and growth from other studies. We created a multistate mark-recapture model with six size classes (states) to estimate survival probability, and we linked it to a state-space count model to derive estimates of size class-specific detection probability and abundance. Because we worked from a count dataset in which 60% of the original observations were of unknown size, we treated size class as a latent property and developed a novel observation model to make use of information where size could be partly observed. Detection probability was negatively associated with alligator size and water level, and positively influenced by water temperature. Survival probability was positively associated with size among the three immature size classes but was relatively similar among the three adult size classes. We detected mixed evidence for a population

decline based on the population growth rates derived from a Lefkovitch matrix constructed from estimated survival and fecundity parameters, and the two site-specific abundance estimates. Here we illustrate the use of IPMs to produce high demographic resolution output of latent population structure that is partially observed during the monitoring process.

Introduction

In wildlife populations, demographic variation in reproductive output, predation risk, or harvest pressure is frequently reflected in sex, age, or size-specific abundances and vital rates. Decision making for conservation often relies on monitoring data, which can be limited in predictive power by the demographic resolution of the data— the scale at which individuals can be assigned to a demographic group. Demographic data with high resolution may contain sex- and/or age-specificity (e.g., two-year-old females), whereas low resolution data collapse multiple demographic groups (e.g., total individuals). The potential consequences of low resolution data are particularly acute for long-lived species in which demographic responses to disturbance may be lagged (Fryxell et al., 2010; Krauss et al., 2010; Menéndez et al., 2006), or for species with complex life history strategies that exhibit wide variation in vital rates among multiple age or size classes (Aubry et al., 2010; Radchuk et al., 2013).

While intensive forms of monitoring (e.g., mark-recapture studies) are likely to produce high-resolution demographic data in which the state of interest (e.g., sex, size) can be perfectly observed, such options may be too costly or time-intensive to implement

on broad spatiotemporal scales. Mark-recapture studies may be particularly difficult to justify for species with high annual hunting mortality (Gauthier et al., 2001; Langvatn and Loison, 1999), wide-ranging species with a low likelihood of recapture (e.g., pelagic fish), or for small or declining populations in which adverse marking or handling effects may outweigh increased demographic resolution (Gibson et al., 2013; Lomba et al., 2010). Alternatively, survey-based monitoring methods (e.g., counts, occupancy) offer the potential for lower expense and increased spatial coverage, but may come at the cost of added uncertainty for some or all states of observed individuals. A common manifestation of state uncertainty is partial observability, in which the demographic state (e.g., sex, age, reproductive status) cannot be determined to the desired level of resolution for all observed individuals (Conn and Cooch, 2009). Managers of monitoring programs with extensive partial observability may resort to reducing the data's demographic resolution to avoid extensive censoring or to reduce bias in population projections (Caswell, 2001), which may ultimately limit the demographic resolution of management actions (e.g., size-structured vs. total individual harvest quotas) and increase the level of uncertainty in their outcomes.

Using data with a relatively low resolution to identify latent demographic structure within populations is a growing area of interest, as it has the potential to produce high resolution results (e.g., age-specific demographic parameters) for a lower cost. For example, Link et al. (2003) developed a model to derive age-structured abundance and survival estimates from a 64-year census of endangered whooping cranes (*Grus americana*) using aggregated, low resolution data that distinguished only two classes of

birds: first-year individuals, and adults. In an extension of the *N*-mixture model framework (Royle, 2004), Zipkin et al. (2014a) incorporated a classification probability term into the detection process to account for state uncertainty when assigning individuals to one of two demographic groups (e.g., adult/juvenile, male/female) during sampling. Though each approach offers a different mechanism to enhance low resolution data, both require relatively large sample sizes of low resolution datasets (e.g., study duration, replicate visits; Link et al., 2003; Zipkin et al., 2014a) that may not be feasible for many monitoring programs.

Integrated population models (hereafter IPMs) offer a flexible, efficient tool to jointly analyze multiple data streams, thus increasing the precision of parameter estimates and providing a standardized error structure to reduce uncertainty (Besbeas et al., 2002; Schaub and Abadi, 2011). In their general form, IPMs connect an abundance analysis of count data (e.g., *N*-mixture, state-space) with the estimation of survival parameters from a capture-recapture model using marked individuals. Incorporating additional data streams (e.g., productivity, harvest) enables the IPM to account for all demographic processes that influence changes in population growth rate (birth/death, immigration/emigration). A comprehensive demographic model allows the estimation of additional parameters, both ecological (e.g., emigration) and observational (e.g., classification rate), that would be inestimable for any of the individual model components in isolation (Arnold et al., 2018; Schaub and Abadi, 2011; Zipkin and Saunders, 2018). Therefore, IPMs present an opportunity to synthesize multiple datasets, often of dissimilar demographic resolutions, in a common framework to identify latent population structure.

The American alligator (*Alligator mississippiensis*) is a species of ecological and economic importance in the southeastern United States (Mazzotti and Brandt, 1994). Throughout their lifespan, alligators undergo a five-fold increase in body size that is paired with ontogenetic shifts in diet and habitat use (Nifong et al., 2015; Subalusky et al., 2009), allowing the species to fill different ecological roles (e.g., prey vs. predator) as they grow (Rootes and Chabreck, 1993; Somaweera et al., 2013). Alligators require over a decade to reach sexual maturity and continue to reproduce throughout their lifespan, which likely exceeds 65 years (Wilkinson et al., 2016). Following two decades of protection by the Endangered Species Act, alligators are currently managed under consumptive use programs throughout most of their range (Rhodes, 2002). The alligator's complex life history, delayed maturity, and long lifespan all underscore the importance of delineating population structure and vital rates at a high resolution to reduce uncertainty in the outcome of consumptive use policy decisions.

We developed an IPM for an alligator population on the middle coast of South Carolina, USA (Fig. 2.1), which is approximately the northern limit at which high alligator densities occur. Specifically, we synthesized data from a long-term, mark-recapture study (1979–2017) and from low-resolution nightlight surveys (count data: 2011–2016) with prolific uncertainty about the size state condition. Our goal was to provide a "proof of concept" for reducing state uncertainty in census data by using a high-resolution dataset to produce abundance estimates that were specific for size classes that spanned the entire size range. We also sought to obtain survival estimates specific to each size class to characterize life history patterns, evaluate environmental variables that

influence detection probability, and investigate the influence of length of the data time series to reduce parametric uncertainty.

Methods

Study area

We studied a coastal population of alligators in Georgetown County, South Carolina, USA (Fig. 2.1; 2681 km^2). The city of Georgetown receives 78–184 cm of annual precipitation; the dry season occurs October–March, and the wet season is June–September. Mean temperatures during the alligator's active season (April–October) range 17–27°C and 8–14°C during brumation (November–March). Georgetown County (hereafter GXN) is comprised of extensive and diverse alligator habitat that includes coastal marsh, wooded wetlands, impounded (diked) wetlands on a mixture of private and public lands. For our analysis, we synthesized alligator public harvest data, nightlight survey counts from multiple coastal rivers, and mark-recapture-recovery data from the Tom Yawkey Wildlife Center (6033 ha; YWC; 33.217°N, -79.236°W), all within GXN.

Tom Yawkey Wildlife Center — We captured alligators on South and Cat Islands within the state-operated YWC which has been closed to alligator hunting since the early 1900s. YWC is part of the headland that separates two river deltas in GXN and is surrounded by marine (>26 salinity parts per thousand; ppt) and brackish water habitats (5–25 ppt) (Fig. 2.1), where mean tidal range is 116 cm. Our sampling area included tidal marsh (2,524 ha) comprised of smooth cordgrass (*Spartina alterniflora*) and black needle rush (*Juncus roemerianus*) and managed impounded wetlands (hereafter impoundments;

1,012 ha) which contained both emergent vegetation (e.g., smooth cordgrass, tall cordgrass (*S. cynosuroides*), and saltmarsh bulrush (*Scirpus robustus*)) and submerged vegetation (e.g., widgeon grass, *Ruppia maritima*). Impoundment water levels were typically maintained at 60 cm, except for a spring draw-down (approx. 5–6 weeks) that promoted seed propagation. Salinity of impounded waters ranged 0–35 ppt and was influenced by management practices and rainfall.

Coastal Rivers — We conducted nightlight surveys (Bayliss, 1987) along two routes: (1) a combination of the Great Pee Dee and Waccamaw Rivers and (2) the South Santee River (Fig. 2.1). The Great Pee Dee and Waccamaw route (GPD; 38.4 km) began at the Samworth Wildlife Management Area boat ramp (33.475°N, -79.186°W) and formed an oval circuit that included sections from each river, as well as two excavated channels that connected each river. The South Santee River route (SAN) started at the Santee Coastal Reserve Wildlife Management Area boat ramp (33.154°N, -79.354°W) and extended 12.8 km upstream.

Field Methods

Mark-recapture study — We captured alligators of all age and size classes to evaluate demographics as part of a long-term (1979–2017) mark-recapture study on YWC. Alligators were captured intermittently using a combination of modified baited trip-snares (Murphy et al., 1983), walk-through snares placed on trails or nest sites (Wilkinson, 1994), camera traps placed at nest sites (for recaptures), snare poles, snatch hooks (Cherkiss et al., 2004), and hand captures (for small alligators only). Annual

capture effort (i.e., duration, intensity) and techniques varied to accommodate different research foci over the 39-year time span, which required targeting different demographic groups or individuals (description in Wilkinson et al., 2016). Except for carcass discoveries or off-site harvest returns of marked individuals, no data were collected during 1983–1992, 1994–2004, and 2008.

Captured individuals were uniquely marked using toe clips (1979–1993) (Wilkinson, 1983), scute notching (1979–2017) (Chabreck, 1963; Wilkinson, 1983), toe tags (Conservation Tags 1005-1 [1979–1982] and 1005-681 [2009–2017], National Band & Tag Company) (Jennings et al., 1991), and passive integrated transponder (PIT) tags (2009–2017) (GPT12, Biomark, Boise, ID) (Eversole et al., 2014). For individuals >120 cm total length (TL), we determined the sex through cloacal examination (Chabreck, 1963) and recorded three standard morphometric measurements (± 0.5 cm): TL, snout-vent length (SVL), and tail girth (TG). Hatchlings captured at a nest were marked with individually identifiable web tags and a scute notching and toe clipping combination that reflected their hatch year (tail scute) and nest number (toe); whereas non-hatchling alligators >30 cm TL were assigned individually identifiable scute notching and toe clipping patterns. For any individual <120 cm TL, we recorded TL and released individuals without determining sex, as cloacal examination is fairly difficult without extensive training for these sizes (P.M. Wilkinson, pers. comm.) and not advised for individuals <50 cm TL (Chabreck, 1963; Joanen and Mcnease, 1978). Following marking and measurements all alligators were released at their capture sites. We acquired all necessary alligator sample collection permits from the South Carolina Department of

Natural Resources (SCDNR), and the study was approved by the Institutional Animal Care and Use Committees at Clemson University (Permit nos. 2015007, 2016059) and the Medical University of South Carolina (Permit no. 3069).

Nightlight Survey Counts — We conducted nightlight surveys on the two survey routes from 2011–2016, excluding 2012, using flat-bottomed boats equipped with a 60–115 horsepower outboard motor. Surveys were initiated ≥ 30 min after sunset and completed ≥ 90 min before sunrise. We did not conduct surveys within ± 1 day of a full moon, during extreme water level events, or during heavy rain or wind (>15 km h^{-1}). We generally restricted surveys to weekdays to avoid increased recreational boat traffic on weekends. Within each year, we conducted 2–8 replicate surveys for each route from early May to mid-August, prior to the onset of alligator nest hatch. At the beginning and end of each survey, we recorded the date, time, personnel present and their designated roles, and environmental conditions. We recorded air temperature (± 0.1º C) and wind speed (± 0.1 km h^{-1}) using a Kestrel 4000 weather meter, and we measured water temperature (± 0.1º C) and salinity (± 0.01 parts per thousand, ppt) at approximately 3.2-km intervals using a YSI EcoSense 300A with a 1-m probe. While conducting each survey, we recorded waypoints for our start and end locations, water measurements, alligator locations, and route deviations using a GPS unit (Garmin GPSMap 62).

During each survey, the boat traveled 5–24 km h^{-1} along the river centerline as two personnel (observers) shined spotlights (Brinkman Q-Beam Max Million III Rechargeable Spotlight, $3x10^6$ CP) into the adjacent water to detect alligator eyeshine (Bayliss, 1987), which reflects a distinct red-orange color. When safe and logistically

feasible, we approached observed alligators (≥10 m distance) to assign individuals into one of six size classes (Table 2.1) based on TL: (1) Hatchling: ≤30 cm; (2) Juvenile: 30–121 cm; (3) Subadult: 122–182 cm; (4) Small Adult: 183–243 cm; (5) Large Adult: 244–304 cm; or (6) Bull: ≥305 cm. When a classification could not be confidently made, the individual was classified as either one of two general age classes that approximately distinguish reproductively mature from immature animals; i.e., "unknown adult" (≥183 cm TL), or "unknown juvenile" (<183 cm TL). Because of their correspondence with age, we refer to these groupings as age classes for ease of presentation. If the alligator could not be confidently placed into any size or age category, we classified the alligator as "unknown" (eyes only). Size classes were based on an allometric relationship of TL (Chabreck, 1966), where 2.54 cm snout length equates to 30 cm (1 ft) TL.

Each survey used ≥2 observers to detect eyeshine. The primary observer determined the size class of all detected alligators. In general, primary observers were individuals with at least two years of experience conducting nightlight surveys, or individuals that had intensive training with a primary observer for 3–4 weeks. Secondary observers were eligible to serve as primary observers when their size classifications of detected alligators agreed with that of the primary observer ≥95% of the time. The means by which we treated size-class data collected by a secondary observer that was not confirmed by a primary observer depended upon the secondary observer's level of experience. If the secondary observer had served as a primary observer previously, then such observations were treated as if they were confirmed by the primary observer. If the secondary observer had prior experience conducting alligator surveys, then the detections by the secondary

observer were recorded, but not the size class assignment. Lastly, if the secondary observer had no prior experience conducting alligator surveys, any detections that were not confirmed by the primary observer, or other experienced personnel who were present (e.g., data recorder, boat operator), were not recorded. If only two personnel were present, data recording and boat operation were handled by the primary and secondary observers, respectively, whereas those duties were covered by additional personnel, when available.

South Carolina Alligator Management — The SCDNR has administered an alligator harvest (hunting) program for public waterways since 2008 (SCDNR, 2017). Each year, the hunting season extends from the second Saturday in September to the second Saturday in October. The alligator's distribution in South Carolina is divided into four "Alligator Management Units" (AMUs; Fig. 2.1), set along county lines, which are allocated an equal number of tags each year, in which one tag permits the harvest of a single alligator >120 cm TL. From 2008–2009, and then again from 2014–2016, 250 tags were allocated to each of the four AMUs. SCDNR increased the number of available tags to 300 from 2010–2013 based on expert opinion and hunter participation rates. SCDNR requires that all hunters who have purchased a tag complete a harvest permit report that includes the date and location of the alligator harvest, take method, and TL. For model building, we used SCDNR public harvest data from GXN for 2011–2016 only, to overlap with the time range of nightlight survey data. Summary statistics and sample sizes for the mark-recapture, nightlight survey, and harvest datasets are provided in Appendix A1. Additionally, SCDNR administers nuisance removal (by euthanasia) and private lands

harvest programs; however, annual amounts of take by these programs are either not quantified or not publicly available for GXN.

Auxiliary Data — We used breeding and nesting productivity data from multiple studies conducted in coastal South Carolina from 1980–1982 (Wilkinson, 1983), as well as sex ratio information (female proportion; *FP*) derived from previous studies (Rhodes and Lang, 1996; Woodward, 1996) or expert opinion (A.J. Lawson, unpubl. data.) to parameterize our models. An expanded methodological description and auxiliary data summary are available in Appendix A2.

Integrated Population Model

Multistate Model Framework— We used a multistate mark-recapture dead-recovery model (Lebreton et al., 2009, 1999) to estimate demographic parameters that were size class-specific within a Bayesian integrated population modeling framework. Multistate models enable state-specific estimation of apparent survival (φ), detection probability ($p.m$), recovery probability (r), and the probability of transitioning among states (ψ) conditioned on survival. Our model included six live states (size classes) and two dead states (Fig. 2.2).

We constructed capture histories for all marked individuals from the YWC study population and assigned each individual to one of the six size classes used in the classification of nightlight survey counts. However, we defined the multistate size classes by SVL (Table 2.1), rather than TL, as alligators often lose portions of their tail as they age; classification by SVL thus prevented the illusion of size shrinkage of animals in

subsequent captures. Because the allometric relationship between SVL and TL (among individuals with intact tails) differed by sex in our study population (Females: SVL = 0.517*TL; Males: SVL = 0.520*TL; Wilkinson et al. 2016), we created a series of SVL-based (cm) size class thresholds for each sex: (1) Hatchling: ≤15.510 (Females), ≤15.600 (Males); (2) Juvenile: 15.511–63.031 (F), 15.601–63.397 (M); (3) Subadult: 63.032–94.547 (F), 63.398–95.097 (M); (4) Small Adult: 94.548–126.064 (F), 95.098–126.796 (M); (5) Large Adult: 126.065–157.581 (F), 126.797–158.495 (M); or (6) Bull: ≥157.582 (F), ≥158.496 (M); (Table 2.1). For capture events at which SVL was not measured, we predicted SVL based on allometric relationships with other measurements taken (e.g., TL minus tail length; as described in Wilkinson et al., 2016) or based on estimated growth from a previous capture (Wilkinson et al., 2016).

Captures of alligators at a size at which sex could not be determined through cloacal examination (Chabreck, 1963) were treated in one of three ways. If the alligator was later captured or found dead at a size at which sex could be determined, the final sex assignment was back-propagated to all previous captures. If the alligator was never reencountered at a size at which sex could be determined and if size class assignment at time of capture was ambiguous without knowledge of the animal's sex (e.g., the size class assignment of an animal measuring 15.55 cm SVL is sex-dependent; Table 2.1), then the alligator was excluded from analysis. However, if size class assignment was unambiguous without knowledge of the animal's sex, then sex was randomly assigned to all captures of the alligator by drawing a value from a Bernoulli distribution in which the

success parameter represented the proportion of females for each size class from the literature (Hatchlings: 0.72, Rhodes and Lang, 1996; Juveniles: 0.37, Woodward, 1996).

Mortality observations (e.g., harvest returns, carcass discoveries) were assigned to an observable, "recently dead" state in the year that they were detected, which allowed for correct accounting of the fact that the animal had lived up to that point. Finally, animals either probabilistically (not observable) or deterministically (observed dead recoveries) transitioned to an absorbing "dead" state that persisted for all subsequent occasions in the animal's capture history.

Alligator growth patterns differ between sexes (Wilkinson et al., 2016; Wilkinson and Rhodes, 1997); therefore we parameterized transition (i.e., growth) probabilities from each size class (j) according to sex (ψ_j^{Sex}). However, we captured relatively few hatchlings or juveniles for which we could eventually determine sex (based on a later recapture), leading us to assume that sex-specific transition probabilities for smaller size classes would be poorly estimated if derived solely within the multistate model. Therefore, in a separate analysis, we estimated sex-specific size class transition probabilities by fitting a body growth model to mark-recapture data and simulating growth of individual alligators. Values from this model then served as fixed values of ψ_j^{Sex} in the multistate model.

We simulated alligator growth using data from Wilkinson et al. (2016), which included a subset of the data used in this study (recaptured individuals of known-sex, 1979–2015) and additional mark-recapture data of juveniles from coastal South Carolina (M. Bara, unpubl. data, 1971–1981; see Wilkinson et al. (2016) for a detailed description

of capture, measurement, and marking techniques and differences between the two datasets). We implemented Markov chain Monte Carlo (MCMC) simulations to estimate sex-specific parameters of the mark-recapture form (Baker et al., 1991) of the Schnute (1981) growth equation:

$$Y_r = \{Y_m^b e^{-a\Delta t} + [y_2^b + y_1^b e^{-a(\tau_1-\tau_2)}]\frac{1-e^{-a\Delta t}}{1-e^{-a(\tau_2-\tau_1)}}\}^{\frac{1}{b}}$$

in which Y_m and Y_r denote the size at marking (first capture) and recapture, respectively, and Δt is the number of whole years between marking and recapture. The τ_1 and τ_2 terms are fixed values that indicate the minimum and maximum ages observed in a population (both sexes: 0–45), whereas y_1 (both sexes: 12.5 cm) and y_2 (females: 135.0 cm, males: 182.8 cm) denote the SVL at ages τ_1 and τ_2, respectively. The growth rate parameter a, the dimensionless shape parameter b, and the standard deviation of the error process σ are estimated quantities under the model. Though Wilkinson et al. (2016) estimated these parameters previously in a maximum likelihood framework, we re-estimated them in the Bayesian framework so that we could incorporate parametric uncertainty in size growth simulations. By taking samples of a, b, and σ from the MCMC chains, we applied the growth model over a 100-year time span to a hypothetical individual of each sex just entering the juvenile size class (Female: 15.5 cm SVL; Male: 15.6 cm SVL). For each sex, we tabulated the frequency of how often an individual in size class j transitioned to size class j+1 for size classes $j = 1,\ldots, 5$, conditioned on the number of years an individual has been in size class j (i.e., their time-in-residence; TIR) ($\psi_{j,TIR}^{Sex}$). Next, we calculated an average of $\psi_{j,TIR}^{Sex}$ by size class j, weighted by the number of simulations in

which the individual in size class *j* reached a given TIR, to reflect the expected ψ_j^{Sex} without respect to TIR (Table 2.1). We ran three chains for 105,000 iterations and discarded the first 5,000 as burn-in with a thinning rate of one. We used non-informative wide priors for all parameters and checked for convergence by visually inspecting the trace plots and confirming that the Gelman-Rubin diagnostic statistic ($\hat{R}$; Gelman et al., 2004) satisfied our accepted convergence threshold ($\hat{R} < 1.15$).

The state process component of our multistate framework represented a typical life cycle model in which individuals could initially be encountered in one of $j = 1,\ldots,6$ size classes (Fig. 2.2). From time *t* to *t*+1 the state process allowed for four possibilities, in which an individual alive in size class *j* could survive with probability φ_j and either (1) remain in the same size class with probability $(1-\psi_j^{Sex})$ or (2) transition to the *j*+1 size class with probability ψ_j^{Sex}. Alternatively, an individual could not survive $(1-\varphi_j)$ and either (3) transition into the recently dead state (*j*=7) in which they were recovered through a carcass discovery or harvest return with probability r_j, or (4) transition to the absorbing dead state (*j*=8) in which they were not recovered $(1-r_j)$. The probability of remaining within the bull size class (*j*=6), conditioned on survival, was fixed to 1.0, as were transitions from hatchling to juvenile size class, the recently dead state to the absorbing dead state, and the probability of remaining in the absorbing dead state. The structure of our model rendered some transitions impossible, including "skipping" a size class (i.e., non-consecutive growth transitions), "shrinking" (i.e., moving from larger to

smaller size classes), or "resurrection" (i.e., moving from a dead state to one of the live states).

Similarly, for the observation process component of our multistate model, an individual alive in size class j could either be detected with probability $p.m_j$ or not detected with probability 1-$p.m_j$. We placed additional constraints on both the process and state components to improve parameter estimation and model convergence. We fixed r_1, r_2, $p.m_1$, and $p.m_2$ to zero because the variation in capture effort for the smallest immature size classes ($j \leq 2$) over our study precluded us from recapturing tagged alligators in the hatchling or juvenile state in subsequent occasions, and we did not observe any dead recoveries of these size classes. We encountered relatively few dead alligators in the larger size classes ($j \geq 3$; Table A1.1); therefore, we constrained the r_j for those size classes to a single recovery parameter r. Finally, because the data were sparse, we did not consider temporal or individual-level (beyond size class) variation in the parameters of the state process. In the development of the integrated population model, we considered a covariate which allowed temporal as well as size class specificity of detection probability.

To estimate parameters φ_j, $p.m_j$, and r given ψ_j^{Sex}, we followed the state-space formulation of Kéry and Schaub (2012) in which a latent categorical state $z_{i,t} \in \{1, 2,\ldots, 8\}$ for individual i at time t, conditional on $z_{i,t-1}$, is modeled as a Markovian process. Given the alligator's previous state $z_{i,t-1}$, the alligator's current state $z_{i,t}$ was drawn from a categorical distribution with component probabilities defined by functions involving φ_j, r, and ψ_j^{Sex}. Observational data on alligator i at time t, $y_{i,t}$, were recorded in one of eight

states: detected in one of the 6 size classes ($y_{i,t}$ = 1,…, 6), recovered dead ($y_{i,t}$ = 7), or not seen ($y_{i,t}$ = 8). We linked observations $y_{i,t}$ to the true latent state $z_{i,t}$ through a categorical distribution with component probabilities defined by functions involving $p.m_j$.

Count observation model— We developed a state-space model to estimate size class-specific abundance ($N_{j,k,t}$) and detection probabilities ($p.d_{j,k,t}$, $p.a_j$, $p.c_j$), in which the observation component incorporated the count data from nightlight surveys. Despite the availability of replicated survey data, for computational efficiency we only used counts from the single survey that had the highest number of total individuals recorded for the year. Nightlight surveys were comprised of three different observation types that represented an increasing level of demographic resolution: (1) Unknown includes individuals that were detected but could not be placed into any size or age class ($unk_{k,t}$ in Fig. 2.3); (2) Aged includes observations in which the individual was assigned to either the immature (size class j unknown but ≤3; $age.im_{k,t}$ in Fig. 2.3) or adult (j unknown but ≥4; $age.ad_{k,t}$ in Fig. 2.3) age class; and (3) Sized includes observations in which the individual was assigned to one of the six size classes ($c_{j,k,t}$ in Fig. 2.3).

To estimate the $N_{j,k,t}$, we created a structure of three models in which numbers of alligators detected at increasingly finer demographic resolution were probabilistically linked to numbers (possibly latent) at coarser resolutions. The Detections level, the coarsest level of resolution, included all three observation types— Unknown, Aged, and Sized. We defined the latent quantity $d_{j,k,t}$ as the number of alligators detected at site k on occasion t that belonged to size class j. This quantity is generally unobservable because not all alligators detected that belong to size class j can be assigned to size class j. We

modeled $d_{j,k,t}$ as the outcome of a binomial process with success probability $p.d_{j,k,t}$ and index parameter $N_{j,k,t}$., i.e., the abundance of alligators in size class j at site k at time t:

$$d_{j,k,t} \sim \text{binomial}(p.d_{j,k,t}, N_{j,k,t}) \quad (2.1)$$

Thus, $p.d_{j,k,t}$ is the overall detection probability for individuals of size class j, whether or not an individual of that class can be assigned as such. The Aggregate level, the next finer level of demographic resolution, considers the Aged and Sized observation types. We defined the latent quantity $a_{j,k,t}$ as the number of alligators assigned either to a size or age class that belonged to size class j. Again, $a_{j,k,t}$ is generally unobservable because it includes alligators belonging to size class j that cannot be determined as such. We modeled $a_{j,k,t}$ as the outcome of a binomial process with success probability $p.a_{,j}$ and index $d_{j,k,t}$:

$$a_{j,k,t} \sim \text{binomial}(p.a_{,j}, d_{j,k,t}) \quad (2.2)$$

Parameter $p.a_{,j}$ is the probability that an individual, conditional on its detection, can be placed into either an aggregated age class (age.im$_{k,t}$, age.ad$_{k,t}$ in Fig. 2.3) or a specific size class. Last, the Classified level, the finest level of demographic resolution, includes only the Sized observations. Here, the count of individuals for a particular size class, site, and occasion, $c_{j,k,t}$, is a directly-observable quantity. We modeled $c_{j,k,t}$ as the outcome of a binomial process with success probability $p.c_{,j}$ and index $a_{j,k,t}$:

$$c_{j,k,t} \sim \text{binomial}(p.c_{,j}, a_{j,k,t}) \quad (2.3)$$

Parameter $p.c_{,j}$ is the probability that an individual, conditional on having been identified to at least an age class, can be placed into a specific size class. Thus, through the parametric linkages among models, all three observation types ultimately inform size

class-specific population abundance. We did not consider site-level differences or temporal variation for the count model detection probabilities for the Aggregate and Count levels; thus, these parameters lack both site (k) and time (t) indexing.

We used a series of sum constraints within JAGS to link the raw observations to the quantities in Eq. 2.1–2.3 above (Plummer, 2013):

$$unk_{k,t} = \sum_{j=1}^{6} d_{j,k,t} - \sum_{j=1}^{6} a_{j,k,t} \tag{2.4}$$

$$age.im_{k,t} = \sum_{j=1}^{3} a_{j,k,t} - \sum_{j=1}^{3} c_{j,k,t} \tag{2.5}$$

$$age.ad_{k,t} = \sum_{j=4}^{6} a_{j,k,t} - \sum_{j=4}^{6} c_{j,k,t} \tag{2.6}$$

In Eq. 2.4, the number of Unknown observations ($unk_{k,t}$) must equal the difference between number of Detection observations, which includes all three data categories (Unknown, Aged, Sized), and the number of Aggregate observations (Aged and Sized only). Eq. 2.5 states that the number of $age.im_{k,t}$ observations must equal the number of Aggregate juveniles ($j \leq 3$) minus Classified immatures. Similarly, in Eq. 2.6, the number of $age.ad_{k,t}$ observations must equal the number of Aggregate adults ($j \geq 4$) minus Classified adults.

Abundance State Process — For the state, or ecological, process component of our state-space model, we integrated the likelihoods for abundance ($N_{j,k,t}$) from the observation component of the state-space model and survival parameters (φ_j) from the multistate mark-recapture model. We completed the specification of the IPM by supplying fixed values of size class transition probability, ψ_j^{Sex}, GXN public harvest data

from the prior year ($h_{j,k,t-1}$ in Fig. 2.3), and auxiliary terms for fecundity and proportion of females in each size class. Within our life cycle model (Fig. 2.2), only females in size classes 4 and 5 could contribute to population growth. Though females (F) were allowed to enter size class 6 (i.e., $\psi_5^F > 0$), we never documented a female with a measurement of SVL that would place it in stage class 6 (Table A1.1). Similarly, extremely few females throughout the alligator's distribution have ever been verified to exceed 305 cm TL (P.M. Wilkinson, pers. comm.). As such, we defined annual fecundity ($f_{k,t}$) for site k as:

$$f_{k,t} = \{(N_{4,k,t} \times FP_4) + (N_{5,k,t} \times FP_5)\} \times (BR \times NS \times CL) \quad (2.7)$$

in which the number of individuals in size classes 4 and 5 is multiplied by the proportion of females for that respective size class (FP_j; Woodward, 1996) to derive the number of females within the breeding size classes. The number of females is multiplied by the proportion of females believed to be breeding in a given year (*BR*) and by the apparent nest survival rate (*NS*) and average clutch size (*CL*) for the YWC population (Wilkinson, 1983; Table A2.1). We modeled the number of young-of-the-year hatchlings (*YOY*; individuals hatched in the current year) on occasion t at site k as a Poisson outcome, with fecundity from the current year as the mean and variance term:

$$YOY_{k,t} \sim \text{Poisson}(f_{k,t})$$

Because we completed all nightlight surveys before hatching in the current nesting season, we never encounter *YOY* hatchlings. Therefore, all hatchlings (j=1) encountered during nightlight surveys in year t were hatched in year t-1 and survived for

approximately six to nine months, and both *f* and *YOY* are modeled as functions of conditions in year *t*-1, not year *t*. The number of individuals in the hatchling size class (N_1) observed during surveys in year *t* at site *k* is therefore binomially distributed as a function of the nine-month hatchling survival rate and *YOY* in year *t*-1 at site *k*:

$$N_{1,t,k} \sim \text{binomial}(\varphi_1^{0.75}, YOY_{t\text{-}1,k})$$

For size classes $j \geq 2$, the number of individuals in year *t* was the sum of the number of surviving individuals entering size class *j* from *j*-1 and the number of individuals that remained in *j* from the previous year, of both sexes. These quantities were stochastic outcomes of binomial draws using the combined survival and transition (growth) probability for individuals entering a new size class ($s_{j\text{-}1,j}$) or remaining in the same size class ($s_{j,j}$), respectively.

$$s_{j-1,j} = \varphi_{j-1} \times (FP_{j-1} \times \psi^{F}_{j-1} + (1 - FP_{j-1}) \times \psi^{M}_{j-1})$$

$$s_{j,j} = \varphi_j \times \{FP_j \times (1 - \psi^{F}_{j}) + (1 - FP_j) \times (1 - \psi^{M}_{j})\}$$

Thus, the hatchling survival rate (φ_1) is applied twice: (1) at a nine-month time-scale from nest hatch in *t*-1 to being observed as a hatchling in year *t* and (2) from being observed as a hatchling in year *t* to surviving to be observed as a juvenile at *t*+1. Given the $s_{j,j'}$, prior year abundances $N_{j,k,t\text{-}1}$, and prior-year harvests $h_{j,k,t\text{-}1}$, the number of individuals that entered a new size class ($n_{j\text{-}1,j}$) or remained in the same size class ($n_{j,j}$) was generated thus:

$$n_{j\text{-}1,j,k,t} \sim \text{binomial}(s_{j\text{-}1,j}, N_{j\text{-}1,k,t\text{-}1} - h_{j\text{-}1,k,t\text{-}1}) \quad (2.8)$$

$$n_{j,j,k,t} \sim \text{binomial}(s_{j,j}, N_{j,k,t\text{-}1} - h_{j,k,t\text{-}1}) \quad (2.9)$$

$$N_{j,k,t} = n_{j\text{-}1,j,k,t} + n_{j,j,k,t} \quad (2.10)$$

Size classes in our study population were exposed to different levels of harvest pressure, as public harvest regulations for alligators in South Carolina prohibit the take of individuals <120 cm TL. Therefore, we assumed $h_{j,k,t} = 0$ for $j \leq 3$ in Eq. 2.8 and $j \leq 2$ in E. 2.9. We allocated public harvest deductions from GXN annually by size class to each site k in proportion to the site's survey route length. As such, we deducted the t-1 harvest totals from the previous year's population size for size class j, before applying the combined growth survival term $s_{j,j'}$. The harvest-adjusted total for each size class at a given site and year represents the sum of individuals that entered a new size class ($n_{j\text{-}1,j,k,t}$) and those that remained in the same size class ($n_{j,j,k,t}$) (Eq. 2.10). Lastly, we were interested in describing site-specific population trends. Therefore, we derived $N_{k,t}^{TOT}$ the sum of all size classes (j=1,…,6) for site k at time t, and annual population growth rate ($\lambda_{k,t}$) by dividing the total number of individuals in the current year ($N_{k,t}^{TOT}$) by that in the previous year.

2.3.4 Sensitivity Analysis — The IPM framework relied upon extensive auxiliary data from other studies (Fig. 2.3; Table A2.1) to estimate our demographic parameters and quantities of interest (e.g., N_j, φ_j). Specifically, we used productivity variables (clutch size, nest success, and female breeding probability) in the fecundity formulation (f; Eq. 2.7) and proportion of females in each size class (FP_j) for the abundance state process; hereafter extrinsic variables. To assess the sensitivity of our results to the mean values of the extrinsic variables (except clutch size), we conducted a perturbation analysis in which we compared outputs from a simplified IPM with the extrinsic variables fixed to their mean values (Table A2.1) to a set of models in which variables were perturbed ±1% one

at a time, in turn. Our sensitivity analysis confirmed that there was not systematic bias associated with any extrinsic variable, though some model parameter outputs were changed substantially (>5%; Table A2.2). Therefore, we elected to incorporate further parametric uncertainty by sampling each extrinsic variable (except clutch size) from a beta distribution in the main analysis. Appendix A2 contains an expanded description of the sensitivity analysis and results.

Global model structure and covariate selection — Our global model incorporated the sampling distributions for auxiliary parameters and included the effects of three covariates. First, we created a covariate for the mark-recapture detection probability ($p.m_{j,t}$) to account for temporal variation in capture effort (CE), which varied in both duration (i.e., number of capture days) and intensity (i.e., number of capture methods used or personnel). Unfortunately, traditional metrics of capture effort or trap days were not consistently recorded. Experiences by us and other principal investigators on the YWC study indicated that at least one alligator was captured each field day (P.M. Wilkinson and T.R. Rainwater, pers. comm.). Therefore, for each day that an alligator was captured, we assigned a "1" if only one capture technique was used, or a "2" if two or more techniques were used. We summed all of the capture day scores within each year and z-standardized (mean: 0.0, SD: 1.0) the scores across years.

Both water level (WL) and temperature (WT) are known to influence detection probability of alligators in nightlight surveys (Fujisaki et al., 2011; Waddle et al., 2015); therefore, we modeled these effects for the count-based detection probability ($p.d_{j,k,t}$). We used the average river gauge-height in feet (± 0.01) during the survey as a measure of

water level. Due to structural and hydrological differences between the two survey sites, we z-standardized water level within each river for a more generalizable interpretation of results. We used the YSI measurements recorded during each survey to determine the average water temperature (± 0.1° C), and we z-standardized across both routes.

We used indicator variable selection to evaluate the potential influence of covariates on detection probabilities, $p.m_{j,t}$ and $p.d_{j,k,t}$ (Hooten and Hobbs, 2015). Indicator variable selection is useful for assessing the degree of support for each of a set of candidate predictors (Hooten and Hobbs, 2015). Using this approach, the covariate's beta coefficient (β_i) is defined as the product of a binary indicator variable (ω_i) and a regression coefficient θ_i:

$$\beta_i = \omega_i * \theta_i$$

$$\omega_i \sim \text{Bernoulli}(p.w_i)$$

$$p.w_i \sim \text{uniform}(0,1)$$

$$\theta_i \sim \text{normal}(0, \sigma_\beta)$$

In each MCMC iteration, the *i*th covariate enters the model as a predictor when ω_i =1 and is excluded from the model when $\omega_i = 0$. Thus, the posterior mean of ω_i roughly reflects the probability of the covariate's inclusion in the model.

All four detection probabilities ($p.m_{j,t}$, $p.d_{j,k,t}$, $p.a_{,j}$, $p.c_{,j}$) were modeled with a logit link, though they differed in the number of covariates and other terms:

$$\text{logit}(p.m_{j,t}) = \beta_j + \beta^{CE} * CE_t$$

$$\beta_j \sim \text{normal}(0, 0.37)$$

where β_j denotes the baseline mark-recapture detection probability for each size class, and β^{CE} is the effect of the capture effort. We also forced into each model (i.e., not part of the variable selection procedure) a size class trend term for the three probabilities for count detection ($p.d_{j,k,t}$, $p.a_{,j}$, $p.c_{,j}$):

$$\text{logit}(p.d_{j,k,t}) = \beta^{d} + \beta^{d.T} * j + \beta^{WL} * WL_{t,k} + \beta^{WT} * WT_{t,k}$$

$$\text{logit}(p.a_{j}) = \beta^{a} + \beta^{a.T} * j$$

$$\text{logit}(p.c_{j}) = \beta^{c} + \beta^{c.T} * j$$

$$\beta^{d}, \beta^{a}, \beta^{c}, \beta^{d.T}, \beta^{a.T}, \beta^{c.T} \sim \text{normal}(0, 0.37)$$

where β^{d}, β^{a}, and β^{c} reflect the baseline detection probabilities, $\beta^{d.T}$, $\beta^{a.T}$, and $\beta^{c.T}$ are the size class (j) trend terms, specific to each detection probability type, and β^{WL} and β^{WT} are the effects of water level and temperature, respectively. All terms in the detection models were given a Jeffreys prior, which is weakly informative on the logit scale. Lastly, we used an identity link to model time-invariant (i.e., constant) survival probability ($\varphi_{j,}$) for each specific size class and for recovery probability (r) for size classes 3–6, both of which used uninformative wide priors from a uniform distribution (0,1).

Due to extensive computational demand, the global model (hereafter G93) was fit using only a subset of the YWC mark-recapture data (1993–2017), along with survey and harvest datasets (2011–2016). We evaluated potential improvements in parameter estimate precision by reducing structural uncertainty and by including additional data. Using the output from the global model, we created a "reduced" model structure that only retained the influential covariates— the indicator for the ith covariate (ω_i) was fixed at 1 if its mean value in the global model exceeded a threshold inclusion level of 0.75, or set

to 0 if below the threshold. Fixing the indicator variables to 1 or 0 in the reduced models reflects our acceptance of a certain level of risk (identified by our inclusion threshold value) of wrongly including or excluding a covariate in exchange for a realized benefit of improved parameter estimate precision associated with a reduction in structural uncertainty. We then ran two versions of the reduced model, one that included the same YWC mark-recapture subset as the global model (hereafter R93) whereas the other contained the entire dataset (hereafter R79; 1979–2017). All three models were run with three chains with a 5,000-iteration adaptive phase, followed by 200,000 iterations with the first 100,000 discarded as burn-in, and a thinning rate of 25. This yielded a combined chain of 12,000 MCMC samples from which we computed posterior distributions of parameters and derived quantities.

Population Growth Assessment — We characterized alligator population trends within GXN using the population growth rates from the demographic parameter estimates and count data. From the linear population dynamics equations above involving the φ_j, ψ_j^{Sex}, and *f* terms, we constructed a six-stage Lefkovtich projection matrix (Caswell, 2001), and we calculated the intrinsic population growth rate (λ^L) using the *popbio* package (Stubben et al., 2016). We computed a posterior distribution for λ^L by performing this calculation for every retained sample of the MCMC.

To evaluate population growth rate from nightlight surveys sites (λ_k^N), we simply divided the site-specific total abundance estimate of the final year by that of the first year from the *i*th MCMC iteration:

$$\lambda_{k,i}^{N} = \frac{N_{k,6,i}^{TOT}}{N_{k,1,i}^{TOT}} \quad (2.11)$$

For both the population growth rates, λ^{L} and λ^{N}, we computed the mean, SD, 95% CRI, as well as the proportion of iterations in which the population was increasing ($\lambda>1$) for all three models. We conducted all simulations and parameter estimation described here, and throughout the manuscript, using the *jagsUI* and *popbio* packages (Kellner, 2015; Stubben et al., 2016) in programs R 3.5.1 (R Core Team, 2018) and JAGS 4.3.0 (Plummer, 2013).

Results

Summary statistics for the mark-recapture, nightlight count, and harvest datasets are available in Appendix A1. Our parameter estimates are presented as the mean of the posterior distribution with their 95% credible intervals (CRI) from the G93 model output, unless otherwise stated. We chose to emphasize G93 model output because it incorporates the most parametric uncertainty; Table A3.1 in Appendix A3 contains a full comparison of output among all models and Table A4.1 in Appendix A4 shows the population growth post-hoc analysis output.

Survival probability

Survival probabilities of the three immature size classes increased with age from hatchlings through subadults (Fig. 2.4). In contrast, survival estimates among the three size classes of adults were relatively similar and also higher compared to immatures (Fig.

2.4). All three models showed a consistent pattern as estimates for survival probability became more precise as observations increased within size classes (i.e., small adults, large adults, and bulls; Fig. 2.4 and Table A3.1). Similarly, point and interval estimates of survival were virtually identical between G93 and R93 for the adult (i.e., data-rich) size classes (Table A1.1). There appeared to be no systematic difference between the survival estimates of '93 models and R79 (e.g., consistently higher or lower than the other model) for the immature size classes, despite model R79 appearing to be more precise overall (Fig. 2.4).

Covariates and detection probabilities

The size class-specific mark-recapture detection probabilities ($p.m_{j,t}$) at mean capture effort (CE) were highest for large adults (0.10; 0.07, 0.14), intermediate for bulls (0.08; 0.05, 0.13) and small adults (0.07; 0.05, 0.10), and lowest for subadults (0.03; 0.00, 0.16). Covariate CE had a high probability of inclusion ($\omega_{CE} = 0.99$) and a positive effect on $p.m_{j,t}$ ($\beta^{CE} = 0.36$; 0.18, 0.54).

For the three detection probabilities that were count-based, the trend across size classes was positive for both $p.a_j$ and $p.c_j$, and negative for $p.d_{j,k,t}$ (Fig. 2.5). Both water level (WL) and temperature (WT) had a high probability of inclusion ($\omega_{WL} = 0.81$, $\omega_{WT} = 1.00$). WL had a weak negative effect ($\beta^{WL} = -0.148$; -0.29, 0.03) on $p.d_{j,k,t}$ (Fig. 2.6a), whereas WT was strongly positive ($\beta^{WT} = 0.41$; 0.32, 0.50; Fig. 2.6b).

Abundance trends

Total alligator abundance ($N_{k,t}^{TOT}$) at each site followed the same general temporal pattern, peaking in 2012 (GPD: 1556; 1219, 1955; SAN: 1877; 1496, 2422) and subsequently declining through 2016 (GPD: 983; 660, 1393; SAN: 1522; 1106, 2097) (Fig. 2.7). Both the average estimated density and total individuals (2011–2016) appeared higher across years for SAN (133 alligators km^{-1}; $\bar{N}^{TOT}$: 1697; 1312, 2249) compared to GPD (34 alligators km^{-1}; $\bar{N}^{TOT}$: 1343; 971, 1700), despite the latter site being longer (38.4 vs. 12.8 river km). Though reducing parametric uncertainty in R93 provided increased precision and slightly lower N^{TOT} estimates compared to G93, the inclusion of additional mark-recapture data in R79 caused a large overall reduction in precision (Fig. 2.7c, 2.7f).

At a finer demographic resolution, temporal patterns for each size class were fairly similar between the two sites (Fig. 2.8). Hatchling abundance at both sites increased sharply from 2011 to 2012, then gradually declined (GPD 2011–2016 mean abundance: 399; 225, 606; range of annual means: 174, 521; SAN: 546; 332, 793; range: 235, 652) (Fig. 2.8a, 2.8b). Subadult (GPD: 182; 118, 277; range: 96, 316; SAN: 211; 140, 319; range: 122, 350), small adult (GPD: 219; 150, 302; range: 156, 255; SAN: 295; 209, 414; range: 237, 326), and large adult (GPD: 208; 135, 310; range: 136, 295; SAN: 306; 215, 461; range: 260, 356) size classes at both sites also exhibited a gradual decline throughout the study, whereas juveniles showed an initial decline from 2011–2012 and then stabilized (GPD:166; 76, 286; range: 138, 216; SAN: 217; 111, 367; range: 182, 282) (Fig. 2.8). Temporal variation in abundance of bulls (size class 6) appeared to differ between sites. The abundance of bulls at GPD remained relatively stable (122; 53, 246;

range: 108, 133) (Fig. 2.8c) while at SAN abundance appeared to increase (122; 63, 226; range: 74, 159) (Fig. 2.8d).

Population growth rates

The Lefkovitch matrix-derived population growth rates (λ^L) had the same mean value (0.93 ± 0.02 SD) across all models, and none of the 95% CRIs overlapped zero, indicating a likely population decline. Similarly, only a single iteration within the R79 samples produced a $\lambda_i^L > 1$ (Table A4.1, Fig. A4.1). In contrast, the abundance derived population growth rates (λ_k^N) varied among sites and models (Table A4.1). G93 consistently produced the highest and least precise λ_k^N for both sites (GPD: 0.71; 0.70, 0.71; SAN: 0.94, 0.94, 0.95), and SAN had a greater proportion of iterations (0.30) that produced $\lambda_k^N > 1$ compared to GPD (0.01), indicating both spatial variation in population growth rates and uncertainty regarding the abundance for SAN (Table A4.1, Fig. A4.2).

Discussion

We constructed the first-ever IPM for crocodilians and are among the first to provide survival estimates, adjusted for imperfect detection, from one of the few multi-decadal crocodilian mark-recapture studies in the world. Our study further elucidates the processes that influence detectability of both alligators (and other crocodilians) during nightlight surveys, including environmental, habitat, and demographic factors (Fujisaki et al., 2011; Shirley et al., 2012; Waddle et al., 2015). Due to their conditional structure, the

detection parameters in our observation model (*p.d*, *p.a*, *p.c*) are defined differently than those in *N*-mixture-based abundance models (Dail and Madsen, 2011; Royle, 2004; Zipkin et al., 2014b) that are increasingly used to analyze nightlight survey data (Fujisaki et al., 2011; Gardner et al., 2016; Waddle et al., 2015). However, both the *p.d* estimates (hereafter detection probability) and covariate effects reported here are comparable to other nightlight studies. The negative relationship between water level and detection probability is well-documented for nightlight monitoring of crocodilians (Fujisaki et al., 2011; Waddle et al., 2015; Woodward and Marion, 1978); as water levels rise, alligators have more volume in which to submerge and evade detection. Similarly, alligator activity (i.e., visibility) is positively correlated with water temperature (Smith, 1975) which subseqently has a positive influence on detection (Gardner et al., 2016; Lutterschmidt and Wasko, 2006; Waddle et al., 2015; Woodward and Marion, 1978; but see Fujisaki et al., 2011), though the relationship may differ among size classes due to metabolic requirements (Lang, 1987).

Our detection probability estimates (range: 0.02–0.07) were similar to those from Florida from Waddle et al. (2015) for all size classes (0.11) and from Fujisaki et al. (2011) for small (0.03) and large alligators (0.09). In contrast, our estimates of detection probability were substantially lower than the estimate of 0.50 for all size classes reported by Gardner et al. (2016) in coastal North Carolina. The lower estimates of detection probability from our study and those in Florida compared to Gardner et al. (2016) could be attributed to study design. Gardner et al. (2016) conducted three temporally replicated surveys within one week to meet the assumption of geographic closure, whereas the two

temporal replicate surveys in both Waddle et al. (2015) and Fujisaki et al. (2011) were spaced at least two weeks apart to ensure sampling independence (Woodward and Moore, 1990) and likely sampled from an open superpopulation (*sensu* this study). While both approaches are valid, the choice in survey design likely depends on management objectives and habitat structure. For example, replicating surveys frequently and closely in time to produce an estimate for a closed population (*sensu* Gardner et al., 2016) may be more appropriate for isolated systems (e.g., lakes) or low-density habitats (e.g., North Carolina; O'Brien and Doerr, 1986) in which the geographic closure assumption is more likely to be met. While frequently replicated surveys may provide realistic estimates of population size for alligator habitats that are densely populated and highly connected (e.g., Florida Everglades, this study), the spatiotemporal dimensions to which such estimates would apply are highly uncertain, as alligator movement and habitat use patterns are often seasonally variable (Nifong and Silliman, 2017; Rosenblatt et al., 2013). Therefore, a "superpopulation" approach with replicates that are widely spaced in time may be more relevant for drawing inference over broader spatiotemporal scales.

Alligator wariness may also be a contributing factor to the size-related alligator detectability patterns we observed and our overall low size classification rate (35%; Table A1.3). Our nightlight survey sites were conducted on areas open to hunting for the South Carolina public harvest program, whereas comparison studies were conducted in areas with no harvest program yet established. While our estimates were similar to those by Fujisaki et al. (2011) and Waddle et al. (2015), it is notable that both studies were able to size-classify >90% of detected alligators. Multiple studies focused on surveying and

monitoring crocodilians have reported a wariness effect that is positively related to body size (Bourquin and Leslie, 2012; Ron et al., 1998; Webb and Messel, 1979). Therefore, if hunting elicits a similar wariness response, such behavior could explain why we detected a negative trend in detection across size classes that contrasts with Fujisaki et al. (2011), especially if alligator hunters tend to target larger individuals.

Wariness could also explain the contrasting patterns we observed between increasing population trends in bulls (Fig. 2.8c–d) and the 34% decline in bulls as a proportion of overall public harvest (2008–2016; Table A1.4). However, the apparent increase in bulls that we detected also may be an artifact of our model structure. For example, the annual harvest deductions in our model we included were derived from self-reported TL by hunters, with no indicator for the tail status (intact or not). Therefore, our harvest deductions may have been biased towards smaller size classes, assuming two alligators with identical SVL but different TL have (roughly) the same survival probability and biological function. Additionally, our abundance estimates are reflective of an open superpopulation which includes all individuals that could potentially be encountered by the nightlight surveys (Royle, 2004). Therefore, the apparent increase in bull abundance could reflect temporal variation in movement patterns, rather than a biological increase. However, both the effects of population-density on alligator growth and intra- or inter-annual movement patterns, particularly in response to harvest pressure, remain relatively unexamined (Lawson et al., 2018). Population trend uncertainty aside, bulls were the least numerous size class by far (Fig. 2.8), which is consistent with

previous studies (Nichols et al., 1976) and somewhat expected, given that the size class is likely all male, and the ca. 24 years required to reach 3.05 m TL (Wilkinson et al., 2016).

In contrast, hatchlings were, on average, the most numerous size class throughout the study, which was largely reflected in the temporal variation of the total population (Fig. 2.7). Here, we present two possible explanations for the initial pattern we observed: an initial spike in hatchling abundance and subsequent steep decline (Fig. 2.8). First, though female alligators are capable of reproduction at 1.8 m TL (Joanen and McNease, 1980), few females begin breeding until at least 2.3 m TL (Wilkinson, 1983). Though the mechanisms behind this phenomenon are not well-understood, one could be that dominant females suppress nesting in smaller, reproductively mature females (P.M. Wilkinson pers. comm.). Thus, the higher removal of larger individuals (including reproductively active females) from the population during the earlier years of the South Carolina public harvest (Table A1.4) could have therefore enabled a density-dependent "release" of numerous, smaller reproductively mature females into breeding activity, leading to an increase in hatchling abundance. However, the lack of monitoring data prior to 2011 precludes an evaluation of this hypothesis.

An alternative, but not mutually exclusive hypothesis, is that the steep increase may reflect a statistical artifact of the model. Abundance for the initial year of the study (2011) was sampled from uninformative priors, whereas abundances in later years were functionally related to prior-year abundances, along with other variables (e.g., Eqs. 8, 9). Both the potential influence of priors and missing data in the following year (2012) introduce some uncertainty regarding the observed steep increase. Therefore, future

versions of this model should evaluate the sensitivity of initial abundance observations to the population trajectory. Additionally, newly-hatched alligators typically remain with their mother for 1–2 years following hatch (McIlhenny, 1935). Alligator hatchlings are often encountered in groups during nightlight surveys, which violates the assumption of independent detections required of binomial mixture models (Royle and Dorazio, 2008), as used here. While our nightlight surveys were designed not to encounter young-of-the-year hatchlings in which non-independent detections may be expected, future iterations of this model could use the beta-binomial mixture model for hatchling abundance, which reduces potential bias in abundance estimates if correlated behavior is present (Martin et al., 2011). Similarly, it is also notable that the credible intervals around the overall population trend increased with the additional survival data in R79 (Fig. 2.7), especially given that the G93 and R79 survival estimates were fairly similar and not systematically lower or higher than one another (Fig. 2.4). Future iterations of the model should explore if incorporating beta distirubtions for the abundance terms or temporal variation in survival would affect the abundance precision and dataset length relationship.

Our data demonstrated that both of our study sites had a similar pattern in the composition of size classes and that both sites exhibited a population decline, though the presence of a decline was less clear for SAN (Fig. A4.2). The public harvest program for alligators in South Carolina may be a contributing factor to the decline, though we cannot rule out other potential environmental or anthropogenic mechanisms (e.g., drought, private harvest). The premise of the public harvest program was that the take of 1,000 alligators distributed among the four AMUs (Fig. 2.1) would amount to a 1% harvest,

based on an expert-elicited population estimate of 100,000 non-hatchling alligators (Bara, 1975, P.M. Wilkinson, pers. comm.), an estimate which has not been revised since the private harvest program initiation in 1995 (Rhodes, 2002; South Carolina Department of Natural Resources, 2017). Given the population decline we detected, a fixed harvest quota of 1,000 tags (raised to 1,200 from 2010–2013; Table A1.3) would become an increasing proportion of the overall population each year, thus, accelerating the rate of population decrease. Incorporating additional information (e.g., private harvest, nuisance removals) may produce survival estimates that are more reflective of biotic factors (e.g., environmental variation) that could subsequently be incorporated into the IPM. In the Florida Everglades, for example, dry years are associated with reduced abundances of alligators (Waddle et al., 2015), water depth during autumn and water year range (maximum – minimum water depth) are positively related to body condition (Brandt et al., 2016), while cold spells do not appear to increase apparent mortality of alligators (Mazzotti et al., 2016). Finally, an assumption of IPMs is that the separate datasets that are incoporated to build the IPM are independent such that individuals do not appear in both datasets, but that the datasets are subject to the same demographic processes and drivers (Abadi et al., 2010; Schaub and Abadi, 2011) though other studies indicate this assumption can be relaxed (Zipkin and Saunders, 2018). In our study the mark-recapture data with extrinsic productivity variables was collected from a protected area while nightlight surveys were conducted at sites exposed to harvest. Nonetheless, we contend that the assumptions of the IPM were still met. Since 2014, five marked individuals from the YWC population have been recovered by the public harvest (Table A1.1), suggesting

that coastsal South Carolina is highly connected and subsequently that impacts of management policies are likely to extend beyond their immediate boundaries.

Despite uncertainty regarding specific drivers of the population declines predicted by our model, the fine-scale demographic resolution survival estimates produced by the IPM offer some, albeit limited, opportunity to compare vital rates among other populations or species, given the dearth of demographic studies in crocodilians. The general pattern of increasing survival rates among immature size (or age) classes and of a leveling off in survival rates among adult size classes has been observed in both American crocodiles (*Crocodylus acutus*) in southern Florida (Briggs-Gonzalez et al., 2017) and Nile crocodiles (*C. niloticus*) in the Okavango Delta (Bourquin and Leslie, 2012). Our estimates of hatchling survival were markedly lower than those reported from a mark-recapture study of alligators at an inland freshwater lake in central Florida (0.41 ± 0.06 SE; Woodward et al., 1987). The difference in hatchling survival could be attributed to salinity regimes in the two systems. Salinity, which is higher at YWC due to its coastal location, adversely affects the physiology of immature alligators and therefore may reduce survival in this age class (Faulkner et al., 2018; Laurén, 1985). In a comprehensive demographic assessment of known-age American crocodiles, a protected species, Briggs-Gonzalez et al. (2017) reported survival estimates of 0.82 ± 0.02 SE for subadults (3–12 year-olds) and 0.88 ± 0.03 for adults (>12 year-olds), both substantially lower compared to our study.

Assessing the survival estimates in aggregate from a life history perspective allows us to better understand which vital rates, or size classes, if altered, are most likely to

affect the population growth rate. Our results, however, are consistent with other studies that suggest alligators, like other crocodilians and long-lived reptiles (Briggs-Gonzalez et al., 2017; Salguero-Gómez et al., 2016 and references therein), can be thought of as a hybrid in the context of life history strategies (Stearns, 1992). The high rates of adult survival we report and delayed age at first reproduction are indicative of a "slow" life history strategy. In contrast, the relatively large clutch size, low survival of the immature size class, and absence of reproductive senescence in alligators (this study, Wilkinson, 1983; Wilkinson et al., 2016) are characteristic of a "fast" life history strategy (Stearns, 1992). Though life history theory predicts that long-lived species are most sensitive to changes in survival (Stearns, 1992), multiple studies in crocodilians and other long-lived reptile species indicate that immature (between ages 1 to first breeding) survival rates may have relatively high elasticity (Briggs-Gonzalez et al., 2017; Salguero-Gómez et al., 2016). Interestingly, in a novel use of IPMs, Koons et al., (2017) demonstrated that changes in vital rates predicted by life history theory to be less sensitive were responsible for long-term, continent-wide declines in Lesser Scaup (*Aythya affinis*) populations. Therefore, future iterations of this IPM that incorporate temporal structure into survival estimates could potentially identify if demographic drivers of realized population growth rates are similar to those identified by prospective analyses that assume asymptotic growth.

Our analysis shows the potential utility of IPMs to identify latent, partially observable, population structure and trends, which can subsequently be used to further refine both harvest policy and the efficiency of monitoring programs. For example,

abundance estimates specific to size classes could enable the use of a proportional harvest policy, in which size classes are harvested in proportion to their occurrence. Similarly, the relationship between water level and temperature on detectability during nightlight surveys could be used to adjust scheduling of monitoring programs to optimize detectability. Lastly, though our finding of little variation in survival rates among adult size classes could be taken as evidence that classification of individuals ≥180 cm TL into specific size classes during nightlight surveys is unecessary, we caution that demographic "coarsening" of monitoring data that may reduce the ability to set objectives specific to size classes (e.g., conserve sensitive size classes) and monitor for other undesirable patterns, such as artificial selection. Alligators and other crocodilians exhibit determinate growth patterns in which individuals reach a terminal size in middle age, rather than growing throughout their lifespan (i.e., indeterminate growth) as previously assumed (Campos et al., 2014; Taylor et al., 2016; Tucker et al., 2006; Wilkinson et al., 2016). Therefore, hunted populations of crocodilians may also be subject to artificial selection on body size (total length), if recreational harvest targets the largest individuals for removal.

Our IPM addresses a widespread, critical challenge in the conservation of species that are difficult to directly observe (e.g. crocodilians, marine mammals) and that also have complex life-history patterns. In many cases the data produced by the preferred monitoring methodology are of a lower demographic resolution than what is needed to both make effective conservation decisions and reduce systemic uncertainty (Link et al., 2003). Worse still, this resolution "mismatch" could further propagate existing structural

uncertainty and partial observability, and ultimately limit conservation actions or management interventions that could otherwise benefit the affected species. Though some monitoring programs could be restructured to obtain the necessary level of resolution, or stopped entirely in favor of promising alternative methodologies (e.g., unmanned aerial vehicles; Ezat et al., 2018), such options severely restrict the use of existing, long-term datasets. Despite their potential low resolution, some long-term datasets may have inherent value for slow-growing or long-lived species in which the effects of management or conservation decisions may operate at a lagged timescale. Similarly, in our multi-model comparison we demonstrated that inclusion of longer-term datasets can sometimes improve estimate precision for multiple parameter types (Fig. 2.4). The IPM described here provides a promising, flexible approach to merge high-resolution demographic data (e.g., mark-recapture) with low-resolution, but less costly, monitoring data to describe and quantify latent demographic structure and population trends. The flexible nature of IPMs offers the ability to synthesize multiple datastreams to produce more precise demographic parameter estimates that can be used in other contexts to guide not only conservation decisions, but also improvements to the design of the monitoring program. Hence, IPMs are a valuable tool in conservation because they provide a means to both increase the resolution and precision of existing data, and potentially improve upon how monitoring data are collected for managed species.

Acknowledgments

We thank the many technicians and volunteers who assisted with nightlight surveys from 2011–2016 and alligator captures at the Yawkey Wildlife Center from 1979–2017. We specifically acknowledge the contributions of Jay Butfiloski, Brad Taylor, Jamie Dozier, and Derrell Shipes who were instrumental in the completion of this study. We are also grateful to the South Carolina Department of Natural Resources, members of the Guillette, Parrott, and Lance Labs, M. Wilkinson, and Y. Kanno who provided extensive logistical support, assistance, and analytical guidance. We also thank A. Woodward, E. Leone, and M. Bara for full use of the Wilkinson et al. (2016) data, and Clemson University for generous allotment of computer time on the Palmetto Cluster. We honor the memory of our coauthor, Kate W. McFadden, a passionate, innovative scientist and conservationist, who initiated this project and inspired those around her to think broadly and to hold themselves to a higher standard personally, intellectually, and professionally, beyond our self-limiting beliefs. This work was supported by the South Carolina Department of Natural Resources [grant numbers 2009094 and 20100899] and the United States Geological Survey [grant numbers G12AC20329 and G15AC00264]. Authors declare no conflict of interest. Any use of trade, firm, or product names is for descriptive purposes only and does not imply endorsement by the U.S. Government. This paper represents Technical Contribution Number 6731 of the Clemson University Experiment Station.

Literature Cited

Abadi, F., Olivier, G., Arlettaz, R., Schaub, M., 2010. An assessment of integrated population models: bias, accuracy, and violation of the assumptions of

independence. Ecology 91, 7–14.

Arnold, T.W., Clark, R.G., Koons, D.N., Schaub, M., 2018. Integrated population models facilitate ecological understanding and improved management decisions. J. Wildl. Manage. 82, 266–274. https://doi.org/10.1002/jwmg.21404

Aubry, A., Bécart, E., Davenport, J., Emmerson, M.C., 2010. Estimation of survival rate and extinction probability for stage-structured populations with overlapping life stages. Popul. Ecol. 52, 437–450. https://doi.org/10.1007/s10144-010-0194-9

Bara, M.O., 1975. American alligator investigations final study report. Columbia, South Carolina, USA.

Bayliss, P., 1987. Survey methods and monitoring within crocodilian management programmes, in: Webb, G.J., Manolis, S.C. (Eds.), Wildlife Management: Crocodiles and Alligators. Surrey Beatty and Sons Proprietary Limited, Sydney, Australia, pp. 157–175.

Bourquin, S.L., Leslie, A.J., 2012. Estimating demographics of the Nile crocodile (Crocodylus niloticus Laurenti) in the panhandle region of the Okavango Delta, Botswana. Afr. J. Ecol. 50, 1–8. https://doi.org/10.1111/j.1365-2028.2011.01285.x

Brandt, L.A., Beauchamp, J.S., Jeffery, B.M., Cherkiss, M.S., Mazzotti, F.J., 2016. Fluctuating water depths affect American alligator (Alligator mississippiensis) body condition in the Everglades, Florida, USA. Ecol. Indic. 67, 441–450. https://doi.org/10.1016/j.ecolind.2016.03.003

Briggs-Gonzalez, V., Bonenfant, C., Basille, M., Cherkiss, M., Beauchamp, J., Mazzotti, F., 2017. Life histories and conservation of long-lived reptiles, an illustration with the American crocodile (Crocodylus acutus). J. Anim. Ecol. 86, 1102–1113. https://doi.org/10.1111/1365-2656.12723

Campos, Z., Mouraõ, G., Coutinho, M., Magnusson, W.E., 2014. Growth of caiman crocodilus yacare in the brazilian pantanal. PLoS One 9, 1–5. https://doi.org/10.1371/journal.pone.0089363

Caswell, H., 2001. Matrix Population Models, Second Edi. ed. Sinauer Associates, Inc., Sunderland, Massachusetts, USA.

Chabreck, R.H., 1966. Methods of determining the size and composition of alligator population in Louisiana. Proc. Southeast. Assoc. Game Fish Comm. 20, 105–112.

Chabreck, R.H., 1963. Methods of capturing, marking, and sexing alligators. Proc. Ann. Conf. Southeast. Assoc. Game Fish Comm. 17, 47–50.

Cherkiss, M.S., Fling, H.E., Mazzotti, F.J., Rice, K.G., 2004. Counting and capturing crocodilians. Gainesville, Florida.

Conn, P.B., Cooch, E.G., 2009. Multistate capture-recapture analysis under imperfect state observation: An application to disease models. J. Appl. Ecol. 46, 486–492. https://doi.org/10.1111/j.1365-2664.2008.01597.x

Dail, D., Madsen, L., 2011. Models for Estimating Abundance from Repeated Counts of an Open Metapopulation. Biometrics 67, 577–587. https://doi.org/10.1111/j.1541-0420.2010.01465.x

Eversole, C.B., Henke, S.E., Ballard, B.M., Powell, R.L., 2014. Duration of marking tags on American Alligators (Alligator mississippiensis). Herpetol. Rev. 45, 223–226.

Ezat, M.A., Fritsch, C.J., Downs, C.T., 2018. Use of an unmanned aerial vehicle (drone) to survey Nile crocodile populations: A case study at Lake Nyamithi, Ndumo game reserve, South Africa. Biol. Conserv. 223, 76–81. https://doi.org/10.1016/j.biocon.2018.04.032

Faulkner, P.C., Burleson, M.L., Simonitis, L., Marshall, C., Hala, D., Petersen, L.H., 2018. Effects of chronic exposure to 12‰ saltwater on the endocrine physiology of juvenile American alligator (Alligator mississippiensis). J. Exp. Biol. jeb.181172. https://doi.org/10.1242/jeb.181172

Fryxell, J.M., Packer, C., Mccann, K., Solberg, E.J., Sæther, B., 2010. Supporting Online Material for Resource Management Cycles and the Sustainability of Harvested Wildlife Populations. Science (80-.). 328, 903–907. https://doi.org/10.1126/science.1185802

Fujisaki, I., Mazzotti, F.J., Dorazio, R.M., Rice, K.G., Cherkiss, M., Jeffery, B., 2011. Estimating trends in alligator populations from nightlight survey data. Wetlands 31, 147–155. https://doi.org/10.1007/s13157-010-0120-0

Gardner, B., Garner, L.A., Cobb, D.T., Moorman, C.E., 2016. Factors Affecting Occupancy and Abundance of American Alligators at the Northern Extent of Their Range. J. Herpetol. 50, 541–547. https://doi.org/10.1670/15-147

Gauthier, G., Pradel, R., Menu, S., Lebreton, J.D., 2001. Seasonal survival of Greater Snow Geese and effect of hunting under dependence in sighting probability. Ecology 82, 3105–3119. https://doi.org/10.1890/0012-9658(2001)082[3105:SSOGSG]2.0.CO;2

Gelman, A., Carlin, J.B., Stern, H.S., Rubin, D.B., 2004. Bayesian Data Analysis.

Chapman & Hall/CRC, Boca Raton, Florida, USA.

Gibson, D., Blomberg, E.J., Patricelli, G.L., Krakauer, A.H., Atamian, M.T., Sedinger, J.S., 2013. Effects of Radio Collars on Survival and Lekking Behavior of Male Greater Sage-Grouse. Condor 115, 769–776. https://doi.org/10.1525/cond.2013.120176

Hooten, M.B., Hobbs, N.T., 2015. A guide to Bayesian model selection for ecologists. Ecol. Monogr. 85, 3–28. https://doi.org/10.1890/14-0661.1

Jennings, M.L., David, D.N., Portier, K.M., 1991. Effect of Marking Techniques on Growth and Survivorship of Hatchling Alligators. Wildl. Soc. Bull. 19, 204–207.

Joanen, T., Mcnease, L., 1978. The cloaca sexing method for immature alligators, in: Proceedings of the Annual Conference of the Southeastern Association of Fish and Wildlife Agencies. p. 32:179-181.

Joanen, T., McNease, L., 1980. Reproductive biology of the American alligator in southwest Louisiana, in: Murphy, J.B., Collins, J.T. (Eds.), Reproductive Biology and Diseases of Captive Reptiles. Contributions to Herpetology, Society for the Study of Amphibians and Reptiles, Lawrence, Kansas, USA, pp. 153–159.

Kellner, K.F., 2015. jagsUI: A wrapper around ‘rjags’ to streamline ‘JAGS’ analyses.

Koons, D.N., Arnold, T.W., Schaub, M., 2017. Understanding the demographic drivers of realized population growth rates. Ecol. Appl. 27, 2102–2115. https://doi.org/10.1002/eap.1594

Krauss, J., Bommarco, R., Guardiola, M., Helm, A., Kuussaari, M., Lindborg, R., Ockinger, E., Partel, M., Pino, J., Poyry, J., Raatikainen, K.M., Sang, A., Stefanescu, C., Teder, T., Zobel, M., Steffan-Dewenter, I., 2010. Habitat fragmentation causes immediate and time- delayed biodiversity loss at different trophic levels. Ecol. Lett. 13, 597–605. https://doi.org/10.1111/j.1461-0248.2010.01457.x

Lance, V., Joanen, T., McNease, L., 1983. Selenium, vitamin E, and trace elements in the plasma of wild and farm-reared alligators during the reproductive cycle. Can. J. Zool. 61, 1744–1751. https://doi.org/10.1139/z83-225

Lang, J.W., 1987. Crocodilian thermal selection, in: Wildlife Management: Crocodiles and Alligators. Surrey Beatty and Sons Proprietary Limited, Sydney, Australia, pp. 301–317.

Langvatn, R., Loison, A., 1999. Consequences of harvesting on age structure, sex ratio and population dynamics of red deer Cervus elaphus in central Norway. Wildlife

Biol. 5, 213–223.

Laurén, D.J., 1985. The effect of chronic saline exposure on the electrolyte balance, nitrogen metabolism, and corticosterone titer in the american alligator, Alligator mississippiensis. Comp. Biochem. Physiol. 81, 217–223. https://doi.org/10.1016/0300-9629(85)90125-2

Lawson, A.J., Strickland, B.A., Rosenblatt, A.E., 2018. Patterns, drivers and effects of alligator movement behavior and habitat use, in: Henke, S.E., Eversole, C.B. (Eds.), American Alligators: Habitats, Behaviors, and Threats. Nova Science Publishers, Hauppauge, NY, USA, pp. 47–77.

Lebreton, J.D., Almeras, T., Pradel, R., 1999. Competing events, mixtures of information and multistratum recapture models. Bird Study 46, S39–S46. https://doi.org/10.1080/00063659909477230

Lebreton, J.D., Nichols, J.D., Barker, R.J., Pradel, R., Spendelow, J.A., 2009. Chapter 3 Modeling Individual Animal Histories with Multistate Capture-Recapture Models. Adv. Ecol. Res. 41, 87–173. https://doi.org/10.1016/S0065-2504(09)00403-6

Link, W.A., Royle, J.A., Hatfield, J.S., 2003. Demographic Analysis from Summaries of an Age-Structured Population. Biometrics 59, 778–785. https://doi.org/10.1111/j.0006-341X.2003.00091.x

Lomba, A., Pellissier, L., Randin, C., Vicente, J., Moreira, F., Honrado, J., Guisan, A., 2010. Overcoming the rare species modelling paradox: A novel hierarchical framework applied to an Iberian endemic plant. Biol. Conserv. 143, 2647–2657. https://doi.org/10.1016/j.biocon.2010.07.007

Lutterschmidt, W.I., Wasko, D.K., 2006. Seasonal Activity, Relative Abundance, and Size-Class Structure of the American Alligator (Alligator Mississippiensis) in a Highly Disturbed Inland Lake. Southwest. Nat. 51, 346–351. https://doi.org/10.1894/0038-4909(2006)51[346:SARAAS]2.0.CO;2

Martin, J., Royle, J.A., Mackenzie, D.I., Edwards, H.H., Ke, M., Gardner, B., 2011. Accounting for non-independent detection when estimating abundance of organisms with a Bayesian approach. Methods Ecol. Evol. 2, 595–601. https://doi.org/10.1111/j.2041-210X.2011.00113.x

Mazzotti, F.J., Brandt, L.A., 1994. Ecology of the American alligator in a seasonally fluctuating environment, in: Everglades: The Ecosystem and Its Restoration. pp. 485–505.

Mazzotti, F.J., Cherkiss, M.S., Parry, M., Beauchamp, J., Rochford, M., Smith, B., Hart, K., Brandt, L.A., 2016. Large reptiles and cold temperatures: Do extreme cold spells set distributional limits for tropical reptiles in Florida? Ecosphere 7, 1–9. https://doi.org/10.1002/ecs2.1439

McIlhenny, E.A., 1935. The alligator's life history. The Christopher Pubhlishing House, Boston, Massachusetts, USA.

Menéndez, R., Megías, A.G., Hill, J.K., Braschler, B., Willis, S.G., Collingham, Y., Fox, R., Roy, D.B., Thomas, C.D., 2006. Species richness changes lag behind climate change. Proc. R. Soc. B Biol. Sci. 273, 1465–1470. https://doi.org/10.1098/rspb.2006.3484

Murphy, T., Wilkinson, P., Coker, J., Hudson, M., 1983. The alligator trip snare: a live capture method. Columbia, South Carolina, South Carolina.

Nichols, J.D., Viehman, L., Chabreck, R.H., Fenderson, B., 1976. Simulation of a commercially harvested alligator population in Louisiana. Louisiana State Univ. Agric. Exp. Stn. Bull. 691, 1–59.

Nifong, J.C., Layman, C.A., Silliman, B.R., 2015. Size, sex and individual-level behaviour drive intrapopulation variation in cross-ecosystem foraging of a top-predator. J. Anim. Ecol. 84, 35–48. https://doi.org/10.1111/1365-2656.12306

Nifong, J.C., Silliman, B., 2017. Abiotic factors influence the dynamics of marine habitat use by a highly mobile "freshwater" top predator. Hydrobiologia 802, 155–174. https://doi.org/10.1007/s10750-017-3255-7

O'Brien, T.G., Doerr, P.D., 1986. Night Count Surveys for Alligators in Coastal Counties of North Carolina. J. Herpetol. 20, 444–448.

Plummer, M., 2013. JAGS: Just another Gibbs sampler.

R Core Development Team, 2018. R: A language and environment for statistical computing.

Radchuk, V., Turlure, C., Schtickzelle, N., 2013. Each life stage matters: The importance of assessing the response to climate change over the complete life cycle in butterflies. J. Anim. Ecol. 82, 275–285. https://doi.org/10.1111/j.1365-2656.2012.02029.x

Rhodes, W.E., 2002. Differential harvest of American Alligators on Private Lands in Coastal South Carolina, in: Crocodiles. Proceedings of the 16th Working Meeting of the Crocodile Specialist Group. IUCN–The World Conservation Union, Gland

Switzerland and Cambridge, UK, pp. 75–79.

Rhodes, W.E., Lang, J.W., 1996. Alligator Nest Temperatures and Hatchling sex rations in coastal South Carolina. Proc. Annu. Conf. Southeast. Assoc. Fish Wildl. Agencies 521–531.

Ron, S.R., Vallejo, A., Asanza, E., Ron, S.R., Vallejo, A., Asanza, E., 1998. Human Influence on the Wariness of Melanosuchus niger and Caiman crocodilus in Cuyabeno, Ecuador. J. Herpetol. 32, 320–324.

Rootes, W.L., Chabreck, R.H., 1993. Cannibalism in the American alligator. Herpetologica 49, 99–107.

Rosenblatt, A., Heithaus, M., Mather, M., Matich, P., Nifong, J., Ripple, W., Silliman, B., 2013. The Roles of Large Top Predators in Coastal Ecosystems: New Insights from Long Term Ecological Research. Oceanography 26, 156–167. https://doi.org/10.5670/oceanog.2013.59

Royle, J.A., 2004. N-Mixture Models for Estimating Population Size from Spatially Peplicated Counts. Biometrics 60, 108–115. https://doi.org/10.1111/j.0006-341X.2004.00142.x

Royle, J.A., Dorazio, R.M., 2008. Hierarchical modeling and inference in ecology: the analysis of data from populations, metapopulations and communities. Academic Press, San Diego, CA, USA.

Salguero-Gómez, R., Jones, O.R., Archer, C.R., Bein, C., de Buhr, H., Farack, C., Gottschalk, F., Hartmann, A., Henning, A., Hoppe, G., Römer, G., Ruoff, T., Sommer, V., Wille, J., Voigt, J., Zeh, S., Vieregg, D., Buckley, Y.M., Che-Castaldo, J., Hodgson, D., Scheuerlein, A., Caswell, H., Vaupel, J.W., 2016. COMADRE: A global data base of animal demography. J. Anim. Ecol. 85, 371–384. https://doi.org/10.1111/1365-2656.12482

Schaub, M., Abadi, F., 2011. Integrated population models: A novel analysis framework for deeper insights into population dynamics. J. Ornithol. 152, S227–S237. https://doi.org/10.1007/s10336-010-0632-7

Schnute, J., 1981. A Versatile Growth Model with Statistically Stable Parameters. Can. J. Fish. Aquat. Sci. 38, 1128–1140. https://doi.org/10.1139/f81-153

Shirley, M.H., Dorazio, R.M., Abassery, E., Elhady, A.A., Mekki, M.S., Asran, H.H., 2012. A sampling design and model for estimating abundance of Nile crocodiles while accounting for heterogeneity of detectability of multiple observers. J. Wildl.

Manage. 76, 966–975. https://doi.org/10.1002/jwmg.348

Smith, E.N., 1975. Thermoregulation of the American Alligator, Alligator mississippiensis. Physiol. Zool. 48, 177–194. https://doi.org/10.2307/30155651

Somaweera, R., Brien, M., Shine, R., 2013. The Role of Predation in Shaping Crocodilian Natural History. Herpetol. Monogr. 27, 23–51. https://doi.org/10.1655/HERPMONOGRAPHS-D-11-00001

South Carolina Department of Natural Resources, 2017. Alligator Hunting Season Report. Columbia, South Carolina, USA.

Stearns, S.C., 1992. The evolution of life histories. Oxford University Press, New York, NY, USA.

Stubben, C., Milligan, B., Maintainer, P.N., 2016. Package 'popbio' : Construction and Analysis of Matrix Population Models.

Subalusky, A.L., Fitzgerald, L.A., Smith, L.L., 2009. Ontogenetic niche shifts in the American Alligator establish functional connectivity between aquatic systems. Biol. Conserv. 142, 1507–1514. https://doi.org/10.1016/j.biocon.2009.02.019

Taylor, P., Li, F., Holland, A., Martin, M., Rosenblatt, A.E., 2016. Growth rates of black caiman (Melanosuchus Niger) in the Rupununi region of Guyana. Amphib. Reptil. 37, 9–14. https://doi.org/10.1163/15685381-00003024

Team, R.C., 2017. R: A language and environment for statistical computing.

Timothy T., T.J.B., R., L., Quinn, 1991. A General Growth Model for Mark Recapture Data. Fish. Res. 11, 257–281.

Tucker, A.D., Limpus, C.J., McDonald, K.R., McCallum, H.I., 2006. Growth dynamics of freshwater crocodiles (Crocodylus johnstoni) in the Lynd River, Queensland. Aust. J. Zool. 54, 409–415. https://doi.org/10.1071/ZO06099

Waddle, J.H., Brandt, L.A., Jeffery, B.M., Mazzotti, F.J., 2015. Dry Years Decrease Abundance of American Alligators in the Florida Everglades. Wetlands 35, 865–875. https://doi.org/10.1007/s13157-015-0677-8

Webb, G., Messel, H., 1979. Wariness in Crocodylus porosus (Reptilia: Crocodilidae). Aust. Wildl. Res. 6, 227–234. https://doi.org/10.1071/WR9790227

Wilkinson, P.M., 1994. A walk-through snare design for the live capture of alligators, in: Proceedings of the 12th Working Meeting of the Crocodile Specialist Group, Volume 2. IUCN–The World Conservation Union, Gland, Switzerland, Switzerland,

pp. 74–75.

Wilkinson, P.M., 1983. Nesting ecology of the American alligator in coastal South Carolina. Study Completion Report. Columbia, South Carolina.

Wilkinson, P.M., Rainwater, T.R., Woodward, A.R., Leone, E.H., Carter, C., 2016. Determinate Growth and Reproductive Lifespan in the American Alligator (Alligator mississippiensis): Evidence from Long-term Recaptures. Copeia 104, 843–852. https://doi.org/10.1643/CH-16-430

Wilkinson, P.M., Rhodes, W.E., 1997. Growth rates of American alligators in coastal South Carolina. J. Wildl. Manage. 61, 397–402.

Woodward, A.R., 1996. Determination of appropriate harvest strategies for alligator management units. Gainesville, Florida.

Woodward, A.R., Hines, T.C., Abercrombie, C.L., Nichols, J.D., 1987. Survival of young American alligators on a Florida lake. J. Wildl. Manage. 51, 931–937. https://doi.org/10.2307/3801762

Woodward, A.R., Marion, W.R., 1978. An evaluation of factors affecting night-light counts of alligators, in: Proceedings of the Annual Conference of Southeast Association of Fish and Wildlife Agencies. pp. 291–302.

Woodward, A.R., Moore, C.T., 1990. Use of crocodilian night count data for population trend estimation. Tallahassee, Florida, USA.

Woodward, A.R., Moore, C.T., Delany, M.F., 1992. Experimental alligator harvest. Final Report. Tallahassee, Florida, USA.

Zipkin, E.F., Saunders, S.P., 2018. Synthesizing multiple data types for biological conservation using integrated population models. Biol. Conserv. 217, 240–250. https://doi.org/10.1016/j.biocon.2017.10.017

Zipkin, E.F., Sillett, T.S., Grant, E.H.C., Chandler, R.B., Royle, J.A., 2014a. Inferences about population dynamics from count data using multistate models: A comparison to capture-recapture approaches. Ecol. Evol. 4, 417–426. https://doi.org/10.1002/ece3.942

Zipkin, E.F., Thorson, J.T., See, K., Lynch, H.J., Grant, E.H.C., Kanno, Y., Chandler, R.B., Letcher, B.H., Royle, J.A., 2014b. Modeling structured population dynamics using data from unmarked individuals. Ecology 95, 22–29. https://doi.org/10.1890/13-1131.1

Table 2.1. Summary information for American alligators (*Alligator mississippiensis*) by size class based on snout-vent length (SVL) ranges, which reflect the minimum and maximum predicted distances in cm from the snout tip to the vent posterior. Predicted total length (TL) range is the predicted distance from snout tip to tail tip in cm, based on established allometric relationships between SVL and TL among individuals with intact tails (Wilkinson et al., 2016). TL range was used to classify detected alligators during nightlight surveys conducted in coastal South Carolina, USA (2011–2016), whereas SVL range was used for assignment of size class in a mark-recapture recovery study at the Tom Yawkey Wildlife Center (Fig. 2.1; 1979–2017). Growth probability reflects the sex-specific probability of an individual in size class *j* at time *t* transitioning to *j*+1 at *t*+1, conditioned on survival.

Size class (*j*)	**Name**	**SVL range (cm)**		**Predicted TL range (cm)**	**Proportion female (PF_j ± SD)**	**Growth prob. (ψ_j)**	**Repro. status**
1	Hatchlings	F:	≤15.510	≤30	0.72 ± 0.02	1.00	Immature
		M:	≤15.600			1.00	
2	Juveniles	F:	15.511–63.031	31–121	0.37 ± 0.02	0.16	
		M:	15.601–63.397			0.17	
3	Subadults	F:	63.032–94.547	122–182	0.47 ± 0.02	0.19	
		M:	63.398–95.097			0.26	
4	Small Adults	F:	94.548–126.064	183–243	0.47 ± 0.07	0.09	Mature
		M:	95.098–126.796			0.19	
5	Large Adults	F:	126.065–157.581	244–304	0.35 ± 0.10	0.01	
		M:	126.797–158.495			0.12	
6	Bulls	F:	≥157.582	≥305	0.00	0.00	
		M:	≥158.496			0.00	

[a]Growth probabilities for j=2,…,5 were estimated though MCMC simulation, whereas all others were fixed values.

Figure 2.1. Map depicting the location of an American alligator capture-mark recovery study (1979–2017) at the Tom Yawkey Wildlife Center (YWC; indicated by the dashed border), and two nightlight survey routes (thick black lines) on the Great Pee Dee and Waccamaw Rivers, and the South Santee River (2011–2016), all within Georgetown County (GXN), South Carolina, USA. The black squares represent boat launches (BL) or stream gauges (SG) that recorded water levels and water temperature for each survey route. The inset shows the four alligator management units in South Carolina subject to a public harvest program: 1. Southern Coastal; 2. Middle Coast, 3. Midlands, and 4. Pee Dee (GXN shaded dark gray).

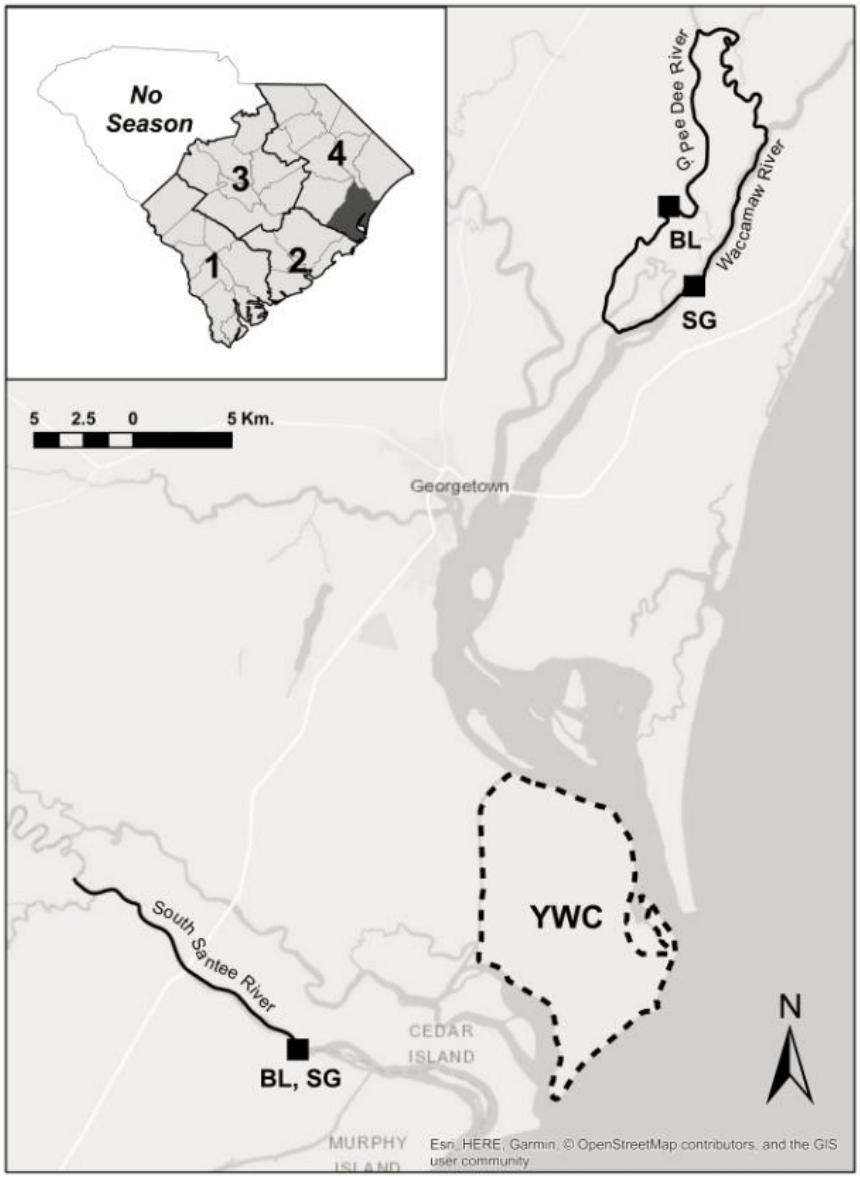

Figure 2.2. An American alligator life cycle diagram. Each circle consists of a single state (j). States 1–6 represent live states as defined by different size classes (Table 2.1), in which the dashed circles ($j \leq 3$) represent immature (non-breeding) size classes and the solid circles ($j \geq 4$) reflect adult (breeding) size classes: 1= hatchlings; 2=juveniles; 3=subadults; 4= small adults; 5=small adults, and 6= bulls. The closed, gray circles reflect a recently dead state (j=7) and an absorbing, terminal, dead state (j=8). The bolded ψ_j terms reflect growth probabilities that were fixed to one. Each year, surviving individuals (φ_j) could remain in the same size class (1- ψ_j^{Sex}; self-looping arrows) or graduate to the next sequential size class (ψ_j^{Sex}; straight right-pointing arrows). Individuals that did not survive (1-φ_j; lower arcs) could either enter the recently dead state if their carcass was recovered (e.g. harvest return of a tagged individual) with probability r, with compulsorily transition to the absorbing state in the following year, or directly enter the absorbing state if their carcass was not encountered (1-r). The upper arc arrows show the reproductive contributions of females in size classes 4 and 5. Fecundity($f_{k,t}$) is the product of size class-specific abundance ($N_{j,k,t}$), female proportion in the size class (FP_j), proportion of breeding females (BR; Wilkinson, 1983); nest survival (NS), and the average clutch size (CL=45), summed for each reproductive size class.

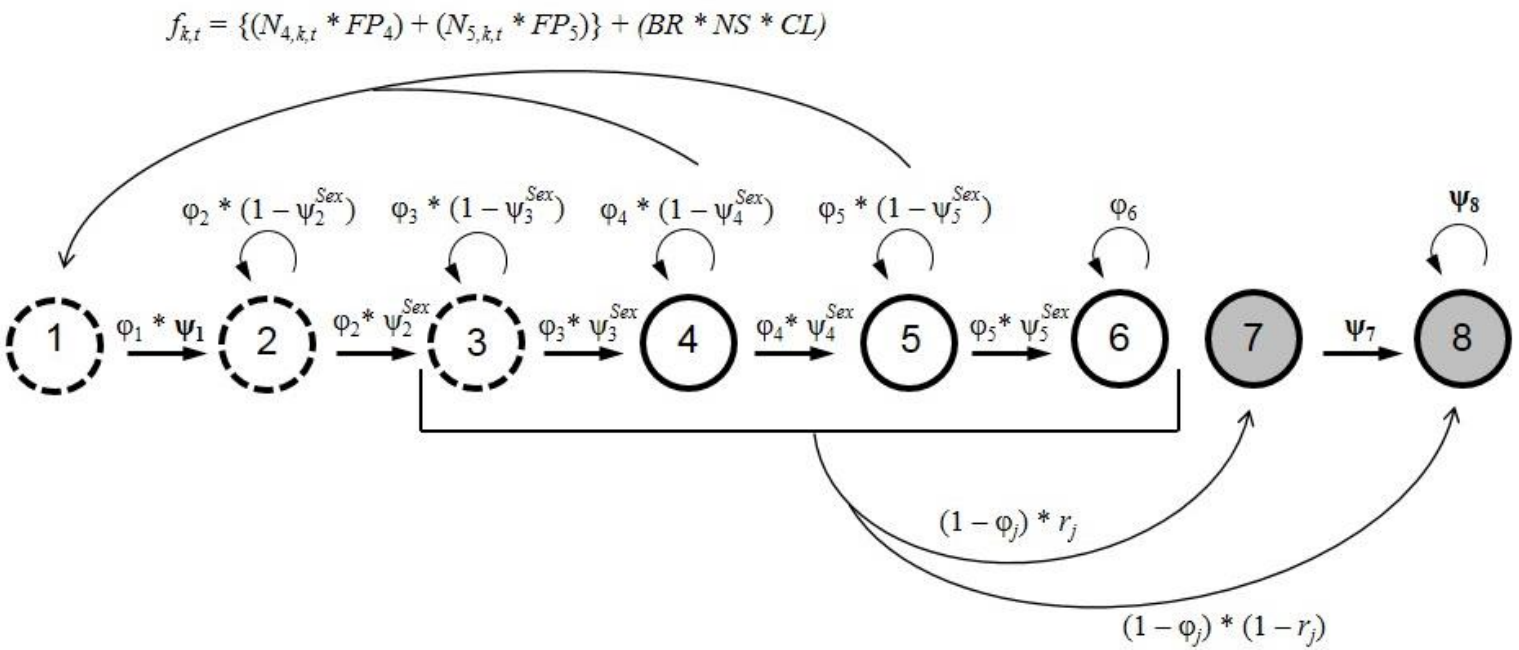
$f_{k,t} = \{(N_{4,k,t} * FP_4) + (N_{5,k,t} * FP_5)\} + (BR * NS * CL)$
$\varphi_2 * (1 - \psi_2^{Sex})$
$\varphi_3 * (1 - \psi_3^{Sex})$
$\varphi_4 * (1 - \psi_4^{Sex})$
$\varphi_5 * (1 - \psi_5^{Sex})$
φ_6
ψ_8
1
$\varphi_1 * \psi_1$
2
$\varphi_2 * \psi_2^{Sex}$
3
$\varphi_3 * \psi_3^{Sex}$
4
$\varphi_4 * \psi_4^{Sex}$
5
$\varphi_5 * \psi_5^{Sex}$
6
7
ψ_7
8
$(1 - \varphi_j) * r_j$
$(1 - \varphi_j) * (1 - r_j)$

Figure 2.3. Directed acyclic graph of an integrated population model (IPM) for American alligators in Georgetown County, South Carolina, USA. Parameters for which we computed posterior distributions are represented by circles whereas observed data, covariates, and extrinsic variables (non-updated) are represented by squares; with indexing for size class (j), site (survey route; k), and year (t). The growth formula represents an alligator growth dataset (g; Wilkinson et al., 2016) that was used to derive transition probabilities for sex-specific growth (ψ_j^{Sex}) outside of the IPM framework. The large dashed box represents the multistate mark-recapture model that used a mark-recapture dataset (m), ψ_j^{Sex}, and a capture effort covariate ($CE_{j,t}$) to estimate probabilities of recovery (r), detection ($p.m_{j,t}$), and apparent survival (φ_j)— a shared parameter within the integrated likelihood for the state-space abundance model. Input to the fecundity formula included the proportion of females in each size class (FP_j; Rhodes and Lang, 1996; Woodward, 1996), the proportion of breeding females (BP; Wilkinson, 1983), and average clutch size (CL) and nest success (NS) at the Tom Yawkey Wildlife Center (Wilkinson, 1983). The bottom row of boxes within the state-space model reflect different types of nightlight survey data: Sized ($c_{j,k,t}$), Aged (immatures: $age.im_{k,t}$, adults: $age.ad_{k,t}$); or Unknown age ($unk_{k,t}$). These data were used to estimate two latent quantities specific to size class, the number of detected and aggregated individuals ($d_{j,k,t}$) and ($a_{j,k,t}$), respectively, and their associated detection probabilities ($p.d_{j,k,t}$) and ($p.a_j$), whereas $p.c_j$ was conditioned on the size-classified counts. We modeled the effects of water level ($WL_{k,t}$) and temperature ($WT_{k,t}$) as survey-level covariates on $p.d_{j,k,t}$. The true number of individuals in each size class ($N_{j,k,t}$) was estimated in the process component of the state space model by fecundity ($f_{k,t}$), ψ_j^{Sex}, and φ_j, as well as the previous year's true number of individuals ($N_{j,k,t-1}$) and GXN harvest ($h_{j,k,t-1}$).

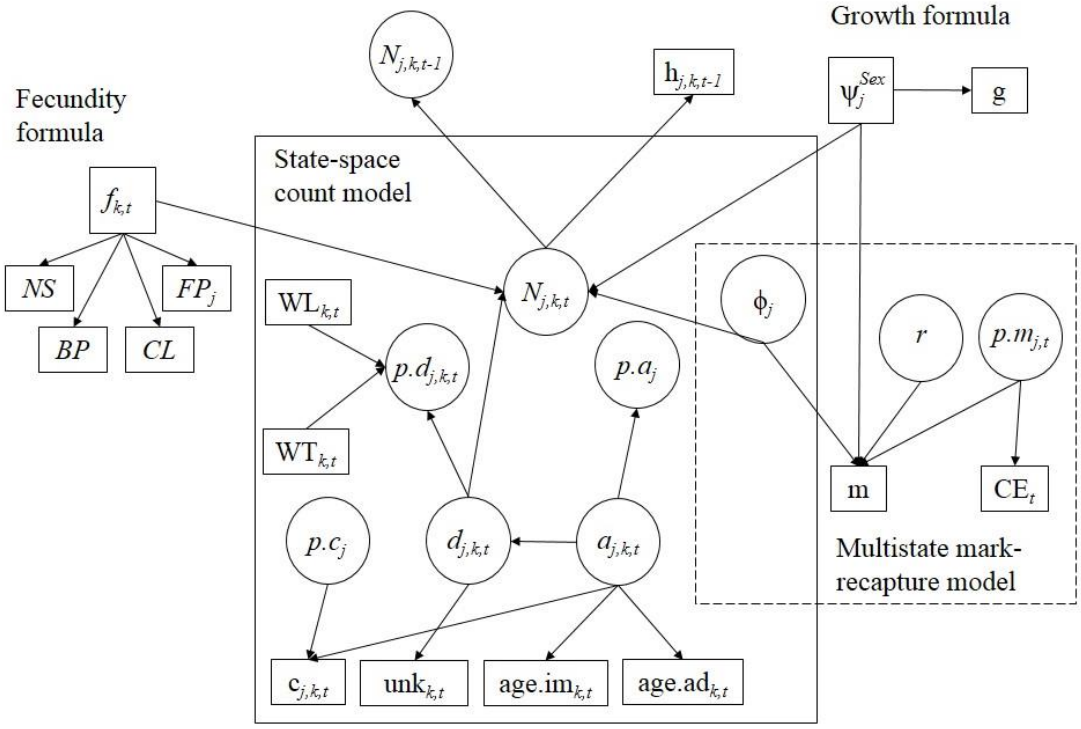
Growth formula
Fecundity formula
State-space count model
Multistate mark-recapture model
$N_{j,k,t-1}$
$h_{j,k,t-1}$
ψ_j^{Sex}
g
$f_{k,t}$
NS
FP_j
BP
CL
$WL_{k,t}$
$N_{j,k,t}$
ϕ_j
r
$p.m_{j,t}$
$p.d_{j,k,t}$
$p.a_j$
$WT_{k,t}$
m
CE_t
$p.c_j$
$d_{j,k,t}$
$a_{j,k,t}$
$c_{j,k,t}$
$unk_{k,t}$
$age.im_{k,t}$
$age.ad_{k,t}$

Figure 2.4. American alligator (*Alligator mississippiensis*) apparent survival estimates (±95% Bayesian credible intervals; CRI) for six size classes in coastal South Carolina, USA, produced from three different integrated population models (IPM). The G93 model (black circles) included alligator mark recapture records from the Tom Yawkey Wildlife Center (YWC) from 1993–2017, nightlight survey count and public harvest data from Georgetown County (Fig. 2.1) from 2011–2016, and indicator variable selection terms (Hooten and Hobbs, 2015) for three covariates. The R93 model (gray triangles) contained the same data as G93, but it included the covariates as certain components of the model structure (by removal of the indicator variable terms). The R79 model (light gray squares) included the full YWC mark-recapture dataset (1979–2017) but was otherwise identical to R93 in data and model structure.

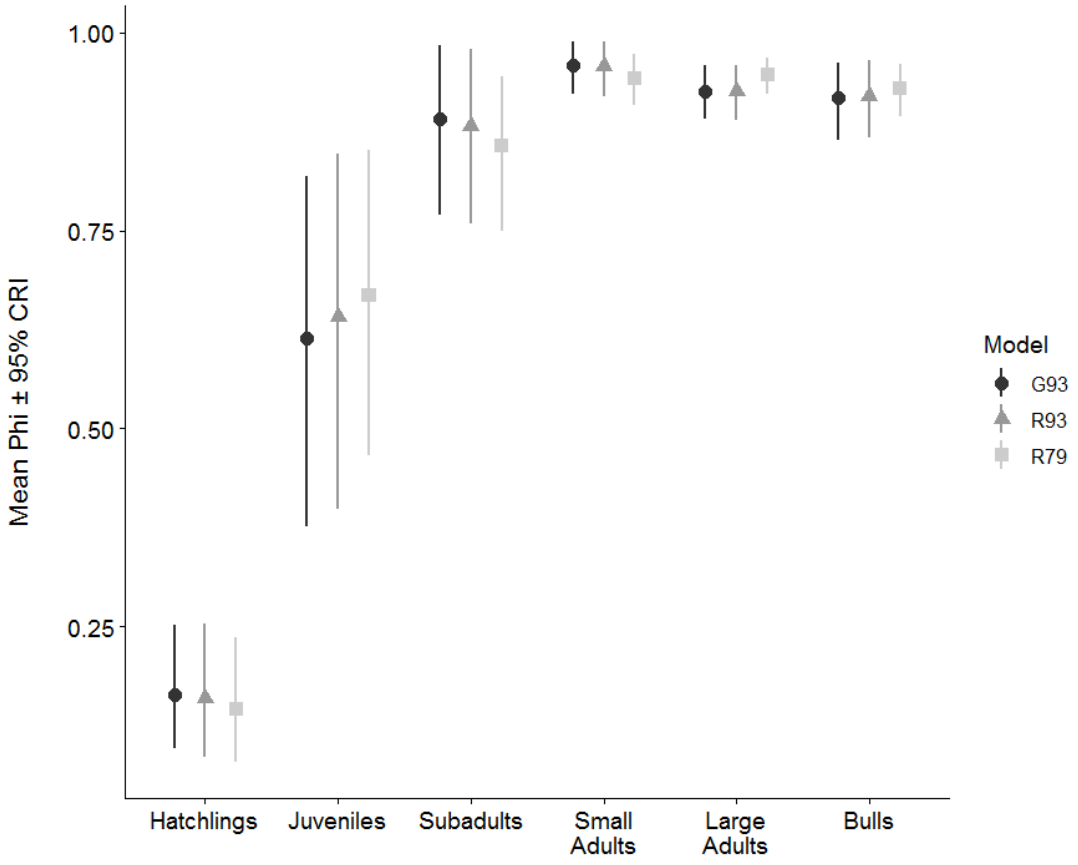

Figure 2.5. Estimated size class-specific American alligator (*Alligator mississippiensis*) detection probabilities during nightlight surveys in coastal South Carolina from 2011–2017. Each color reflects a specific size class. Probability of detection (*p.d*; left columns) is the probability of detecting an alligator. Probability of aggregation (*p.a*; center columns) is the probability of being able to determine an alligator's age or specific size class, conditioned on its detection. Probability of classification (*p.c*) is the probability of assigning an alligator to a specific size class, conditioned on successful aggregation. All estimates are from the G93 population model.

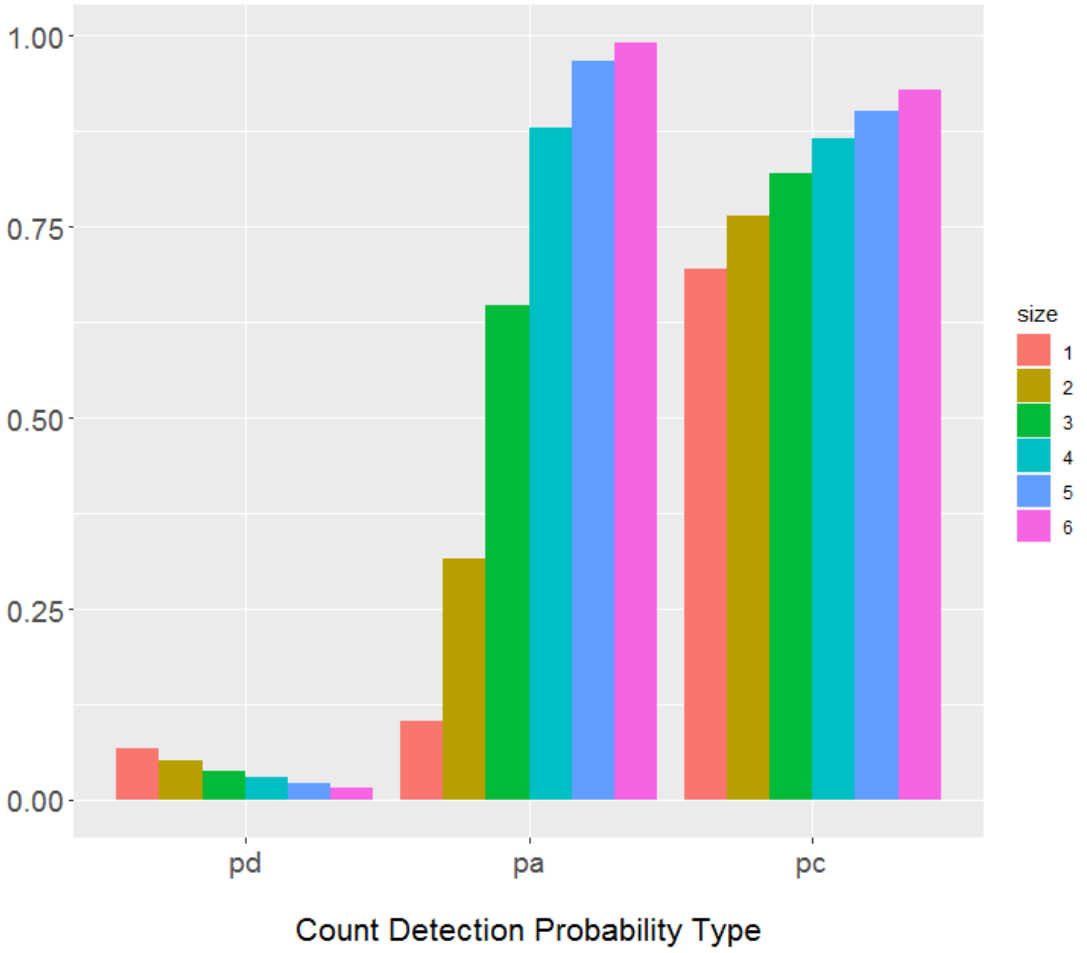

Figure 2.6. Effects of (a.) relative water level and (b.) water temperature on size class-specific detection probability ($p.d_{j,k,t}$) of American alligators (*Alligator mississippiensis*) observed during nightlight surveys in coastal South Carolina, USA (2011–2016). We used water level data (± 0.01 ft) recorded by a stream gauge every 15 minutes during all nightlight surveys, and we z-standardized data values within each survey route. Therefore, relative water level on the x-axis in (a.) reflects the z-standardized values of the maximum range in water levels observed on a single river during May 1st–August 21st across all years of the study at mean temperature (28.6°C).

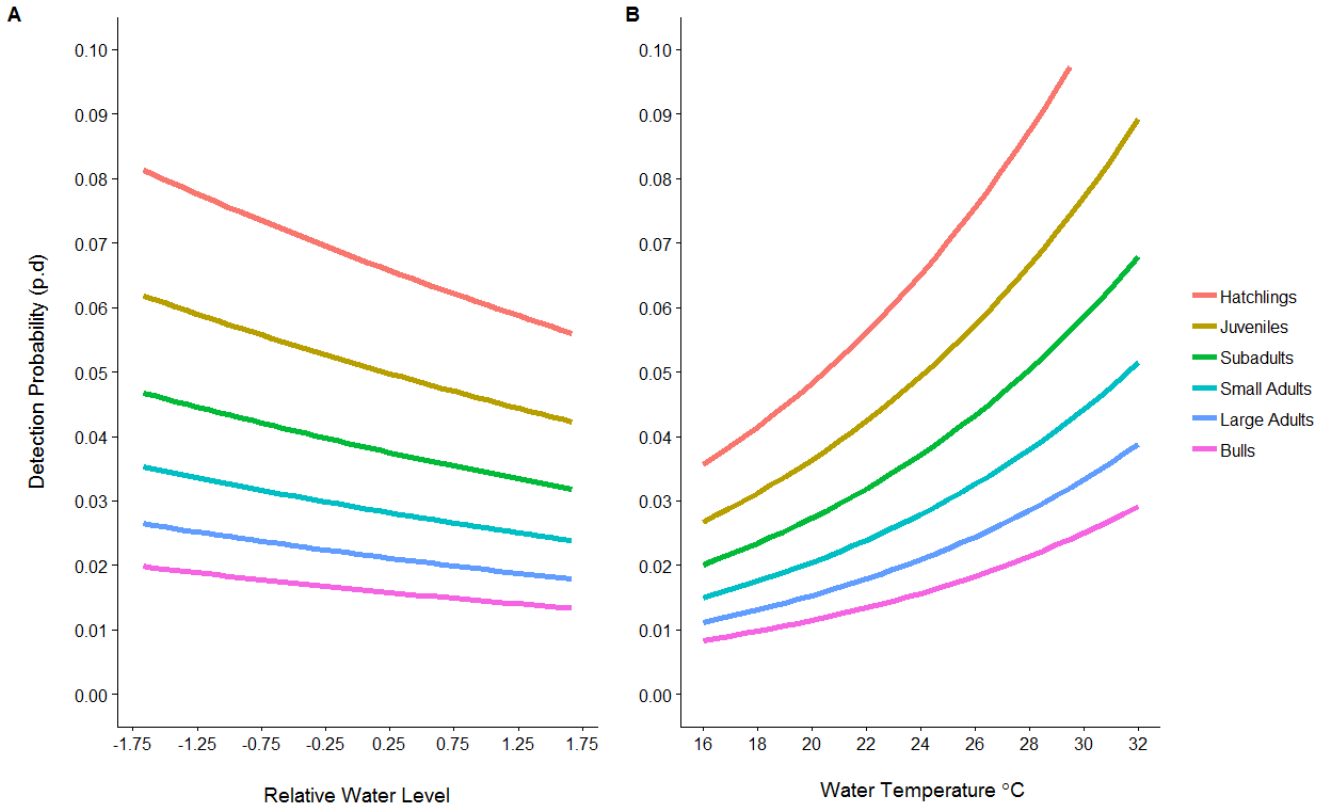

Figure 2.7. Total American alligator (*Alligator mississippiensis*) abundance (all size classes) on the Great Pee Dee and Waccamaw River (top panels) and South Santee River (bottom panels) surveys from 2011–2016. Abundance estimates were produced under three integrated population models: (1) G93 (left column); (2) R93 (center); and (3) R79 (right). The dark gray shaded area represents the 95% Bayesian credible interval (CRI).

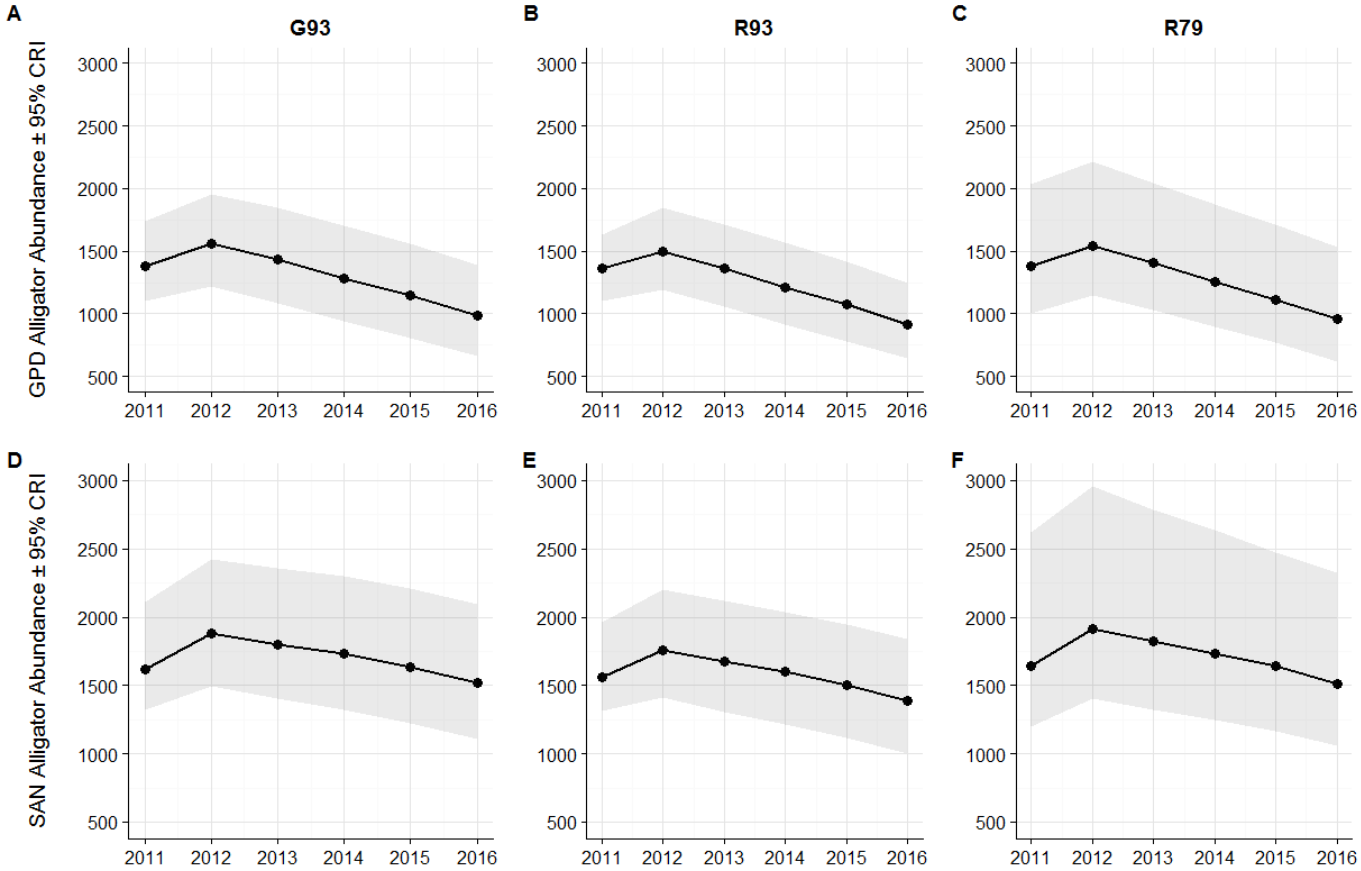

Figure 2.8. Size class-specific American alligator (*Alligator mississippiensis*) abundance estimates from nightlight survey counts on the Great Pee Dee and Waccamaw Rivers (left panels) and the South Santee River (right panels) from 2011–2016 in coastal South Carolina, USA. The top panels (a, b) show abundance estimates for immature size classes (closed points; 1–3) and the bottom show adult size classes (open points; 4–6). The error bars represent 95% Bayesian credible intervals. All size class estimates were produced by the G93 integrated population model.

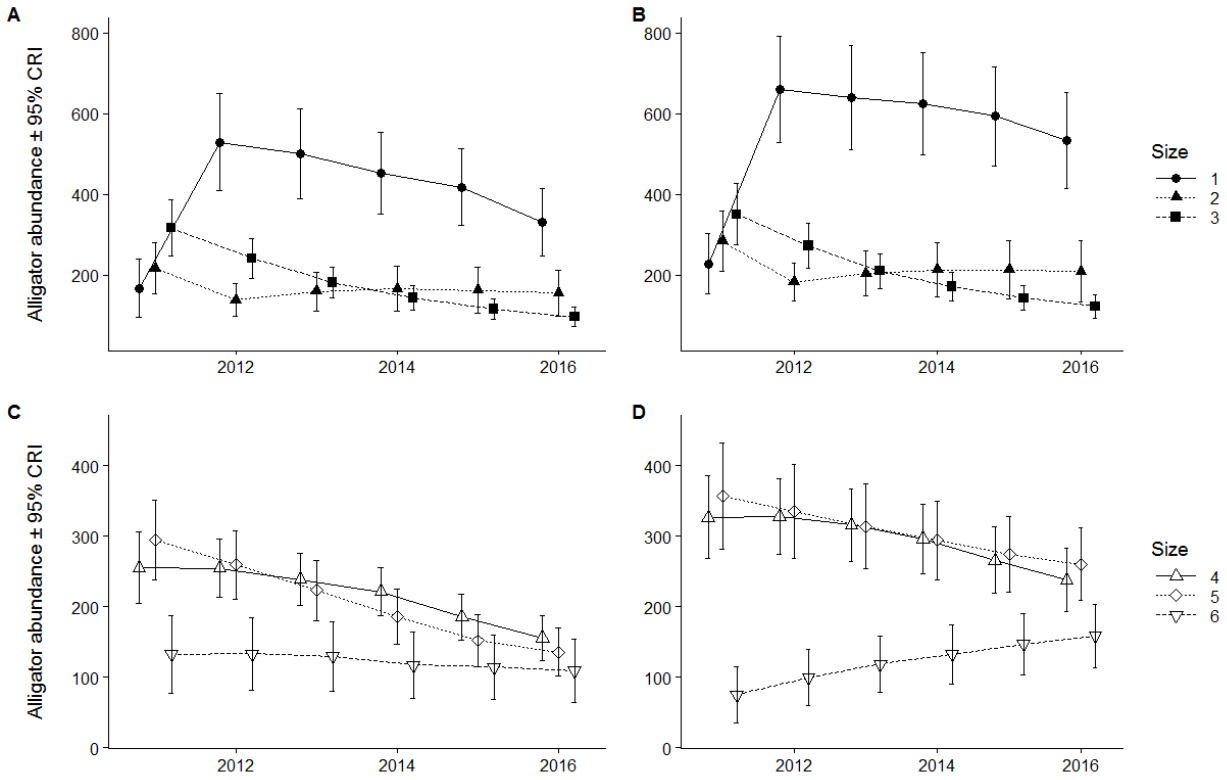

CHAPTER THREE

OPTIMIZATION OF SURVEY DESIGN FOR A CRYPTIC APEX PREDATOR TO REDUCE UNCERTAINTY IN CONSERVATION DECISION-MAKING

Abstract

Robust monitoring programs are the backbone of effective decision-making in wildlife population management. Reliability of monitoring data is heavily influenced by study design components including spatiotemporal replication of surveys, population characteristics (e.g., density, harvest pressure), and detection probabilities. Following 50 years of closure, the state of South Carolina, USA, re-opened populations of American alligator (*Alligator mississippiensis*; hereafter alligator) to harvest on public lands in 2008. Substantial uncertainties existed as to how local factors may influence the reliability of abundance estimates intended to inform harvest quotas. We simulated alligator population dynamics under nine scenarios across a range of population density and harvest rates. We generated count data based on expected detection probabilities specific to South Carolina, from nine different survey designs that differed in spatial and temporal replication. The count data were analyzed in an *N*-mixture model and used to identify an annual harvest quota. Our goal was to evaluate tradeoffs in temporal and spatial replication, given initial population density and harvest rate, and to identify an optimal monitoring design based on two fundamental objectives: maximizing financial effectiveness and minimizing ecological and management uncertainty. We quantified these objectives with multiple criteria including survey effort, changes to stage class

proportions, and abundance estimate bias and precision. In general, the reliability of abundance estimates was more sensitive to temporal replication, rather than spatial, and the *N*-mixture models routinely overestimated abundance; both of which could be attributed to the inherently low detection probability. Population declines induced by overestimating abundance were mostly reflective of a substantial reduction in two of the three adult stage classes. Our analysis illustrates the power of simulation-based approaches to evaluate tradeoffs in survey designs and how survey designs may interact with intrinsic factors (population density, management actions) in stage-structured populations.

Introduction

Monitoring the state of a population, community, or ecosystem is of fundamental interest to ecologists and conservation practitioners (Yoccoz et al. 2001). Monitoring data can be used to identify long term trends (Mosnier et al. 2015, Sedinger et al. 2017), generate hypotheses to test ecological theory (Cremer et al. 2018), and inform conservation or management decisions (Link et al. 2003, Lindenmayer et al. 2012). The ability of a management decision or action to achieve a desired outcome can be limited due to partial observability of the system which, in turn, determines the ability of the monitoring data to produce unbiased and precise (i.e., reliable) estimates of latent quantities (Kendall and Moore 2012). The reliability of monitoring data is ultimately determined by the design of the monitoring program itself which may consider aspects such as temporal and spatial replication, inter-observer variability, or detectability

(Williams et al. 2002, Moore and Kendall 2004, Shirley et al. 2012). Assessing whether a monitoring program is designed to provide sufficiently unbiased and precise estimates of latent quantities (e.g., abundance) to achieve the desired level of certainty associated with a decision or management outcome should occur prior to monitoring, though it often is evaluated after implementation (Martin et al. 2007).

One of the primary issues affecting the reliability of monitoring data is the assessment of detectability during sampling (Moore and Kendall 2004, Guillera-arroita et al. 2010). Index-based approaches that assume constant detectability are poorly situated to inform management decisions because their assumptions are rarely validated, and factors that affect the state (i.e., ecological) and detection processes may be confounded (Nichols et al. 2000, Anderson 2001, Yoccoz et al. 2001). However, monitoring programs designed for use in abundance estimation frameworks that adjust for imperfect detection (e.g., *N*-mixture models; Royle 2004) are not immune to producing unreliable inference. For example, insufficient spatiotemporal replication of surveys can generate positive relative-bias (i.e., overestimation) in abundance estimates, particularly if the target being monitored has low detectability (Williams et al. 2002). Similarly, extensions of abundance estimators that incorporate additional complexities such as open populations (Dail and Madsen 2011), stage-structure (Zipkin et al. 2014b), or imperfect state-assignment (Zipkin et al. 2014a) typically require additional spatiotemporal replication for unbiased estimation. The necessary level of demographic resolution (e.g., stage-specific abundance vs. total individuals) in the data and model complexity, however, is ultimately determined by the management objectives (Nichols and Williams 2006).

Data simulation is a powerful tool to evaluate how tradeoffs in the design and implementation of monitoring programs, including spatiotemporal replication, demographic resolution, and the models used to analyze monitoring data may influence the effectiveness of management decision-making, by reducing partial observability, structural uncertainty, or both (Zurell et al. 2010, Kendall and Moore 2012, Kéry and Royle 2016). By simulating data, the true values of the latent quantities can be generated from probability distributions with known parameters. The "true" latent quantities are simulated from an underlying ecological model, and are then virtually surveyed by a specified monitoring program design. The virtual monitoring data (e.g., counts) are then fed into a statistical model to produce estimates that are compared against the underlying virtual population (i.e., truth) to assess quantities such as relative bias and variance of the parameter estimates. Data simulation may be particularly beneficial for decision-making about rare or cryptic species that are difficult to sample, occur at low densities, or have low detectability ("Using Multiple Methods to Assess Detection Probabilities of Forest-Floor Wildlife" 2011, Mcintyre et al. 2012, Couturier et al. 2013). Similarly, in stage-structured populations, both detectability and vital rates may vary substantially among life stages (Unger et al. 2013, Crouse et al. 2016, Lawson 2019), and in such cases data simulation also can be an effective tool to assess monitoring strategies.

We implemented a simulation approach to evaluate potential tradeoffs in the design of a monitoring program for American alligators (*Alligator mississippiensis*; hereafter alligator). Specifically, we considered the interaction of the spatiotemporal replication of the monitoring program with an ecological attribute, initial population density, and a

management-focused attribute, harvest rate. Modified vital rates for alligators were used to simulate stage-structured dynamics under varying initial population densities, harvest rates, and survey designs. We virtually sampled the population by generating count data based on the specified true abundance of the underlying population and expected detection probabilities, then used an *N*-mixture model framework (Royle 2004) to analyze the simulated counts. We simulated annual harvest over a twenty-year period by setting a harvest quota based on the abundance estimate output from the model, and we distributed the quota across stage classes of the simulated population.

We then used a decision analytic framework to quantify the model output for each survey design and for every initial population density and harvest scenario. We did so based on objective criteria to maximize financial effectiveness of conducting surveys and to minimize ecological and management uncertainty, given that a monitoring plan met an eligibility criterion of low extinction risk. Specifically, we quantified a suite of biological parameters, including population growth, extinction probability, and changes in stage (stage class) proportions. We also quantified the effect of the survey design on the bias and precision of the estimates, and an index of survey effort (i.e., cost).

Methods

Case Study

Our study is focused on the population of alligators occupying coastal South Carolina, USA. The range for alligators in coastal South Carolina is comprised of diverse aquatic habitats including artificial (diked) wetlands, coastal marsh, wooded swamp,

rivers, and ponds. South Carolina is the approximate northern limit at which alligator densities are comparable to those in Florida and Louisiana, regions regarded as having highly productive alligator habitat (Woodward and Moore 1990, Lawson 2019). Alligators in South Carolina are managed under nuisance removal (by euthanasia) and harvest programs on private (initiated 1995) and public (2008) lands. Annual take by the nuisance removal and harvest programs on private lands are either not quantified or not publicly available. Since its inception, the South Carolina Department of Natural Resources (SCDNR) public harvest program has administered a fixed annual statewide quota of 1,000–1,200 alligator tags, in which one tag permits the harvest of a single alligator ≥122 cm total length (TL; distance from snout to tail tip) (SCDNR 2017). Given the fixed nature of SCDNR's harvest quota system, maximizng the number of alligators in the population serves as a proxy for maximizing the number of harvested alligators.The initial quota was assumed to represent 1% of the total statewide population, based on a consensus-estimate among local alligator biologists in the 1970s of 100,000 non-hatchling alligators (Bara 1975, P.M. Wilkinson, pers. comm.) that is still in use despite extensive changes to consumptive use policies (Rhodes, 2002; SCDNR, 2017). However, in recent years the popularity of the alligator harvest has exceeded the available tags (SCDNR 2017); in which only hunters drawn by the lottery (limit: 1 lottery ticket per hunter) may purchase one tag. Furthermore, the funding structure for the SCDNR public harvest program is relatively unique—revenue generated through the sale of lottery tickets, hunting licenses and tags directly supports alligator research and monitoring within the state (e.g., Lawson 2019), as well as administration of the harvest

programs. Thus the ability of the funding structure to support monitoring programs of high intensity (i.e., high spatiotemporal coverage) positively scales with the size of the harvest, which itself, if under a fixed rate of harvest, increases with overall abundance of alligators available for harvest

In 2011, SCDNR initiated a standardized monitoring protocol for boat-based nightlight surveys on rivers and lakes (description in Chapter 2). From early May to mid-August each year (prior to most hatchling emergence and the harvest season), temporally replicated surveys were conducted on each route (water body), though the number and duration between replicates varied depending on the year and survey route. Though the annual harvest quota has been held constant since 2014, SCDNR intends for survey data to be used to produce estimates of annual abundance needed to inform time-varying management decisions (e.g., harvest quotas). However, uncertainties exist regarding how to optimize the design of the monitoring program to reduce the uncertainty in the outcome of harvest decisions, given the expected detection probabilities for the survey protocol and alligator densities observed in South Carolina.

To evaluate potential tradeoffs in the design of nightlight surveys, we simulated growth, abundance assessment, and harvest of a theoretical alligator population. We conducted simulations across 81 scenarios that differed in gradation of four main attributes (Table 3.1). One attribute, initial population density, reflected a biological state that potentially affected performance of alternative sampling designs. From a fixed starting density, the simulated population was projected through time, and its density was estimated annually based on simulated count data arising from a given survey design.

Thus, annual population density was measured imperfectly in the simulations. Initial population densities (number of alligators per replicate survey unit) were based on observed densities in South Carolina (Chapter 2). The second attribute, harvest rate (fraction of the total population removed by harvest), was controlled by managers, but its degree of control in simulations was affected by measurement error of population density, resulting in disagreement between apparent harvest rate (fraction of estimated abundance harvested) and realized harvest rate. Harvest rates were set as ± 0.5% of the current putative rate of 1% (i.e., 0.5%, 1%, and 1.5%) (SCDNR 2017, Lawson 2019).

The last two attributes, number of sites (spatial replicates) and number of temporal replicates (visits), were perfectly controlled by managers and constituted the alternative survey design variables. For this analysis we defined "site" as a 0.5-km segment within a river-based survey route. This distance represents an estimate of maximum daily movement and was also used in previously published *N*-mixture analyses for alligators (Fujisaki et al. 2011, Waddle et al. 2015). For the current SCDNR monitoring program, each river survey route (n=10) is approximately 16 km in length (16.5 ± 3.3 SD, range: 10.3–19.4 km), resulting in 32 sites per route. As such, the intermediate number of sites (Table 3.1) is approximately equivalent to 10 river survey routes and represents SCDNR's current spatial coverage. To provide a geographic context for number of sites (i.e., sampling frame), we determined that the intermediate number of sites represents approximately 4% of the available habitat in rivers and large creeks (8,000 sites total) in South Carolina based on the flowline layer in the U.S. National Hydrography Dataset. Finally, the number of temporal replicates (i.e., the number of times a route is surveyed

within a year) was chosen based on assessing effort from previous studies, which range from two (Fujisaki et al. 2011, Waddle et al. 2015) to three (Gardner et al. 2016), and from monitoring efforts in South Carolina, which range from two to eight (Chapter 2). Though the values used to parameterize our simulation scenarios were chosen from empirical data and management practices specific to alligator populations in South Carolina, the framework we used is generalizable to other crocodilian populations or to other size or age-structured species. All statistical analyses were performed in the R statistical program (R Core Development Team 2017).

Population Simulation

Projection matrix construction.— We constructed a size-structured (six size stages), Lefkovitch matrix (Caswell 2001) to project alligator population dynamics for both sexes over an annual time step. The model structure reflects a hypothetical post-breeding/pre-harvest census, which contrasts with the timing of the pre-breeding census currently used in South Carolina. The existing pre-breeding census conducted by SCDNR is timed to minimize violations of demographic closure by completing the final replicate surveys before hatchling emergence (late August) and initiation of the private- and public-harvest seasons (mid-September). In contrast, the monitoring design in our simulation reflects an idealized scenario in which the number of individuals to be immediately exposed to harvest in the current year can be estimated and used to determine the current year's harvest quota.

Alligators exhibit substantial inter-individual variation in growth patterns (Wilkinson et al. 2016), and reproductive maturity is dependent on body length, rather than age (Joanen and McNease 1980, Wilkinson 1983). Therefore, each stage class (j) was defined by TL as follows: (1) Hatchling: ≤ 30 cm; (2) Juvenile: 31–121 cm; (3) Subadult: 122–182 cm; (4) Small Adult: 183–243 cm; (5) Large Adult: 244–304 cm; or (6) Bull: ≥ 305 cm (Table 3.2). Any surviving individual entering the time step may remain in the same stage class or transition (grow) to the next sequential stage class during each time step. Thus, growth rate (G_j) represents the combined probability of both surviving and transitioning to the next stage class, whereas retention rate (P_j) is the combined probability of surviving and remaining in a stage class. We defined the G_j and P_j elements of the projection matrix as follows:

$$P_j = \varphi_j * (1-\psi_j) \quad (3.1)$$

$$G_j = \varphi_j * \psi_j \quad (3.2)$$

From t to t+1, φ_j is the probability of an individual in stage j surviving, and ψ_j is the probability of an individual transitioning (i.e., growing) from stage j to j+1. We parameterized the stage-specific G_j and P_j rates using apparent survival (φ_j) and growth transition (ψ_j) probabilities from an integrated population model for alligators in South Carolina that used an identical stage class structure (Chapter 2). Because our projection model lacked sex-specificity, we calculated the weighted means for each ψ_j based on the proportion of each sex (Table 3.2) in the departure stage (i.e., the stage an individual is in at the beginning of an interval).

In our model, hatchling production was determined by number of females from small adult and large adult stage classes only, as females are not capable of breeding until they reach 183 cm TL and rarely exceed 305 cm TL (bulls) (Joanen and McNease 1980). We defined fecundity as:

$$F_j = BP * CL * NS * FP_j \quad (3.3)$$

in which *BP* is average female breeding probability, *CL* is average clutch size, *NS* is average probability that at least one egg in a nest hatches, and FP_j is average proportion of females in stage class *j* (Table 3.2). Components *BP*, *CL*, *NS*, and FP_1 (average proportion of hatchlings that were female) of F_j were estimated from alligator nesting studies in South Carolina (Wilkinson 1983, Rhodes and Lang 1996), and female proportions for non-hatchling stage classes were estimated from an experimental harvest study in Florida (Woodward 1996). See Appendix A2 for expanded field methodology descriptions and sample sizes for each variable.

Perfect information simulation.— We conducted simulations of a statewide population subject to harvest under perfect monitoring information (PI; detection probability = 1.0) of abundance to provide a theoretical maximum of alligators that could be produced. This maximum served as a standard for comparison against alternative conditions of imperfect detection, reflected across the 81 simulation scenarios. As an initial step, we required that the projection matrix produce an increasing population in the absence of harvest; i.e., we required a value >1 for the dominant eigenvalue, λ, of the matrix. We chose to focus on the linkage between monitoring program designs and

management actions (i.e., harvest) which would be absent from a no-harvest scenario, therefore, the imperfect detection simulations did not include a 0% harvest rate.

The projection matrix we initially parameterized (using values in Table 3.2) yielded a declining population under absence of harvest (0.98). In an earlier iteration of our simulation framework, before the survival probabilities in Lawson (2019) were available, we used five-stage alligator population projection matrices described in Dunham et al. (2014) to determine the minimum λ value ($\approx$1.015) needed to sustain a population under any of the three harvest rates (Table 3.1) under PI. Though the survival probabilities in Lawson (2019) accounted for the effects of the public harvest, they did not account for the private harvest and for the nuisance removals and thus may have been lower than expected under non-harvest conditions. To account for this potential bias and ensure that the projection matrix met the minimum λ threshold for harvest sustainability, we conducted an elasticity analysis to identify which elements of the projection matrix would produce the largest proportional change in λ (i.e., the most elastic). Retention rate P_4 was the most elastic element followed by P_5 and P_3 (Table B1.1); we then incrementally increased φ_j within the P_j and G_j terms for stages 3–5 (bold values in Table 3.2) until the projection matrix produced a $\lambda \geq 1.015$. We used the *popbio* package (Stubben et al. 2016) to conduct an elasticity analysis and estimate λ.

We conducted 12 PI simulations for combinations of three initial population densities and four harvest rates (including a no harvest scenario), as well as 81 imperfect detection simulations for the three initial population densities, harvest rates (0% harvest not considered), temporal replicates, and spatial replicates (Table 3.1). For all population

simulations, we initialized (at time t = 1) each simulated alligator population density (d) at a stable stage distribution (the corresponding eigenvector of the dominant eigenvalue of the projection matrix; Table 3.2). We selected initial abundance in each stage class, $n_{j,d,1}$, so that the sum of all stage class abundances divided by the full sampling frame of 8,000 sites equaled the specified population density per site:

$$d = \frac{\sum_{j=1}^{6} n_{j,d,1}}{8{,}000} \tag{3.4}$$

in which d is equal to the simulated density level (10, 30, or 60 alligators per site; Table 3.1) at t=1. For the no-harvest PI scenario the vector of stage-specific abundances at each time step t was then multiplied by the projection matrix (**L**) to produce abundances at the next time step:

$$\begin{bmatrix} n_{1,d,t+1} \\ n_{2,d,t+1} \\ n_{3,d,t+1} \\ n_{4,d,t+1} \\ n_{5,d,t+1} \\ n_{6,d,t+1} \end{bmatrix} = \begin{bmatrix} P_1 & 0 & 0 & F_4 & F_5 & 0 \\ G_1 & P_2 & 0 & 0 & 0 & 0 \\ 0 & G_2 & P_3 & 0 & 0 & 0 \\ 0 & 0 & G_3 & P_4 & 0 & 0 \\ 0 & 0 & 0 & G_4 & P_5 & 0 \\ 0 & 0 & 0 & 0 & G_5 & P_6 \end{bmatrix} \times \begin{bmatrix} n_{1,d,t} \\ n_{2,d,t} \\ n_{3,d,t} \\ n_{4,d,t} \\ n_{5,d,t} \\ n_{6,d,t} \end{bmatrix} \tag{3.5}$$

For the simulations that incorporated a harvest rate, we then determined the annual harvest quota ($H_{d,r,t}$):

$$H_{d,r,t} = \sum_{j=1}^{6} n_{j,d,t} \times r \tag{3.6}$$

in which $H_{d,r,t}$ in Eq. 3.6 is the total number of individuals to be harvested for a given initial density, harvest rate, and year. Note that the harvest quota includes the sum of individuals from all stage classes, whereas SCDNR harvest regulations only permit the

take of alligators ≥122 cm TL ($j \geq 3$). To accommodate the harvest of only legal stage classes, the harvest rates (r) in our model reflects the proportion of individuals from all stage classes (j: 1–6) that is equivalent to a desired harvest rate of harvestable stage classes ($j \geq 3$) at a stable stage distribution. For example, 0.5% of the individuals in harvestable stage classes is equivalent to 0.14% of the total population based on the stable stage distribution of **L** (Table 3.1). For ease in reporting, when referencing harvest rates in the text explicitly we will use the values that are in relation to the harvestable stage classes (e.g., 0.5%, 1.0%, 1.5%) rather than the total population (Table 3.1), though the latter quantity is what was used in the model. Note that translation of harvest rates to the total population at each time step (both PI and imperfect detection) relied on use of this invariant stable stage distribution despite change in the underlying stage distribution over the course of the simulation. Therefore, PI represents a theoretical situation in which abundance can be perfectly observed, but the size-class specific abundances are unknown for the purposes of implementing harvest, though those quantities are available in the simulation for heuristic purposes. Our decision to treat the stage distribution as a latent quantity in PI was based on an expert consensus that adjustments to a monitoring program were unlikely to produce meaningful improvements in ability to assign individuals to stage classes due to extreme alligator wariness and habitat structure, but that the total individual estimates could be improved upon (A. Lawson, umpubl. data).

In order to ensure that the annual harvest quota ($H_{d,r,t}$) was only applied to harvestable stage classes, we created the vector, **hsp**, to specify the proportion of the harvest quota that would be applied to each stage class:

$$\mathbf{hsp} = \begin{bmatrix} 0.00 \\ 0.00 \\ 0.04 \\ 0.30 \\ 0.40 \\ 0.26 \end{bmatrix}$$

in which the first two elements of **hsp** ensure that 0% of the total number of individuals to be harvested will come from $j \leq 2$. Additionally, either because of selectivity by hunters, availability to hunters, or both, alligators are not harvested in proportion to their abundance among stage classes. Therefore, the remainder of **hsp** reflects the average proportion of alligators harvested from stage classes $j \geq 3$ based on SCDNR public harvest records from Georgetown County, South Carolina (2008–2017), the focal county of the Lawson (2019) integrated population model. Next, to determine the number of individuals to be harvested from each stage class ($h_{j,d,t}$), **hsp** is multiplied by the annual harvest quota:

$$\begin{bmatrix} h_{1,d,r,t} \\ h_{2,d,r,t} \\ h_{3,d,r,t} \\ h_{4,d,r,t} \\ h_{5,d,r,t} \\ h_{6,d,r,t} \end{bmatrix} = \mathbf{hsp} \times H_{d,r,t} \tag{3.7}$$

In the final step, the $h_{j,d,r,t}$ vector is subtracted from the $n_{j,d,r,t}$ vector and then multiplied by the projection matrix **L**:

$$\begin{bmatrix} n_{1,d,r,t+1} \\ n_{2,d,r,t+1} \\ n_{3,d,r,t+1} \\ n_{4,d,r,t+1} \\ n_{5,d,r,t+1} \\ n_{6,d,r,t+1} \end{bmatrix} = \mathbf{L} \times \left(\begin{bmatrix} n_{1,d,r,t} \\ n_{2,d,r,t} \\ n_{3,d,r,t} \\ n_{4,d,r,t} \\ n_{5,d,r,t} \\ n_{6,d,r,t} \end{bmatrix} - \begin{bmatrix} h_{1,d,r,t} \\ h_{2,d,r,t} \\ h_{3,d,r,t} \\ h_{4,d,r,t} \\ h_{5,d,r,t} \\ h_{5,d,r,t} \end{bmatrix} \right) \tag{3.8}$$

Imperfect detection simulations.— The dynamics described in Eqs. 4–8 represent a PI scenario in which the total number of individuals to harvest each year ($H_{d,r,t}$) to achieve a target harvest rate is determined without error because the population is perfectly observed (i.e., the count is a true census). In practice, detection probability (p) is typically < 1, and hence abundance is imperfectly observed during a survey. Consequently, $H_{d,r,t}$ must be calculated from an abundance estimate rather than a true or known value. A major advantage of data simulation is that true abundance (N) is known and can be compared to abundance estimates (N') produced from a model that uses count data simulated under different survey designs or values for p.

We used the *simNmix* function in the *AHMbook* package (Kéry and Royle 2016) to simulate non stage-specific count data for each of the 81 scenarios. Data were based on the number of sites, number of temporal replicates, mean p (Chapter 2), and N (density in Table 3.1; Chapter 2). The p estimates reported by (Chapter 2) were negatively influenced by stage class and water level, and positively influenced by water temperature. To match the lack of stage class-specificity of the simulated count data produced from *simNmix*, we collapsed the detection probability estimates from Lawson (2019) by calculating the weighted mean of the size-specific detection probabilities (range: 0.02–0.07 at mean water level and temperature), using the stable stage class distribution of **L**

as weights. The weighted mean *p* was not updated throughout the simulation based on the relative proportions of each stage class. However, to add stochasticity to our simulations reflecting variability in detection during nightlight surveys due to temporally varying stage class composition and environmental conditions, and we used the weighted mean and weighted standard deviation*1.15 to derive beta distribution parameters *a* and *b*. For every time step, *p* was then sampled from a beta distribution and subsequently used within the *simNmix* function.

The simulated count data produced by *simNmix* were then fed into an *N*-mixture model (Royle 2004) using the *pcount* function in the *unmarked* package (Fiske and Chandler 2011). *N*-mixture models use spatiotemporally replicated count data to estimate the mean number of individuals per site *s* in year *t*, $N'_{s,t}$, and detection probability (p'):

$$c_{s,k,t} \sim \text{binomial}(\tilde{N}_{s,t}, p'_{k,t}) \quad (3.9)$$

$$\tilde{N}_{s,t} \sim \text{Poisson}(N'_{s,t}) \quad (3.10)$$

such that $c_{s,k,t}$ in Eq. 3.9 is the number of individuals counted (detected) at site *s* during visit (temporal replicate) *k* in year *t*, and $\tilde{N}_{s,t}$ is true abundance as realized under the estimation model. In Eq. 3.10, true abundance at site *s* in year *t* is Poisson distributed with the mean-variance parameter, $N'_{s,t}$. We imposed no model structure (i.e., no survey or site covariates) on the $p'_{k,t}$ and $N'_{s,t}$ terms, and set the upper integration parameter for the likelihood function (*K*) to 1000, which represents a maximum mean site abundance (density) value.

To fully evaluate the effects of the design of a monitoring program on population viability, we linked the outcome of the *N*-mixture model estimates to the underlying virtual population (i.e., true abundance) through the following equation:

$$H_{d,r,m,l,t} = (N'_{d,r,m,l,t} \times 8{,}000) \times r \tag{3.11}$$

in which $N'_{d,r,m,l,t}$ is the estimate of $N_{s,t}$ (mean abundance in year *t* for site *s*), from a survey design with *m* temporal and *l* spatial replicates, in a population with *r* harvest rate and *d* initial density. Note that in Eq. 3.11 *r* reflects the apparent harvest rate, and we have removed the site (*s*) indexing because our *N*-mixture model did not incorporate site effects, and site-level abundance is extrapolated to a statewide estimate by multiplying by the total number of sites. The annual harvest quota, $H_{d,r,m,l,t}$, and the harvest taken from each stage class, $h_{j,d,r,m,l,t}$, are calculated exactly as outlined in Eq. 3.6–3.7, except that the quantities are based on estimated abundance (*N*′) rather than true abundance (*N*). Similarly, as in Eq. 3.8, the harvests $h_{j,d,r,m,l,t}$ are deducted from the true number of individuals in each stage class $n_{j,d,r,m,l,t}$, and the associated vectors are multiplied by the projection matrix **L** to produce the true number of individuals for each stage class in year *t*+1. Therefore, the realized harvest rate $(\hat{r})$ for a scenario is obtained by dividing the sum of $h_{j,d,r,m,l,t}$ by the sum of $n_{j,d,r,m,l,t}$ in Eq. 3.8. The process just described is then repeated beginning with Eq. 3.4 which is used to update the true mean abundance per site (density) and is then fed into the *pcount* function to simulate survey data for year *t*+1. For each of the imperfect detection scenarios, we conducted 100 simulations over 20 years.

Monitoring program design decision analysis

The selection of an optimal monitoring program design ultimately depends on the management objectives. For each initial population density and harvest rate scenario (n=27), we implemented a multi-step process to evaluate each of the nine potential designs for the monitoring program (3 temporal replicate levels x 3 site levels). First, we imposed constraints that the monitoring program had to have an associated extinction percentage $\leq 5\%$ and $\lambda \geq 0.98$ to be considered. These constraints were meant to eliminate monitoring plans that could put the alligator population at a relatively higher risk of a steep population decline and perhaps spurring intensive and expensive management interventions for recovery (e.g., harvest closure, reintroduction). Given that a plan was able to meet these constraints, we identified two fundamental objectives on which to evaluate the remaining potential monitoring program designs: (1) maximize financial effectiveness, and (2) minimize ecological and management uncertainty. We selected these two broad fundamental objectives because they reflect a common tradeoff that management agencies are often faced with: developing a management strategy that reduces partial controllability— the inability to achieve a desired management outcome— given limited financial resources.

The first fundamental objective, maximizing financial effectiveness, is the "efficiency" of a monitoring plan, based on minimizing costs (survey effort) and maximizing revenue (maximizing abundance and subsequent harvest potential). The second fundamental objective is comprised of two components, ecological and management, and is a measure of the plan's ability to reduce the uncertainty of management outcomes. We defined the ecological component as minimizing changes to

stage class proportions over 20 years. Alligators have highly complex, size-structured social systems (Lang 1987, J. Zajdel unpubl. data), and it is unknown how populations may respond to perturbations, such as harvest or artificial selection, that would cause changes to the size distribution. The management component of the second fundamental objective is a measure of a plan's ability to limit relative bias and improve precision of abundance estimates. We parameterized each fundamental objective with a series of means objectives— mechanisms by which the fundamental objective can be accomplished. We describe the constraints and means objectives, in turn:

Constraints.— To estimate extinction probability (*EP*), we summed the number of simulations in which total abundance (of all stage classes) had reached zero by the final year of the simulation. Because we conducted 100 simulations per scenario, the scenario-specific number of extinctions is reported here as a percentage. To parameterize our second constraint, we estimated λ based on the true total of individuals (all stage classes) in year 21 divided by total individuals in year 1. If the monitoring program within the density x harvest scenario had ≤ 5 simulations in which the population went extinct and $\lambda \geq 0.98$, it was eligible for consideration. For the latter constraint, we allowed plans that produced a slight negative growth rate to be considered in case there was a desire to reduce alligator densities (e.g., reducing human-alligator-conflict).

1a. Minimize survey effort.— We created an index of survey effort (*EF*), which is reflective of financial cost, for each potential monitoring program design (n=9) by multiplying the number of temporal replicates (m) by the number of spatial replicates (l):

$$EF = m \times l$$

in which smaller values of $EF_{m,l}$ reflect lower effort (i.e., less expensive) whereas larger values reflect higher effort (i.e., more expensive). Note that this index assumes that increasing the number of temporal or spatial replicates incurs the same financial cost.

1b. Maximize abundance.— The PI simulations represented a theoretical maximum for the size of alligator populations that could be produced for a given initial population density and harvest rate. Therefore, we evaluated the performance of each monitoring program based on the proportion of total individuals (all stage classes) remaining in year 21 (the outcome of the 20th harvest) relative to total individuals in year 21 under the PI scenario for the same population density and harvest rate:

$$MA_{d,r,m,l} = \frac{\sum_{j=1}^{6} n_{j,d,r,m,l,21}}{\sum_{j=1}^{6} PI_{j,d,r,21}} \tag{3.12}$$

We included the *MA* means objective within the financial effectiveness fundamental objective (FO_1) because revenue generated by the private and public alligator harvest programs is applied directly to the SCDNR alligator research and monitoring. Maximizing abundance is a proxy for the number of harvested alligators (for a set *r*), therefore maximizing both the total population size and the number of harvested alligators can increase available funds for monitoring.

2a. Minimize changes to stage class proportions.— We calculated the mean number of individuals in each stage class for each year across simulations for a given scenario and divided mean stage class-specific abundance by the total to obtain the proportion of individuals in each stage class (sp_j). Next, we computed the absolute value of the percent

change in each sp_j from t=1 (i.e., the stable stage distribution) to t=21. We then obtained the weighted mean of the percent change of absolute values using the stable stage distribution (i.e., relative proportions of each stage in year 1) for the weights. This produced a single estimate of changes in stage class structure ($SC_{d,r,m,l}$) for a given scenario:

$$SC_{d,r,m,l} = \sum_{j=1}^{6}\left(\left|\frac{sp_{j,d,r,m,l,21} - sp_{j,d,r,m,l,1}}{sp_{j,d,r,m,l,1}}\right| \times sp_{j,1}\right) \quad (3.13)$$

We acknowledge that our measure of changes in stage class proportions, $SC_{d,r,m,l}$, reflects both changes in *sp* that would occur under the $PI_{d,r}$ counterpart as well as those attributed to the specific monitoring design (*m*, *l*).

2b. Minimize relative bias.— For t = 1–20 (t=21 only contained true values) of every simulation *i*, we computed the relative bias between the estimated mean abundance per site $(N'_{d,r,m,l,t,i})$ from the *N*-mixture model (Royle 2004) and the true value $(N_{d,r,m,l,t,i})$:

$$RB_{d,r,m,l,t,i} = \frac{N'_{d,r,m,l,t,i} - N_{d,r,m,l,t,i}}{N_{d,r,m,l,t,i}} \quad (3.14)$$

We then averaged across simulations, and then across years to produce a scenario-specific mean relative bias $(RB_{d,r,m,l})$. All of the *RB* values we calculated were > 0.00 (i.e., overestimation), therefore we opted to use the raw relative bias scores rather than the absolute value.

2c. Minimize uncertainty.— We computed the standard deviation of the estimated mean abundance per site across simulations for every time step, and then computed the

overall mean of the standard deviations across years for each scenario as a measure of uncertainty ($UC_{d,r,m,l}$).

Objective weighting.— Within each of the nine initial density x harvest scenarios, we scaled each of the *k* means objective values from 0 to 1, in which 0 was the least optimal value observed, and 1 was the most optimal value observed. We used a different scaling formula, depending on whether the k^{th} means objective was minimized or maximized:

$$MO'_{k,d,r} = \frac{\max(MO_{k,d,r}) - MO_{k,d,r,i}}{\max(MO_{k,d,r}) - \min(MO_{k,d,r})} \tag{3.15}$$

$$MO'_{k,d,r} = \frac{MO_{k,d,r,i} - \min(MO_{k,d,r})}{\max(MO_{k,d,r}) - \min(MO_{k,d,r})} \tag{3.16}$$

Eq. 3.15 was used for means objectives to be minimized (*EF*, *SC*, *RB*, *UC*), where each value *i* for means objective *k* within initial density *d* and harvest rate *r* was subtracted from the maximum means objective value within the *d* x *r* scenario and the difference divided by the difference between the maximum and minimum values for that objective. Eq. 3.16 was used for *MA* only, as it was the only means objective that was maximized. Here, the numerator is the difference between the objective value and the minimum value observed, whereas the denominator is the same as in Eq. 3.15.

Within each initial population density and harvest scenario, plans that met the eligibility criteria were scored based on two weighted-sum formulas for each fundamental objective:

$$FO_{1,d,r} = (0.5 \times EF') + (0.5 \times MA'_{d,r}) \tag{3.17}$$

$$FO_{2,d,r} = (0.50 \times SC'_{d,r}) + (0.25 \times RB'_{d,r}) + (0.25 \times UC'_{d,r}) \quad (3.18)$$

For each fundamental objective within an initial density and harvest scenario, each scaled means objective value ($MO'_{k,d,r,i}$) was multiplied by an objective weight (sum of weights = 1) and summed together to derive the fundamental objective value (FO_k). The FO_1 means objectives, *EF* and *MA*, were weighted equally (Eq. 3.17), whereas half of the FO_2 weight was assigned to the "ecological uncertainty" means objective (*SC*) and the other half was distributed evenly between the two "management uncertainty" means objectives, *RB* and *UC* (Eq. 3.18). Lastly, we summed FO_1 and FO_2 within each initial density (*d*) and harvest (*r*) scenario (i.e., they were given equal weights). Therefore, for each harvest and initial density combination, the eligible monitoring plan with the highest $OP_{d,r}$ (Eq. 3.17) reflects the optimal plan:

$$OP_{d,r} = FO_{1,d,r} + FO_{2,d,r} \quad (3.19)$$

Results

The λ of the original projection matrix (**L′**) we constructed from the Lawson (2019) vital rates was 0.98; which was most elastic to retention of small adults (P_4; 0.317), large adults (P_5; 0.169), and subadults (P_3; 0.153). We increased the survival term within the growth and retention elements for each of these stages (Eqs. 1, 2) by 4% to produce the final projection matrix (**L**) that was used in the simulations (Table 3.2). Matrix **L** projected positive growth under absence of harvest (λ = 1.018), and it reflected the same elasticity order of elements as **L′**. Full output from the elasticity analyses and both stable stage distributions are provided in Appendix S1. As we required in our preliminary

modeling of **L′**, under the perfect information simulation, the projection matrix (**L**) produced positive population growth rates for the three harvest rates (Fig. 3.1) and harvest closure (0%)

In general, abundance trends appeared to be more sensitive to increases in temporal replication than site replication when harvest was based on imperfect observation of the population (Figs. 3.1, 3.2). All initial density x harvest (high/intermediate/low density x 0.5/1.0/1.5% hereafter) scenarios had at least one monitoring program design that met the eligibility criteria (Table 3.3). Both the number of eligible plans and λ varied negatively with harvest rate for a given initial population density, and both varied positively with initial population density for a given harvest rate (Table 3.3, Fig. 3.2b). High initial density x 0.5% yielded the most eligible plans (n=8) of the nine possible (Table 3.3c), whereas both low and medium initial density x 1.5% only had one eligible plan. The maximum λ we observed was 1.31 for high initial density x 0.5% at maximum survey effort (Table 3.3c) whereas the lowest (0.00) was for low initial density x 1.5% at minimal survey effort (Table 3.3a).

The raw (un-scaled) means objective values (*EF, MA, RB, SC, UC*) all showed slightly different relationships regarding variation with harvest rate (for a given initial population density) and initial population density (for a constant harvest rate; not explicitly stated hereafter) (Table 3.3, Fig. 3.2). Note that contrasting patterns among means objectives are expected, as the optimal values for *MA* are maximized, whereas the remainder (*EF, SC, RB, UC*) are minimized Increasing harvest rate resulted in increasing *EP*, whereas increased initial population density reduced *EP* (Fig. 3.2a), and the opposite

relationships were observed for λ. The highest *EP* we observed was 99 for low initial density x 1.5% with minimal survey effort, followed by 93 at 1.0% harvest rate at the same initial density and survey effort (Table 3.3a). However, all initial population density x harvest rate scenarios had at least two survey designs associated with an *EP* of zero (Table 3.3). As such, at high initial densities, the maximum *EP* observed was 2 for 1.5% harvest and minimal survey effort (Table 3.3c). All optimal plans (those having greatest value of OP among eligible plans within scenario; bold rows in Table 3.3) had an *EP* of zero.

Maximizing total alligator abundance (*MA*) as a proportion of the theoretical maximum under PI varied negatively with harvest rate and positively with initial density (Fig. 3.2c). Among optimal plans, *MA* averaged 0.91 ± 0.04 SD and ranged from 0.87 for low density x 1.0% harvest and 0.97 for high density x 0.5% harvest. When combined (Eq. 3.17) with the minimize effort (*EF*) means objective, which did not vary by harvest rate or initial density, FO_1 averaged 0.72 ± 0.09 and varied from 0.5 (low density x 1.5%) to 0.77 (intermediate density x all harvest) across optimal plans (Table 3.3).

Relative bias (*RB*) negatively varied with initial population density and positively varied with harvest rate (Fig. 3.2d) though the latter relationship was particularly weak for middle and high initial densities. Among optimal plans, *RB* averaged 0.64 ± 0.38 and varied from 0.33 (high initial density x 0.5%) to 1.54 (low initial density x 0.5%), in which lower values are more optimal. Across all initial density x harvest scenarios, *RB* ranged from 0.17 (high x 0.5/1.0% at maximum effort) to 92.77 (low x 1.5% at minimal effort), indicating that the models consistently overestimated abundance for all scenarios.

Weighted mean percent change in stage classes (*SC*) varied positively with harvest and negatively with initial density (Fig. 3.2e). Among optimal plans, *SC* averaged 0.02 ± 0.01 and varied from 0.01 (high/intermediate initial density x 0.5%) to 0.03 (all initial densities x 1.5%) (Table 3.3), in which lower values are more optimal. Abundance estimate uncertainty (*UC*) varied positively with initial density, and did not vary with harvest rate (Fig. 3.2f). Among optimal plans, *UC* averaged 80.83 ± 22.69 and varied from 37.82 (low density x 1.5%) to 105.15 (high density x 1.5%) in which lower values are more optimal. After combining the scaled means objective values (Eq. 3.18, FO_2 averaged 0.97 ± 0.03 and varied from 0.94 (high initial density x all harvest; low x 0.5%) to 1.0 (low/intermediate density x 1.5%) across optimal plans (Table 3.3). Finally, all nine optimal monitoring plans contained six replicate surveys and 320 sites (Table 3.3), with the exception of the low initial density x 1.5%, which selected six replicate surveys and 640 sites.

Discussion

Effective conservation decision-making necessitates a thorough assessment of how ecological, management, and survey-level attributes interact to influence the precision and accuracy (i.e., reliability) of monitoring data used to predict the outcomes of said decisions (Bunnefeld et al. 2011, Kendall and Moore 2012). We focused on how the reliability of alligator abundance estimates (N') used to set annual harvest quotas were influenced by survey effort (number of temporal replicates and sites), for varying gradations of initial population density and harvest. Increasing both temporal and spatial

replication improved the reliability of N' across all initial density and harvest scenarios (*RB*, *UC* in Table 3.3); though temporal replicates had a stronger influence than the number of sites (Figs. 3.1, 3.2). In contrast, Yamaura et al. (2016) reported that increasing the number of sites, rather than temporal replicates, improved the reliability of abundance and species richness parameters in community *N*-mixture models using simulated data. Multiple occupancy simulation studies indicate, however, that when detection probability is low (as in our study), increasing temporal replication will have a greater improvement on occupancy probability estimate precision and bias than increasing the number of sites (Tyre et al. 2003, Guillera-arroita et al. 2010, McKann et al. 2013, Sanderlin et al. 2014).

The greater sensitivity of N' reliability to temporal replication at low detection probabilities likely explains the uniform selection for maximum temporal replication across all optimal survey designs (Table 3.3). The mean detection probability estimate (0.05 ± 0.02 SD) we used to parameterize the beta distribution (to produce random values for each time step of a simulation) is from unreplicated within-year counts (Chapter 2), but is similar to other nightlight survey studies in which temporally replicated surveys were spaced at least two weeks apart (Fujisaki et al. 2011, Waddle et al. 2015). In contrast, Gardner et al. (2016) reported a 0.50 detection probability based on three replicate surveys conducted within one week. As such, detection probability of alligators appears to be negatively correlated with the interval between replicate surveys— more individuals are likely to enter or exit the survey unit as the duration between replicates increases which violates the geographic closure assumption and lowers the probability of

encountering a given individual (Chapter 2). The tradeoff between temporal and spatial replication appears to be a function of detection probability (Tyre et al. 2003, McKann et al. 2013); detection probability is, in turn, influenced by the time interval between replicate surveys, which is ultimately constrained by the duration of the primary occasion (i.e., the time period in which replicate surveys are conducted). For example, if the primary occasion duration is relatively long (e.g., months), additional temporal replicates beyond the maximum of six that we examined could continue to improve the precision and accuracy of abundance estimates. In contrast, a shorter primary occasion duration (e.g., one week) would necessitate a shorter time interval between replicate surveys and ultimately limit the number of replicate surveys that could be conducted. However if the shorter interval produced a higher detection probability, the reliability of N' could become more sensitive to the number of sites, rather than temporal replicates (Tyre et al. 2003, Royle et al. 2016).

The primary occasion sampling duration issue is an important caveat for the real-world application of our results. We simulated a post-breeding pre-harvest survey structure which is not currently feasible in South Carolina because the hatchling emergence period (mid-August through September) overlaps with harvest (mid-September to mid-October). In contrast, the detection probabilities and initial densities used to parameterize our simulation were derived from the single replicate survey with the highest number of detected alligators, of 2–8 replicate surveys conducted within the May—mid-August (pre-breeding) primary occasion sampling period each year (Chapter 2). As discussed, the detection probability estimates we used were consistent with other

studies that used a study design with a large duration between surveys (≥ two weeks) (Fujisaki et al. 2011, Waddle et al. 2015). That said, implementing any of the optimal survey designs, all of which selected six replicate surveys (Table 3.3), is highly unrealistic using the post-breeding pre-harvest structure that we simulated, regardless of the duration between replicate surveys. Though most nests have hatched by the end of September, alligators begin to reducing their daily movements and enter brumation approximately mid-October (A. Lawson, unpubl. data), further reducing their detectability during surveys due to increased usage of their winter dens, and likely reducing their availability for harvest. We acknowledge that the phenological limitations of a post-breeding pre-harvest survey structure represent a major limitation for application of our results.

We acknowledge two additional caveats associated with the post-breeding pre-harvest sampling structure used in our simulation. First, the temporal scale at which the count data were applied to inform harvest decisions is not a realistic representation of how monitoring data would likely be used by SCDNR. Specifically, the post-breeding pre-harvest surveys we simulated could not be used to set harvest quotas in the current year (as done in the simulations), as the harvest tag lottery opens on May 1 (SCDNR 2017), meaning that a dynamic harvest quota would need to be determined in advance, based on estimated abundance in the previous calendar year. Second, given the established effects of water level (negative) and temperature (positive) on detection probability (Chapter 2), our simulation assumed that these variables showed similar patterns in variation during pre-breeding pre-harvest surveys conducted in May through

mid-July (i.e., the period used to parameterize the simulation) and post-breeding pre-harvest surveys conducted in late-September through October (i.e., the period in which our simulated surveys would occur). In South Carolina, both water temperatures and levels are generally lower in spring and increase throughout the summer into fall (A. Lawson, unpubl. data). Therefore, given the counteractive effects of water level and temperature on detection probability, we posit that this assumption was generally met, though future iterations of this model should formally test this assumption.

Detection probability was a stochastic element in our simulation, as a new value was drawn from a beta distribution at each time step of each simulation. We inflated the variance around the mean ($0.05 \pm 0.02 \times 1.15\,\mathrm{SD}$) to reflect variable environmental conditions (water temperature and level) that would affect detectability during each survey. We used the weighted mean of the stage class-specific detection probabilities in Chapter 2— which negatively varied according to size (stage) class— based on the relative proportions of each stage class within the stable stage distribution of **L** (Table 3.1) to derive the mean detection probability to parameterize the beta distribution. However, detection probability was not updated to reflect the changing relative proportions of each stage class (Figs. 3.3, 3.4) at each time step. In general, the changes in stage class distribution followed a similar pattern— a decrease in the proportion of large adults and bulls that was compensated by an increase in subadults and small adults (Fig. 3.3). The combination of negative variation in detection probability across stage classes (Chapter 2) and smaller stage classes comprising a greater proportion of the population (Fig. 3.4) would create an overall increase in detection probability over time.

The magnitude of the change in detection probability would be driven by the change in *SC*, meaning that change in detection probability was negatively influenced by initial population density (e.g. Fig. 3.3a vs. 3.3c) and positively influenced by harvest rate (Fig. 3.2e). Therefore, the mean value of detection probability used in simulations was likely biased low and further explains the selection for temporal replication for the optimal survey design. Despite the potential issue in our approach, we note that the overall range in mean detection probability from bulls to hatchling reported in Lawson (2019) was relatively small (0.02–0.07), and the inflated variation we added to detection may have buffered our results from this potential bias to some extent.

Relative stage class proportions shifted over time for all imperfect detection (Figs. 3.3, 3.4) and perfect information scenarios (except no-harvest PI), indicating that imperfect detection was not the driving force of the changes. A more likely cause is that the adult stage classes ($j \geq 4$) were not harvested in proportion to their availability in the population (i.e., $\mathbf{hsd_j} > sp_j$; Table 3.2). Thus, it is important to emphasize that the virtual managers in both the PI and imperfect detection scenarios were not positioned to observe the changes in stage class proportions through the simulated monitoring data. Though the underlying, "true" alligator population contained stage-specific abundances for the entire statewide population, the simulated monitoring data reflected the mean number of alligators (of all stage classes) per site. We chose to simulate total individuals for the count data, as opposed to stage class specific abundances, as it was more reflective of SCDNR's monitoring efforts, in which 60% of the alligator observations are of unknown stage class (Chapter 2). Total number of individuals is also reflective of monitoring data

collected in Mississippi and North Carolina (Gardner et al. 2016, Strickland et al. 2018). That said, the annual harvest quota (H) was calculated based on the product of the apparent harvest rate (r) applied at the population level (Table 3.1), not just the harvestable stage classes, and the total population size (Eq. 3.6). This becomes problematic if changes to the relative stage class proportions occur, because proportion of harvestable stage classes ($j \geq 3$) within the total population becomes a fluctuating, latent quantity that is unobservable to managers, given the monitoring data structure. Put into context, at stable stage distribution, in which the relative stage class proportions are constant, a 1% apparent harvest rate of harvestable stage classes is equivalent to a 0.0028% harvest rate of the total population. If the proportion of harvestable stage classes within the population declines, the manager would be unable to detect the change, due to the lack of stage class-specific abundance estimates in the monitoring data. Therefore, continuing to implement a 0.0028% apparent harvest rate of the total population would result in a realized harvest rate that exceeds the apparent harvest rate of 1% of the harvestable stage classes (Fig. 3.5).

Both the true abundance of the total population (N; all stage classes) and the stage class proportions are treated as latent quantities within the imperfect detection scenarios. For the PI scenarios, N was perfectly observed (i.e., no need for estimation of N'), but we decided to treat the stage class distribution as a latent quantity for the purposes of setting a harvest quota. Therefore, a virtual manager within a PI scenario would know the true number of individuals within the population but would not be able to detect changes in the stage class portions. Despite extensive experimentation and modifications to

nightlight survey monitoring protocols, decreasing the number of unknown size observations below ~55% does not appear to be feasible in South Carolina riverine habitats (A- Lawson, personal communication). Therefore, we believed modeling *N* as a perfectly observed quantity and stage class proportions as a latent quantity under PI was reasonable and a more useful comparison to the imperfect detection scenarios.

The changes to stage class proportions, particularly the reduction of larger stage classes, highlights another potential weakness in our simulation. We used extinction probability (*EP*) for the total population as a constraint for selecting the optimal survey design, though this quantity may have been underestimated. In a post-hoc analysis, we computed the average extinction percentage for bulls for each population density and compared it to the extinction probability for the total population. Overall, the average *EP* for bulls was substantially higher compared to the *EP* for the total population at each initial population density (Bulls: 28 (L), 8 (I), 1.7 (H); Total: 22.1, 2.6, 0.1). Though increasing the initial population density reduced the overall *EP* for both groups, it increased the magnitude of the difference between them. This result is problematic because the harvest proportions (**hsp**) were not re-allocated following the extinction of a particular stage class. Consequently, under a simulation in which bulls went extinct, their absence was not compensated for by increasing the harvest proportion in the remaining stage classes. This implies that *EP* was likely underestimated— as increasing the proportional harvest in the remaining stage classes would have accelerated the population decline and increased *EP*. The extent of the impact of this scenario may be ameliorated, however, because our model assumed that hunter participation and hunter success were

both 100%. In practice, participation and success typically averages 86.3% and 65%, respectively (SCDNR 2017), meaning that we may have overestimated *EP* for the total population, potentially counter-acting the issue of not reallocating the harvest. Similarly, our decision to begin the simulation at the stable stage distribution of **L** also likely underestimated *EP* relative to current conditions within the alligator population of South Carolina, which has been subject to size-selective harvest for over a decade. Future improvements of this simulation could be improved by incorporating a dynamic rather than static harvest distribution step and potentially incorporating stochastic variables (sampled from a distribution) that reflect hunter participation and success.

Simulation-based approaches can provide a mechanistic understanding of why the outcomes of management actions, informed by imperfect monitoring data, do not match the expected trends under PI (Martin et al. 2011, Kendall and Moore 2012). Though the PI simulations indicated population growth was possible under all harvest rates, many of the underlying (true) population trajectories resulted in declines, particularly for relatively low survey effort (Fig. 3.1). The relative bias (*RB*) values indicated that the *N*-mixture models uniformly overestimated abundance (positive bias; Table 3.3). Even in the most ideal scenario (high density x 0.5% harvest), the optimal design had a substantial relative bias (0.33 in Table 3c). Both *RB* and *UC* increased with harvest rate and declined with population density and harvest rate. As an example in Fig. 3.6, under high initial population density at 1% harvest, the differences between N' and N under PI are greatly reduced at maximum survey effort. As such, the implications of both pervasive positive bias and estimate imprecision (uncertainty) in the abundance estimates

(relative to truth) provide a mechanistic explanation as to why the population trajectory in every scenario was lower than the PI equivalent.

The decision framework we constructed (Fig. 3.7) is flexible and can therefore address specific needs of management agencies or specific aspects of harvest programs. Our two constraint criteria, *EP* and λ, were in strong agreement with one another, as there were no instances in which $EP > 0.05$ also had $\lambda \geq 0.98$, or vice-versa. Thus, including both constraints as quantities was likely redundant. Financial cost is frequently evaluated within the context of decision analysis for monitoring wildlife populations. Though our decision model incorporated financial considerations for the selection of an optimal survey design, we suggest there is an opportunity to improve upon its inclusion. For example, revenue for monitoring and research in South Carolina is directly tied to the amount of harvest (lottery ticket and permit sales), which is unique among all other states in the alligator's distribution (T. Gancos Crawford, unpubl. data). Therefore, a modeling approach that considered the quantity of permit or lottery ticket sales needed to cover the cost of each temporal replicate survey could better evaluate potential abundance thresholds needed to justify the addition of increasing survey effort to produce additional revenue. Decision-makers could evaluate if the cost of adding a temporal replicate to improve abundance estimates (relative to perfect information) and increase the harvest quota, exceeds the potential revenue gained from the increased sales of alligator harvest lottery tickets, licenses, and tags, afforded from the increased quota. Similarly, an improved understanding of how hunter participation and interest (i.e., revenue

generation) relates to abundance and densities, including specific stage classes would enable a more realistic simulation.

Finally, we note that our second fundamental objective, minimizing management and ecological uncertainty deviates from typical decision-analytic frameworks for harvested populations (Robinson et al. 2016). However, in alligator populations, substantial uncertainty exists regarding how alligator populations may respond if stage class proportions are perturbed or potentially extirpated (e.g., bulls). For example, Wilkinson et al. (2016) recently reported that growth in alligators is determinate, rather than indeterminate as previously assumed, and the mechanisms controlling terminal size (e.g., genetics) remain uncertain. Similarly, a recent study examining alligator genetics and long-term nesting data in South Carolina determined that the largest males (i.e., bulls) are the sires associated with the majority of nests (J. Zajdel, pers. comm.). It remains uncertain if smaller males that may not be capable of attaining bull size could potentially fulfill the reproductive role of bulls should that stage class become locally extirpated due to disproportionate harvest patterns. Therefore, given the substantial ecological uncertainties in how alligator populations may respond to harvest policies, we decided to combine ecological and management uncertainty into a single fundamental objective. However, many of the attributes that we measured (e.g., *MA*, *EP*, λ) could be easily restructured into different fundamental objectives in other species or ecosystems.

Our study highlights the utility of simulation-based approaches to identify complex relationships and tradeoffs in the design of monitoring plans for stage-structured species. Specifically, we determined that increasing temporal rather than spatial replication was

more likely to reduce uncertainty and bias associated with abundance estimates, though initial population density and harvest rate affect the magnitude of uncertainty within the temporal and spatial framework. All of the optimal plans, derived from our simulations for a given population density x harvest rate scenario, selected for the maximum number of temporal replicates and the intermediate number of sites, with the exception of the low density x 1.5% harvest scenario, which selected for maximum survey effort. However, our analysis also indicated that even under the most optimal conditions to reduce bias (high initial population density and 0.5% harvest), the relative bias rates remained relatively high (> 0.17), leading to an overestimate of abundance and harvest quotas which subsequently resulted in a population decline. This finding is particularly problematic, as abundance reported by other studies with comparable detection probability estimates derived from two temporal replicates (Fujisaki et al. 2011, Waddle et al. 2015) could have been overestimated as well. Future studies should evaluate how changes to survey structure, such as the interval between replicate surveys, or selectively surveying under conditions (e.g., low water level and high temperatures; Lawson 2019) could potentially shift the spatiotemporal replication tradeoff we described.

Evaluating patterns at the stage class-level through a life history lens is also particularly valuable as it enables an understanding of how populations are likely to respond to unsustainable harvest of specific demographic groups. This understanding can provide the opportunity for earlier intervention if reliable monitoring data enable earlier detection of problematic demographic trends. Combining a population simulation within a decision-analytic framework is an informative way to discern how populations respond

to management actions (e.g. monitoring, harvest quotas) and to evaluate the effectiveness of said actions within near universal-constraints faced by conservation practitioners: effective conservation in the face of uncertainty and limited resources.

Acknowledgements

We thank Phil Wilkinson and Allan Woodward for their extensive contributions to the studies used to parameterize this model, as well as Clemson University for generous allotment of computer time on the Palmetto Cluster. We honor the memory of our coauthor, Kate W. McFadden, an innovative conservation biologist, who inspired those around her to collaborate think broadly to solve complex issues in conservation. This work was supported by the South Carolina Department of Natural Resources [grant numbers 2009094 and 20100899] and the United States Geological Survey [grant numbers G12AC20329 and G15AC00264]. Authors declare no conflict of interest. Any use of trade, firm, or product names is for descriptive purposes only and does not imply endorsement by the U.S. Government.

Literature Cited

Anderson, D. R. 2001. The need to get the basics right in wildlife field studies. Wildlife Society Bulletin 29:1294–1297.

Bara, M. O. 1975. American alligator investigations final study report. Columbia, South Carolina, USA.

Bunnefeld, N., E. Hoshino, and E. J. Milner-gulland. 2011. Management strategy evaluation : a powerful tool for conservation ? 26:441–447.

Caswell, H. 2001. Matrix Population Models. Second Edi. Sinauer Associates, Inc.,

Sunderland, Massachusetts, USA.

Couturier, T., L. De Bioge, and E. Pratique. 2013. Estimating Abundance and Population Trends When Detection Is Low and Highly Variable : A Comparison of Three Methods for the Hermann ' s Tortoise 77:454–462.

Cremer, M. J., A. C. Holz, C. M. Sartori, B. Schulze, R. L. Paitach, and P. C. Simões-Lopes. 2018. Behavior and Ecology of Endangered Species Living Together: Long-Term Monitoring of Resident Sympatric Dolphin Populations. Pages 477–508*in* M. R. Rossi-Santos and C. W. Finkl, editors.Advances in Marine Vertebrate Research in Latin America: Technological Innovation and Conservation. Springer International Publishing, Cham.

Crouse, D. T., L. B. Crowder, H. Caswell, and L. B. Crowder. 2016. A Stage-Based Population Model for Loggerhead Sea Turtles and Implications for Conservation Stable URL : http://www.jstor.org/stable/1939225 REFERENCES Linked references are available on JSTOR for this article : You may need to log in to JSTOR to access t 68:1412–1423.

Dail, D., and L. Madsen. 2011. Web Supplementary Materials Models for Estimating Population Size from Repeated Counts of an Open Population. Biometrics 1:1–7.

Dunham, K., S. Dinkelacker, and J. Miller. 2014. A stage-based population model for American alligators in northern latitudes. The Journal of Wildlife Management 78:440–447.

Fiske, I., and R. Chandler. 2011. **unmarked** : An *R* Package for Fitting Hierarchical Models of Wildlife Occurrence and Abundance. Journal of Statistical Software 43.

Fujisaki, I., F. J. Mazzotti, R. M. Dorazio, K. G. Rice, M. Cherkiss, and B. Jeffery. 2011. Estimating trends in alligator populations from nightlight survey data. Wetlands 31:147–155.

Gardner, B., L. A. Garner, D. T. Cobb, and C. E. Moorman. 2016. Factors Affecting Occupancy and Abundance of American Alligators at the Northern Extent of Their Range. Journal of Herpetology 50:541–547.

Guillera-arroita, G., M. S. Ridout, and B. J. T. Morgan. 2010. Design of occupancy studies with imperfect detection:131–139.

Joanen, T., and L. McNease. 1980. Reproductive biology of the American alligator in southwest Louisiana. Pages 153–159*in* J. B. Murphy and J. T. Collins, editors.Reproductive biology and diseases of captive reptiles. Contributions to

Herpetology, Society for the Study of Amphibians and Reptiles, Lawrence, Kansas, USA.

Kendall, W. L., and C. T. Moore. 2012. Maximizing the utility of monitoring to the adaptive management of natural resources. Pages 74–98*in* R. A. Gitzen, J. J. Millspaugh, A. B. Cooper, and D. S. Licht, editors.Design and Analysis of Long-term Ecological Monitoring Studies. Cambridge University Press, Cambridge, UK.

Kéry, M., and J. A. Royle. 2016. Applied hierarchical modeling in ecology. Elsevier, London, Unied Kingdom.

Lang, J. W. 1987. Crocodilian behavior: implications for management. Pages 273–294*in* G. J. Webb, S. C. Manolis, and P. J. Whitehead, editors.Wildlife Management: Crocodiles and Alligators. Surrey Beatty and Sons Proprietary Limited, Sydney, Australia.

Lawson, A. J. 2019. Reducing uncertainty in conservation decision-making for American alligators. Clemson University.

Lindenmayer, D. B., G. E. Likens, A. Andersen, D. Bowman, C. M. Bull, E. Burns, C. R. Dickman, A. R. Y. A. Hoffmann, D. A. Keith, M. J. Liddell, A. J. Lowe, D. J. Metcalfe, S. R. Phinn, J. Russell-smith, N. Thurgate, and G. M. Wardle. 2012. Value of long-term ecological studies:745–757.

Link, W. A., J. A. Royle, and J. S. Hatfield. 2003. Demographic Analysis from Summaries of an Age-Structured Population. Biometrics 59:778–785.

Martin, J., W. M. Kitchens, and J. E. Hines. 2007. Importance of well-designed monitoring programs for the conservation of endangered species: Case study of the snail kite. Conservation Biology 21:472–481.

Martin, J., J. A. Royle, D. I. Mackenzie, H. H. Edwards, M. Ke, and B. Gardner. 2011. Accounting for non-independent detection when estimating abundance of organisms with a Bayesian approach. Methods in Ecology and Evolution 2:595–601.

Mcintyre, A. P., J. E. Jones, E. M. Lund, F. T. Waterstrat, J. N. Giovanini, S. D. Duke, M. P. Hayes, T. Quinn, and A. J. Kroll. 2012. Forest Ecology and Management Empirical and simulation evaluations of an abundance estimator using unmarked individuals of cryptic forest-dwelling taxa. Forest Ecology and Management 286:129–136.

McKann, P. C., B. R. Gray, and W. E. Thogmartin. 2013. Small sample bias in dynamic occupancy models. The Journal of Wildlife Management 77:172–180.

Moore, C. T., and W. L. Kendall. 2004. Costs of detection bias in index-based population monitoring. Animal Biodiversity and Conservation 27:287–296.

Mosnier, A., T. Doniol-Valcroze, J. F. Gosselin, V. Lesage, L. N. Measures, and M. O. Hammill. 2015. Insights into processes of population decline using an integrated population model: The case of the St. Lawrence Estuary beluga (Delphinapterus leucas). Ecological Modelling 314:15–31.

Nichols, J. D., J. E. Hines, J. R. Sauer, F. W. Fallon, J. E. Fallon, and P. J. Heglund. 2000. A Double-Observer Approach for Estimating Detection Probability and Abundance from Point Counts. The Auk 117:393–408.

Nichols, J. D., and B. K. Williams. 2006. Monitoring for conservation 21.

R Core Development Team. 2017. R: A language and environment for statistical computing. R Foundation for Statistical Computing, Vienna, Austria.

Rhodes, W. E. 2002. Differential harvest of American Alligators on Private Lands in Coastal South Carolina. Pages 75–79Crocodiles. Proceedings of the 16th Working Meeting of the Crocodile Specialist Group. IUCN–The World Conservation Union, Gland Switzerland and Cambridge, UK.

Rhodes, W. E., and J. W. Lang. 1996. Alligator Nest Temperatures and Hatchling sex rations in coastal South Carolina. Proc. Annu. Conf. Southeast. Assoc. Fish and Wildl. Agencies:521–531.

Robinson, K. F., A. K. Fuller, J. E. Hurst, B. L. Swift, A. Kirsch, J. Farquhar, D. J. Decker, and W. F. Siemer. 2016. Structured decision making as a framework for large-scale wildlife harvest management decisions. Ecosphere 7:e01613.

Royle, J. A. 2004. N-Mixture Models for Estimating Population Size from Spatially Peplicated Counts. Biometrics 60:108–115.

Royle, J. A., Y. Yamaura, and M. Ke. 2016. Study of biological communities subject to imperfect detection : bias and precision of community N-mixture abundance models in small-sample situations:289–305.

Sanderlin, J. S., W. M. Block, J. L. Ganey, R. Mountain, U. S. F. Service, and S. P. Knoll. 2014. Optimizing study design for multi-species avian monitoring programmes:860–870.

Sedinger, J. S., T. V. Riecke, A. G. Leach, and D. H. Ward. 2017. The Black Brant Population Is Declining Based on Mark Recapture. The Journal of Wildlife Management:1–11.

Shirley, M. H., R. M. Dorazio, E. Abassery, A. A. Elhady, M. S. Mekki, and H. H. Asran. 2012. A sampling design and model for estimating abundance of Nile crocodiles while accounting for heterogeneity of detectability of multiple observers. The Journal of Wildlife Management 76:966–975.

South Carolina Department of Natural Resources. 2017. Alligator Hunting Season Report. Columbia, South Carolina, USA.

Strickland, B. A., F. J. Vilella, and R. D. Flynt. 2018. Long-term spotlight surveys of American alligators in Mississippi, USA. Herpetological Conservation and Biology 13:331–340.

Stubben, C., B. Milligan, and P. N. Maintainer. 2016. Package "popbio" : Construction and Analysis of Matrix Population Models.

Tyre, A. J., B. Tenhumberg, S. A. Field, D. Niejalke, K. Parris, and H. P. Possingham. 2003. Improving precision and reducing bias in biological surveys: estimating false-negative error rates. Ecological Applications 13:1790–1801.

Unger, S. D., T. M. Sutton, and R. N. Williams. 2013. Projected population persistence of eastern hellbenders (Cryptobranchus alleganiensis alleganiensis) using a stage-structured life-history model and population viability analysis. Journal for Nature Conservation 21:423–432.

Using Multiple Methods to Assess Detection Probabilities of Forest-Floor Wildlife. 2011. 75:423–431.

Waddle, J. H., L. A. Brandt, B. M. Jeffery, and F. J. Mazzotti. 2015. Dry Years Decrease Abundance of American Alligators in the Florida Everglades. Wetlands 35:865–875.

Wilkinson, P. M. 1983. Nesting ecology of the American alligator in coastal South Carolina. Study Completion Report. Columbia, South Carolina.

Wilkinson, P. M., T. R. Rainwater, A. R. Woodward, E. H. Leone, and C. Carter. 2016. Determinate Growth and Reproductive Lifespan in the American Alligator (Alligator mississippiensis): Evidence from Long-term Recaptures. Copeia 104:843–852.

Williams, B. K., J. D. Nichols, and M. J. Conroy. 2002. Analysis and management of animal populations. Academic Press.

Woodward, A. R. 1996. Determination of appropriate harvest strategies for alligator management units. Gainesville, Florida.

Woodward, A. R., and C. T. Moore. 1990. Use of crocodilian night count data for population trend estimation. Tallahassee, Florida, USA.

Yoccoz, N. G., J. D. Nichols, and T. Boulinier. 2001. Monitoring of biological diversity in space and time. Trends in Ecology & Evolution 16:446–453.

Zipkin, E. F., T. S. Sillett, E. H. C. Grant, R. B. Chandler, and J. A. Royle. 2014a. Inferences about population dynamics from count data using multistate models: A comparison to capture-recapture approaches. Ecology and Evolution 4:417–426.

Zipkin, E. F., J. T. Thorson, K. See, H. J. Lynch, E. H. C. Grant, Y. Kanno, R. B. Chandler, B. H. Letcher, and J. A. Royle. 2014b. Modeling structured population dynamics using data from unmarked individuals. Ecology 95:22–29.

Zurell, D., U. Berger, J. S. Cabral, F. Jeltsch, C. N. Meynard, T. Münkemüller, N. Nehrbass, J. Pagel, B. Reineking, B. Schröder, and V. Grimm. 2010. The virtual ecologist approach: Simulating data and observers. Oikos 119:622–635.

Table 3.1. Conditions for the simulation of an American alligator (*Alligator mississippiensis*) population, contrasting initial alligator population densities, harvest rates, temporal replication, and spatial replication. For each of the 81 possible combinations of conditions (scenarios), we projected growth of the population over twenty years. The harvest rate columns reflect the proportion of the population that was removed relative to harvestable stage classes ($j \geq 3$; left) and the total population ($j \geq 1$). Though we applied the total population harvest rate in the model, the number of individuals harvested within each stage class was determined by the harvest proportion vector (**hsp**; Table 3.2) to reflect selective harvest of different stage classes and ensure no individuals in $j < 3$ were removed.

		Harvest rate			
	Initial alligator density (#/site)	Harvestable sizes ($j \geq 3$)	Total population ($j \geq 1$)	Temporal replicates	Spatial replicates (Sites)
Low	10	0.5%	0.0014%	2	160
Intermediate	30	1.0%	0.0028%	4	320
High	60	1.5%	0.0042%	6	640

Table 3.2. Stage class life table summary for American alligators (*Alligator mississippiensis*) in South Carolina, USA. We constructed a six-stage Lefkovitch population projection matrix, using parameters from the primary literature, and performed additional calculations when necessary. All values contained in the table were used in the simulation with the exception of survival probabilities in parentheses, which were increased by 4% to the bolded terms, to attain a positive population growth rate for simulation. Harvest proportion is the stage class distribution of harvested alligators (**hsp** vector). Sources are from South Carolina unless otherwise stated, and are reported in the footnotes.

Stage class (*j*)	Name	Total length range (cm)	Female proportion $FP_j \pm$ SD[a]	Survival prob. $\varphi_j \pm$ SD[b]	Transition prob. $\psi_{j,j+1} \pm$ SD[c]	Fecundity	Stable stage dist. (**L**)	Harvest proportion
1	Hatchlings	≤30	0.72 ± 0.02	0.16 ± 0.04	1.00		0.54	0.00
2	Juveniles	31–121	0.37 ± 0.02	0.61 ± 0.11	0.17 ± 0.01		0.18	0.00
3	Subadults	122–182	0.47 ± 0.02	**0.93** (0.89 ± 0.06)	0.22 ± 0.04		0.06	0.04
4	Small Adults	183–243	0.47 ± 0.07	**0.99** (0.96 ± 0.02)	0.15 ± 0.05	4.07	0.08	0.30
5	Large Adults	244–304	0.35 ± 0.10	**0.97** (0.93 ± 0.02)	0.08 ± 0.05	3.03	0.08	0.40
6	Bulls	≥305	0.00	0.92 ± 0.03	0.00		0.06	0.26
Productivity Terms[d]:		*NS* = 0.70	*BP* = 0.275	*CL* = 45				

[a]Hatchlings: Rhodes and Lang 1996; Juveniles–Large Adults: Woodward 1996 (Florida)
[b]Lawson 2019

[c]Calculated weighted mean of sex-specific growth probabilities in Lawson (2019) for each transition using the female proportion. Sex-specific growth probability estimates originally derived from Wilkinson et al. (2016)
[d]Calculated from public alligator harvest records for Georgetown County, South Carolina 2008–2017 (SCDNR 2017)
[f]Nest success (*NS*), breeding probability (*BP*), and clutch size (*CL*) from Wilkinson (1983), multiplied by FP_j (Woodward 1996) for stage-specific fecundity

Table 3.3. Summary of decision objectives for an American alligator (*Alligator mississippiensis*) population simulation to identify an optimal monitoring program design based on population density and harvest rate. We evaluated nine potential monitoring programs that differed based on the number of sites (160, 320, or 640 spatial replicates), and temporal replicates (2, 4, or 6). The nine potential monitoring program designs were evaluated within nine different initial population density (a. high, b. intermediate, or c. low) and harvest rate (0.5, 1.0, or 1.5% of the perceived number of harvestable alligators) scenarios. For a monitoring plan to be eligible for consideration, we used two constraints: (1) population growth rate (λ) ≥ 0.98 and an extinction probability (*EP*) ≤ 0.05. We used two fundamental objectives (FO) to evaluate the eligible monitoring program designs: (1) maximize financial effectiveness and (2) maximize population persistence. FO_1 included two means objectives: (1) minimize effort (*EF*) and (2) maximize abundance (*MA*; Eq. 3.12). FO_2 included three means objectives: (1) minimize changes in stage class structure (*SC*; Eq. 3.13); (2) minimize relative bias (*RB*; Eq. 3.14); and (3) minimize uncertainty (SD) of abundance estimates (*UC*). Each means objective was assigned a weight and used to create a weighted sum associated with each *FO* (Eqs. 3.17–18). The *FO* scores for each monitoring plan design were added together within each of the nine density x harvest scenarios to produce a final optimization (*OP*) score (Eq. 3.19). The bolded rows represent the optimal monitoring design within each density x harvest scenario, conditioned on eligibility.

a. Low Density			*Constraints*			*Max. Financial Effect.*			*Min. Ecol. & Mang. Uncertainty*				
Harvest	Temp. Reps.	Sites	λ	*EP*	Eligible	*EF*	*MA*	FO_1	*SC*	*RB*	*UC*	FO_2	*OP*
0.5	2	160	0.13	0.50	No	320	0.10	0.50	0.20	53.41	285.61	0.00	0.50
0.5	2	320	0.25	0.31	No	640	0.19	0.51	0.15	35.56	276.36	0.21	0.72
0.5	2	640	0.61	0.01	No	1280	0.46	0.57	0.07	11.71	213.10	0.61	1.18
0.5	4	160	0.59	0.06	No	640	0.45	0.66	0.06	14.36	223.91	0.63	1.28
0.5	4	320	0.89	0.00	No	1280	0.67	0.70	0.03	6.20	166.86	0.79	1.48
0.5	4	640	1.22	0.00	Yes	2560	0.91	0.66	0.01	1.09	67.38	0.96	1.62
0.5	6	160	1.02	0.00	Yes	960	0.77	0.80	0.02	3.22	129.57	0.86	1.66
0.5	**6**	**320**	**1.17**	**0.00**	**Yes**	**1920**	**0.88**	**0.73**	**0.02**	**1.54**	**88.51**	**0.94**	**1.66**
0.5	6	640	1.27	0.00	Yes	3840	0.96	0.50	0.01	0.53	42.80	1.00	1.50
1	2	160	0.03	0.93	No	320	0.02	0.50	0.15	77.61	261.03	0.05	0.55

1	2	320	0.09	0.63	No	640	0.08	0.49	0.17	43.50	242.53	0.13	0.62
1	2	640	0.31	0.30	No	1280	0.26	0.50	0.10	20.49	196.20	0.48	0.98
1	4	160	0.35	0.25	No	640	0.29	0.60	0.10	18.91	202.05	0.49	1.10
1	4	320	0.45	0.06	No	1280	0.37	0.56	0.12	11.00	184.08	0.48	1.04
1	4	640	0.98	0.00	Yes	2560	0.80	0.62	0.03	1.59	78.44	0.93	1.55
1	6	160	0.71	0.03	No	960	0.58	0.72	0.06	5.72	139.92	0.73	1.45
1	**6**	**320**	**1.07**	**0.00**	**Yes**	**1920**	**0.87**	**0.75**	**0.02**	**0.91**	**50.79**	**0.99**	**1.74**
1	6	640	1.12	0.00	Yes	3840	0.91	0.50	0.02	0.61	45.41	1.00	1.50
1.5	2	160	0.00	0.99	No	320	0.00	0.50	0.33	92.77	271.23	0.00	0.50
1.5	2	320	0.05	0.77	No	640	0.05	0.48	0.29	48.98	238.61	0.22	0.70
1.5	2	640	0.17	0.49	No	1280	0.15	0.45	0.15	23.61	195.25	0.56	1.01
1.5	4	160	0.21	0.46	No	640	0.18	0.56	0.14	30.65	213.08	0.54	1.10
1.5	4	320	0.40	0.15	No	1280	0.35	0.56	0.09	12.57	171.38	0.72	1.28
1.5	4	640	0.79	0.01	No	2560	0.70	0.57	0.05	2.35	94.77	0.90	1.47
1.5	6	160	0.64	0.04	No	960	0.57	0.73	0.06	4.80	123.37	0.84	1.56
1.5	6	320	0.81	0.00	No	1920	0.71	0.67	0.05	2.28	89.09	0.90	1.58
1.5	**6**	**640**	**1.01**	**0.00**	**Yes**	**3840**	**0.89**	**0.50**	**0.03**	**0.51**	**37.82**	**1.00**	**1.50**

b. Intermediate Density			*Constraints*			*Max. Financial Effect.*			*Min. Ecol. & Mang. Uncertainty*				
Harvest	Temp. Reps.	Sites	λ	*EP*	Eligible	*EF*	*MA*	FO_1	*SC*	*RB*	*UC*	FO_2	*OP*
0.5	2	160	0.58	0.00	No	320	0.44	0.50	0.09	11.06	355.95	0.00	0.50
0.5	2	320	0.82	0.00	No	640	0.61	0.62	0.05	6.28	311.89	0.40	1.03
0.5	2	640	0.95	0.00	No	1280	0.72	0.63	0.03	4.08	258.16	0.62	1.26
0.5	4	160	0.97	0.00	No	640	0.73	0.73	0.03	4.05	264.79	0.63	1.36
0.5	4	320	1.15	0.00	Yes	1280	0.86	0.77	0.02	1.83	182.37	0.83	1.61
0.5	4	640	1.27	0.00	Yes	2560	0.95	0.67	0.01	0.62	90.99	0.99	1.66
0.5	6	160	1.16	0.00	Yes	960	0.87	0.83	0.02	1.67	174.51	0.83	1.66
0.5	**6**	**320**	**1.28**	**0.00**	**Yes**	**1920**	**0.96**	**0.77**	**0.01**	**0.51**	**82.12**	**0.99**	**1.77**
0.5	6	640	1.27	0.00	Yes	3840	0.96	0.50	0.01	0.52	90.81	0.98	1.48
1	2	160	0.21	0.09	No	320	0.17	0.50	0.21	21.64	327.24	0.00	0.50
1	2	320	0.39	0.03	No	640	0.32	0.55	0.13	11.32	296.95	0.36	0.92
1	2	640	0.54	0.00	No	1280	0.44	0.55	0.10	5.38	262.72	0.56	1.11
1	4	160	0.68	0.00	No	640	0.55	0.72	0.06	5.21	242.83	0.68	1.40
1	4	320	0.89	0.00	No	1280	0.73	0.74	0.04	2.16	180.71	0.84	1.58
1	4	640	1.10	0.00	Yes	2560	0.90	0.68	0.02	0.64	96.32	1.00	1.68
1	6	160	0.94	0.00	No	960	0.76	0.82	0.04	1.69	164.69	0.87	1.68
1	**6**	**320**	**1.10**	**0.00**	**Yes**	**1920**	**0.90**	**0.77**	**0.02**	**0.65**	**99.36**	**0.99**	**1.76**
1	6	640	1.09	0.00	Yes	3840	0.89	0.49	0.02	0.74	108.36	0.99	1.48
1.5	2	160	0.06	0.43	No	320	0.05	0.50	0.35	38.09	312.36	0.00	0.50
1.5	2	320	0.25	0.11	No	640	0.22	0.56	0.17	18.03	276.63	0.44	1.00
1.5	2	640	0.33	0.04	No	1280	0.29	0.51	0.14	8.56	246.36	0.59	1.10
1.5	4	160	0.46	0.00	No	640	0.41	0.67	0.11	5.12	230.17	0.68	1.35

1.5	4	320	0.69	0.00	No	1280	0.61	0.70	0.08	2.31	170.06	0.81	1.51
1.5	4	640	0.95	0.00	No	2560	0.84	0.65	0.03	0.71	97.16	0.97	1.63
1.5	6	160	0.77	0.00	No	960	0.69	0.79	0.05	1.69	152.91	0.88	1.66
1.5	**6**	**320**	**1.01**	**0.00**	**Yes**	**1920**	**0.89**	**0.77**	**0.03**	**0.48**	**75.87**	**1.00**	**1.77**
1.5	6	640	0.94	0.00	No	3840	0.83	0.46	0.03	0.78	107.61	0.96	1.43

c. High Density			*Constraints*			*Max. Financial Effect.*			*Min. Ecol. & Mang. Uncertainty*				
Harvest	Temp. Reps.	Sites	λ	*EP*	Eligible	*EF*	*MA*	FO_1	*SC*	*RB*	*UC*	FO_2	*OP*
0.5	2	160	0.94	0.00	No	320	0.71	0.50	0.03	4.30	341.25	0.00	0.50
0.5	2	320	1.04	0.00	Yes	640	0.78	0.60	0.02	2.98	320.01	0.28	0.88
0.5	2	640	1.10	0.00	Yes	1280	0.83	0.59	0.02	2.27	260.52	0.42	1.01
0.5	4	160	1.16	0.00	Yes	640	0.87	0.75	0.02	1.69	251.19	0.55	1.30
0.5	4	320	1.22	0.00	Yes	1280	0.92	0.75	0.01	1.00	191.93	0.72	1.46
0.5	4	640	1.28	0.00	Yes	2560	0.96	0.64	0.01	0.49	128.12	0.87	1.51
0.5	6	160	1.22	0.00	Yes	960	0.92	0.78	0.01	1.07	193.32	0.73	1.51
0.5	**6**	**320**	**1.29**	**0.00**	**Yes**	**1920**	**0.97**	**0.75**	**0.01**	**0.33**	**92.87**	**0.94**	**1.69**
0.5	6	640	1.31	0.00	Yes	3840	0.99	0.50	0.01	0.17	60.63	1.00	1.50
1	2	160	0.51	0.00	No	320	0.42	0.50	0.11	6.13	347.23	0.00	0.50
1	2	320	0.70	0.00	No	640	0.57	0.59	0.07	3.54	314.66	0.34	0.93
1	2	640	0.78	0.00	No	1280	0.64	0.56	0.05	2.82	264.35	0.49	1.05
1	4	160	0.90	0.00	No	640	0.73	0.74	0.04	1.91	251.81	0.63	1.37
1	4	320	1.03	0.00	Yes	1280	0.84	0.75	0.03	1.05	186.10	0.79	1.54
1	4	640	1.13	0.00	Yes	2560	0.92	0.64	0.02	0.50	122.42	0.92	1.55
1	6	160	1.05	0.00	Yes	960	0.85	0.80	0.02	0.98	177.40	0.82	1.62
1	**6**	**320**	**1.15**	**0.00**	**Yes**	**1920**	**0.94**	**0.74**	**0.02**	**0.37**	**94.97**	**0.94**	**1.68**
1	6	640	1.19	0.00	Yes	3840	0.97	0.50	0.02	0.17	59.30	1.00	1.50
1.5	2	160	0.23	0.02	No	320	0.21	0.50	0.20	10.74	342.12	0.00	0.50
1.5	2	320	0.42	0.00	No	640	0.37	0.57	0.13	4.92	314.36	0.36	0.93
1.5	2	640	0.51	0.00	No	1280	0.45	0.53	0.10	3.55	270.41	0.52	1.05

1.5	4	160	0.69	0.00	No	640	0.61	0.73	0.06	2.10	245.07	0.67	1.40
1.5	4	320	0.88	0.00	No	1280	0.78	0.74	0.04	1.06	181.25	0.82	1.57
1.5	4	640	1.00	0.00	Yes	2560	0.88	0.63	0.03	0.50	120.99	0.92	1.56
1.5	6	160	0.84	0.00	No	960	0.74	0.77	0.05	1.24	189.52	0.80	1.57
1.5	**6**	**320**	**1.01**	**0.00**	**Yes**	**1920**	**0.90**	**0.73**	**0.03**	**0.44**	**105.15**	**0.94**	**1.67**
1.5	6	640	1.08	0.00	Yes	3840	0.95	0.50	0.02	0.19	59.38	1.00	1.50

Figure 3.1. Comparison of abundance patterns over 20 years for a simulated population of American alligators (*Alligator mississippiensis*) of all stage classes at a low initial density (10 alligators site^{-1}). True realized abundance of all stage classes is shown for imperfect detection (solid lines) and perfect information (dashed lines), as a function of the harvest rate (colors) for harvestable stage classes ($j \geq 3$). The gray paneling in in each cell describes survey design attributes: the number of sites (160/320/640; rows), and the number of temporal replicates (2/4/6; columns). The perfect information lines for intermediate and high initial densities (Table 3.1) show the same trajectory as the low density scenario shown here, but with a different y-intercept.

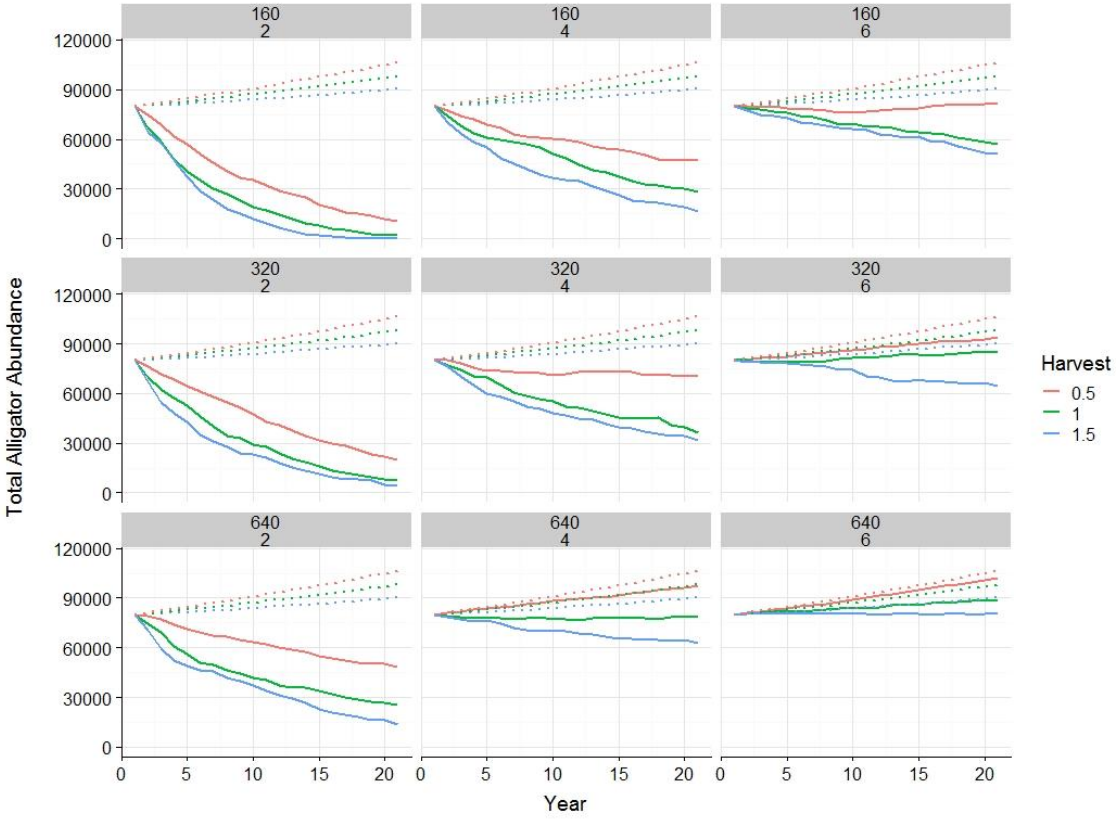

Figure 3.2. Variability in constraint and means objective values as a function of harvest rate and initial population density for population simulations of American alligators (*Alligator mississippiensis*). The mean value ± SD bars for all nine possible survey designs (Table 3.1) associated with each initial population density and harvest rate are shown in each panel. (a) Extinction percentage (*EP*) is the number of simulations out of 100 total in which the total population declined to zero; (b) lambda (λ) is the population growth rate; (c) maximum abundance (*MA*) is the population size in the final year of the imperfect detection simulation divided by the population size under the perfect information counterpart; (d) relative bias (*RB*) indicates deviation of the estimated density under imperfect detection compared to the true value (Eq. 3.14); (e) percent change in stage distribution (*SC*) is the absolute value of mean percent change in each stage class, weighted by the stable stage distribution of **L** (Eq. 3.13); (f) uncertainty (*UC*) is the standard deviation of estimated mean abundance across simulations at each time step, averaged across years.

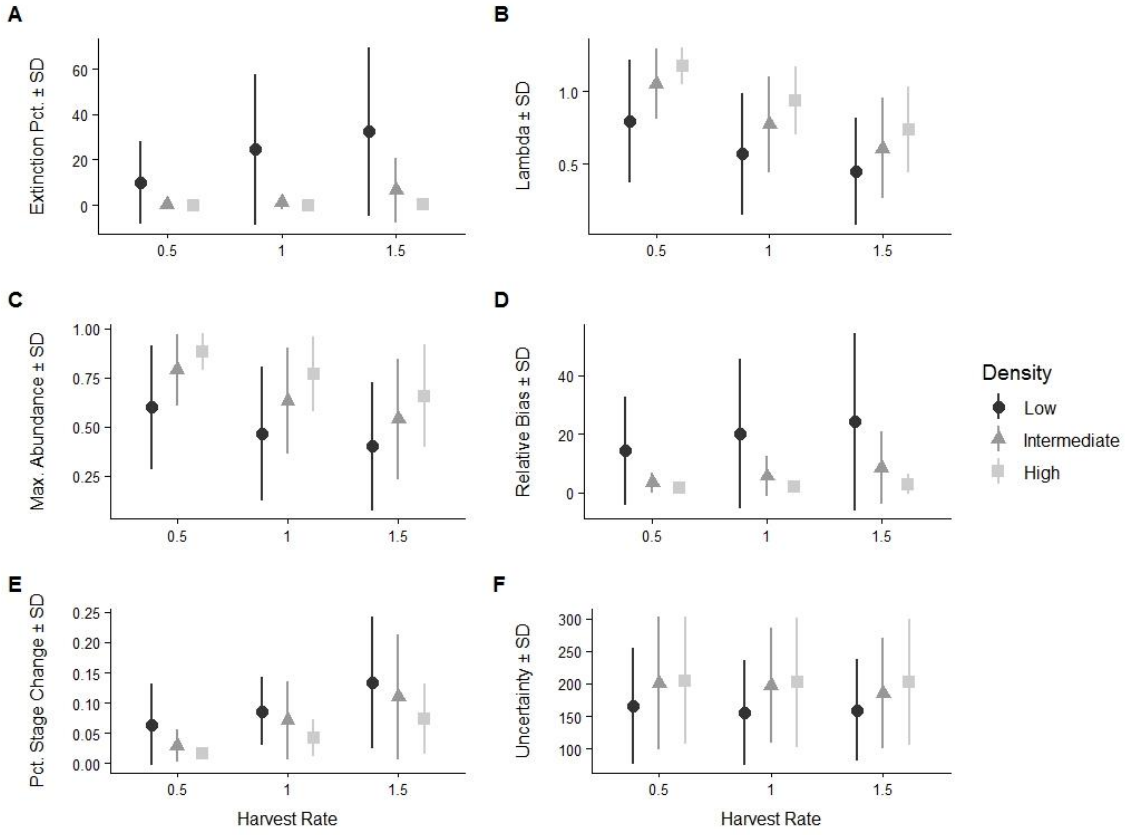

Figure 3.3. Changes in stage class distributions of American alligator (*Alligator mississippiensis*) simulated under imperfect detection over years as a function of survey attributes and harvest rate (Table 3.1). Percent change (y-axis) is the absolute value of mean percent change (between first and last years of simulation) in each stage class, weighted by the stable stage distribution of **L** (Eq. 3.13) and is shown for the three different harvest rates of stages $j \geq 3$ (colored bars) for (a) low, (b) intermediate, and (c) high initial population densities within each panel. The gray paneling in in each cell describes survey design attributes: the number of sites (160/320/640; rows), and the number of temporal replicates (2/4/6; columns). Note that y-axis differs among panels a–c.

a.

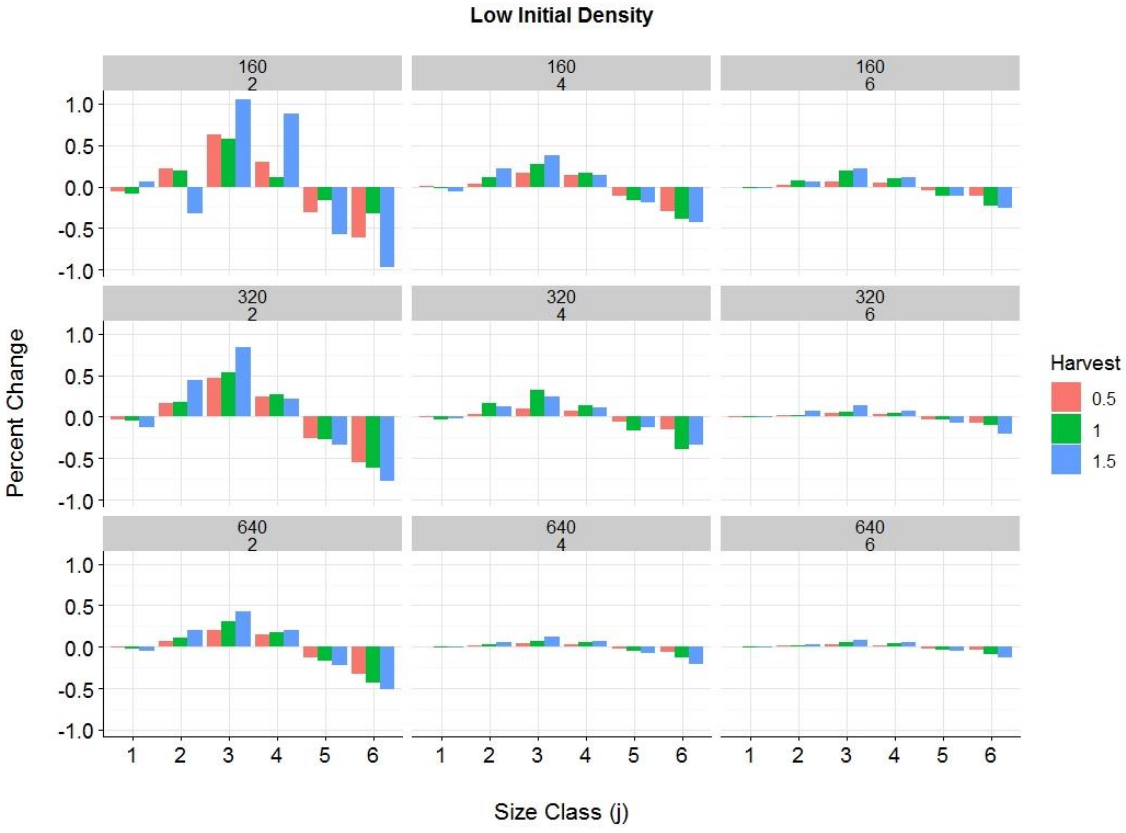

Figure 3b

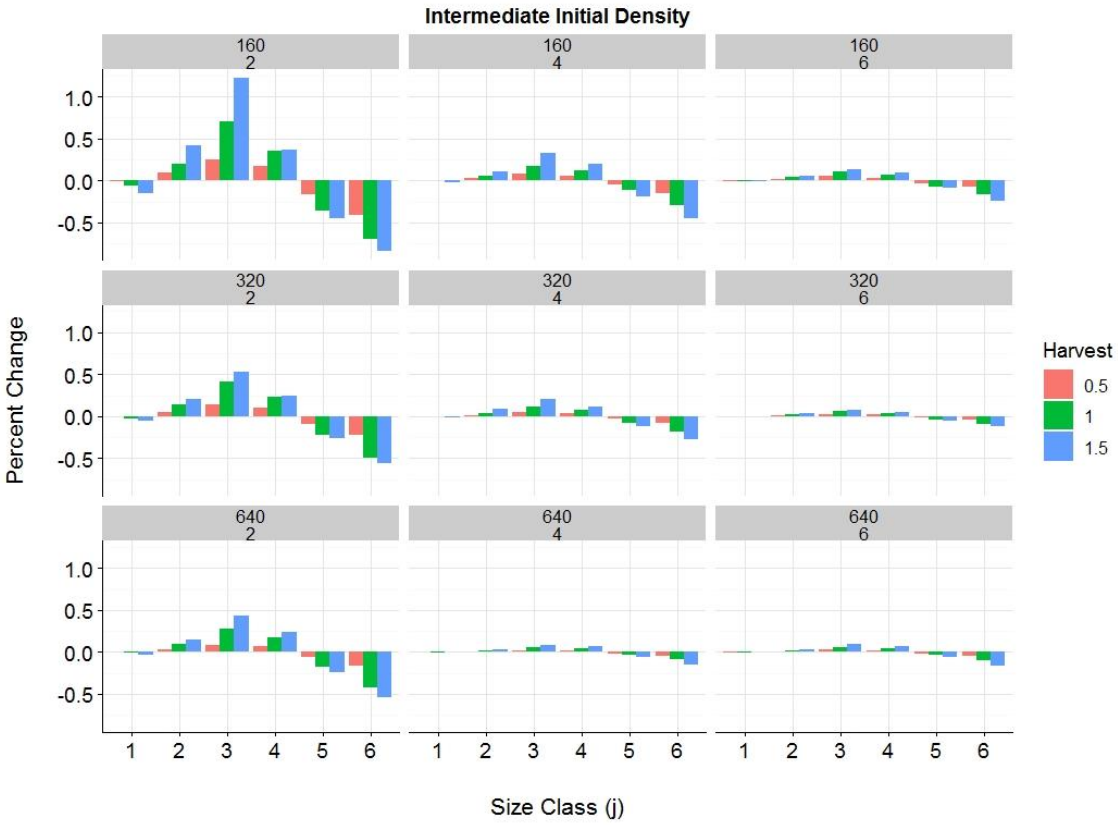
Intermediate Initial Density
160
2
160
4
160
6
320
2
320
4
320
6
640
2
640
4
640
6
1.0
0.5
0.0
-0.5
1
2
3
4
5
6
Percent Change
Size Class (j)
Harvest
0.5
1
1.5

Figure 3c.

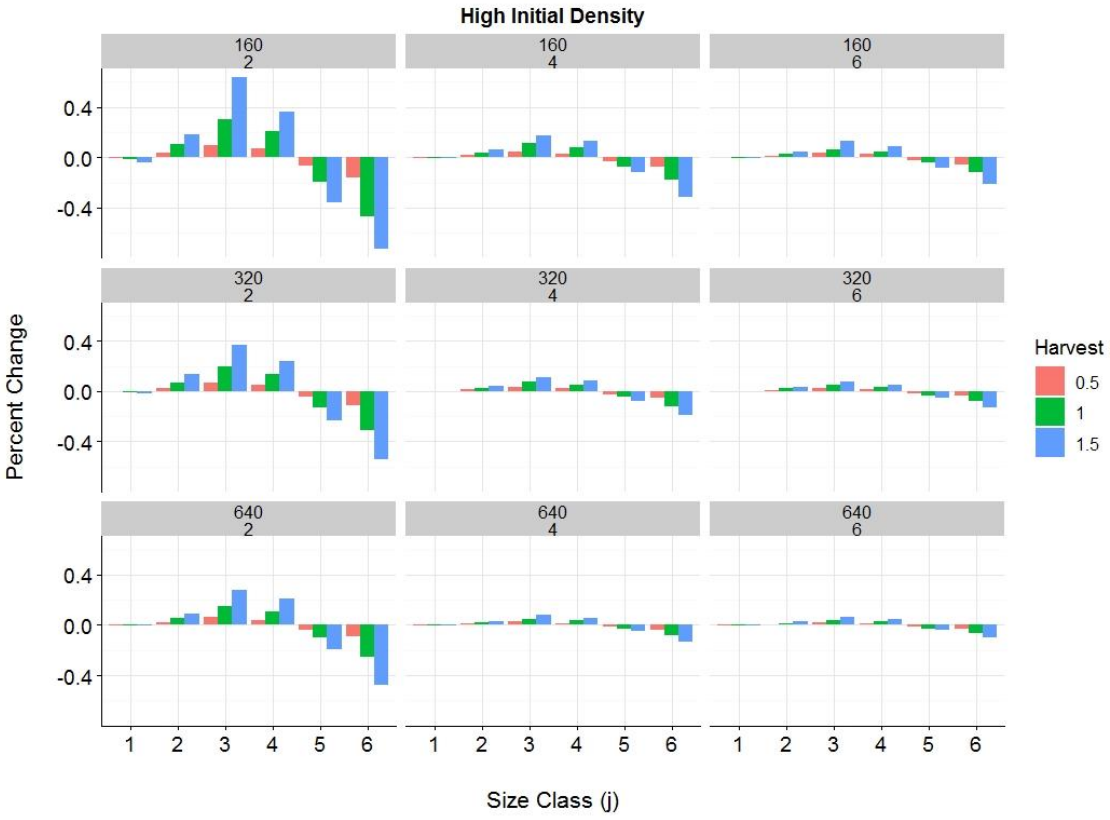
High Initial Density
160
2
160
4
160
6
320
2
320
4
320
6
640
2
640
4
640
6
0.4
0.0
-0.4
1
2
3
4
5
6
Percent Change
Size Class (j)
Harvest
0.5
1
1.5

Figure 3.4. Changes in the proportion of American alligator (*Alligator mississippiensis*) harvestable stage classes ($j \geq 3$) surveyed at maximum effort (Table 3.1) over 20 years. The solid lines show the true underlying proportion of each stage class (color) relative to their initial proportion under the stable stage distribution of **L** (dot-dash lines). The gray paneling in in each cell describes the initial population density (Low/Intermediate/High; rows), and the apparent harvest rate of stage classes $j \geq 3$ (0.5/1/1.5%; columns).

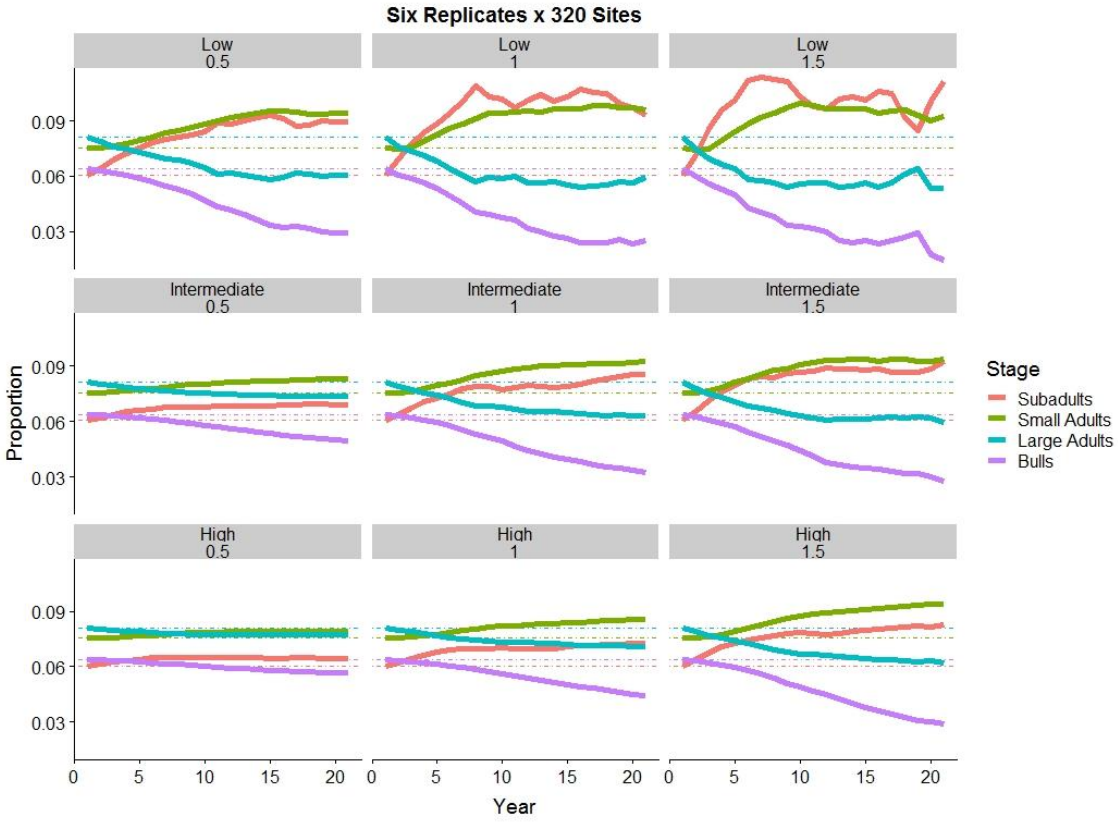

Figure 3.5. Comparison of apparent and realized harvest rate of American alligator (*Alligator mississippiensis*) populations over 20 years simulated under imperfect detection with maximal temporal replication (six visits). The y-axis reflects the harvest rate as applied to the total population (j: 1–6) whereas the line colors in the legend refer to the apparent harvest rate as a function of harvestable stage classes only ($j \geq 3$). The dashed lines reflect the apparent (i.e. intended) harvest rate, whereas the solid lines reflect the realized (i.e., actual) rate. The gray paneling in in each cell describes the number of survey sites (160/320/640; rows), and the initial population density (10/30/60; columns).

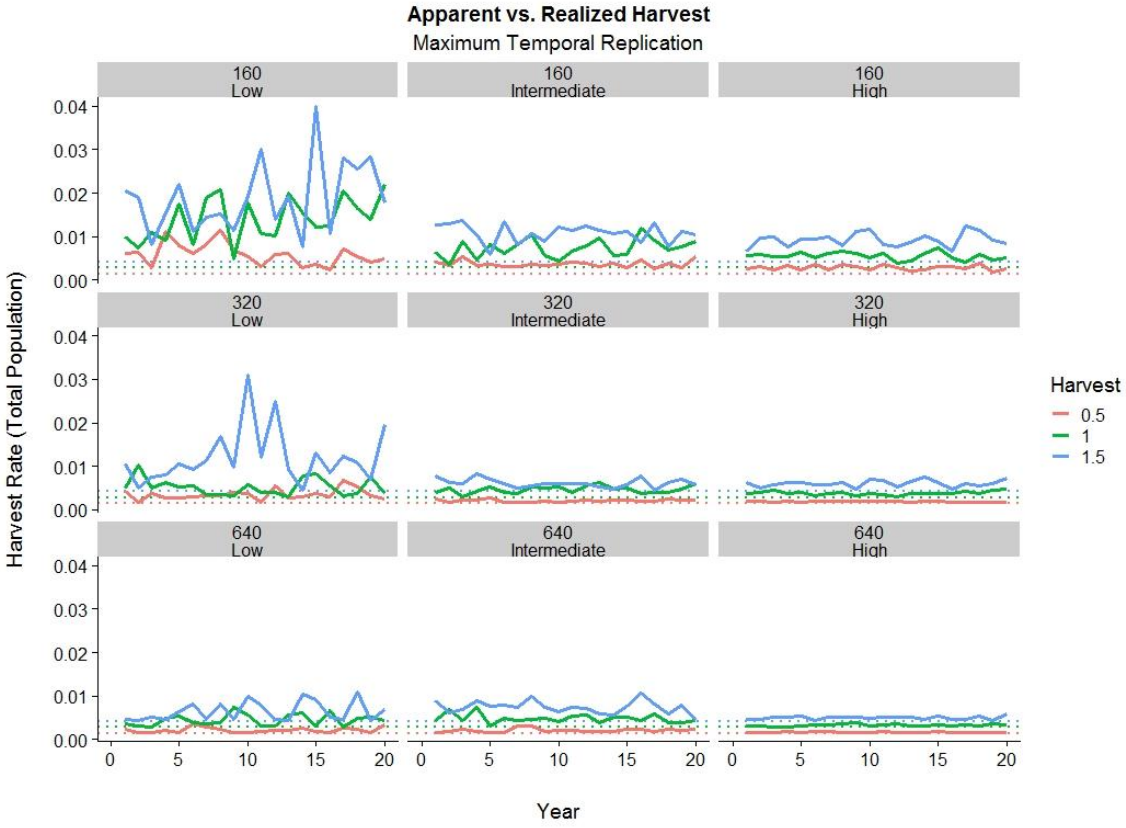

Figure 3.6. Comparison of density patterns over 20 years for a simulated population of American alligators (*Alligator mississippiensis*) of all stage classes at a high initial population density (60 alligators site^{-1}) subject to 1% harvest for $j \geq 3$ (Table 3.2). The dashed line shows the estimated population density produced by the *N*-mixture model with ± SD in the shaded area. The solid line shows the true realized density under imperfect detection, whereas the dotted line shows the same under perfect information. The gray paneling in in each cell describes survey design attributes: the number of sites (160/320/640; rows), and the number of temporal replicates (2/4/6; columns).

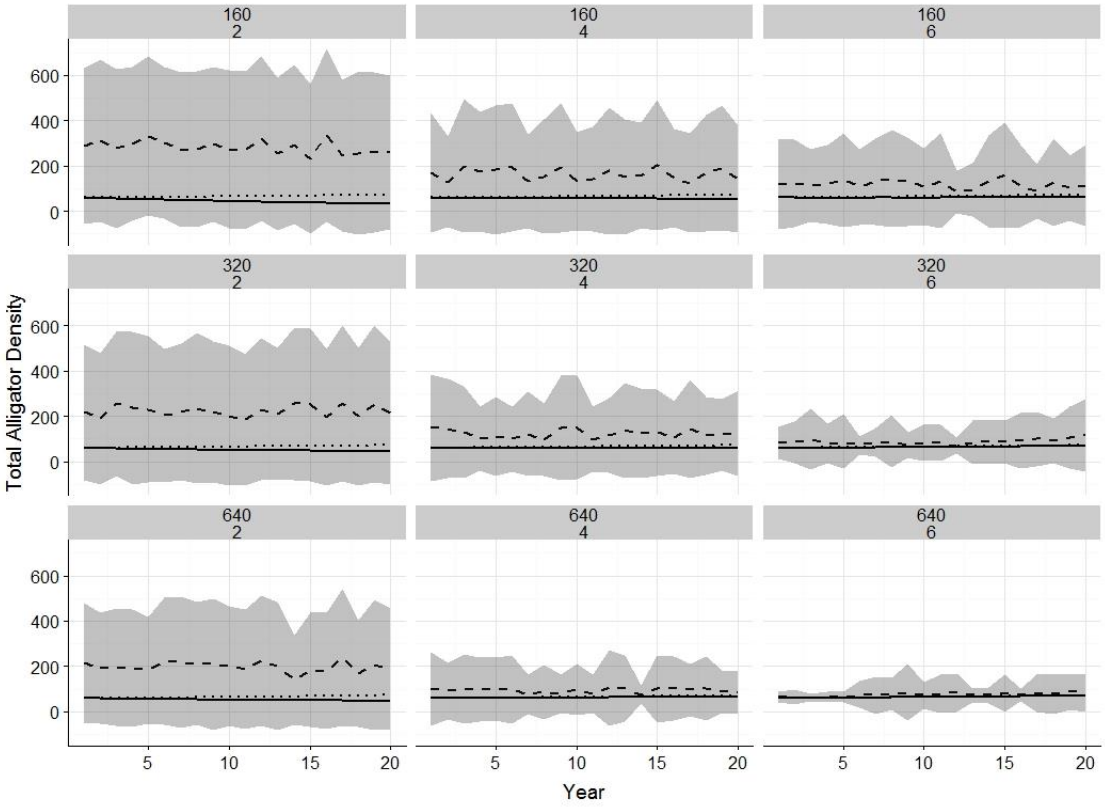

Figure 7. Representation of potential survey designs for American alligators (*Alligator mississippiensis*) as quantified by fundamental objectives (axes). The x-axis reflects FO_1 (maximize financial effectiveness; Eq. 3.17) whereas FO_2 (minimize ecological and management uncertainty; Eq. 3.18) is on the y-axis, in which higher values for both *FO*s represent a more optimal value. The red points indicate survey designs that have declining population growth rate ($\lambda<1.0$) whereas the blue reflects a stable or increasing population ($\lambda\geq1.0$). The triangles represent eligible plans that met both of the constraints ($\lambda\geq0.98$, $EP\leq5\%$), whereas the circles represent plans in which at least one of the criteria was not met. The gray paneling within each section (a–c) lists the apparent harvest rate for stage classes $j\geq3$ (0.5%/1.0%/1.5%; columns). The data point that represents the most optimal plan (*OP* in Eq. 3.19 is maximized) for each initial population density (a. low, b. intermediate, and c. high) and harvest rate combination is circled.

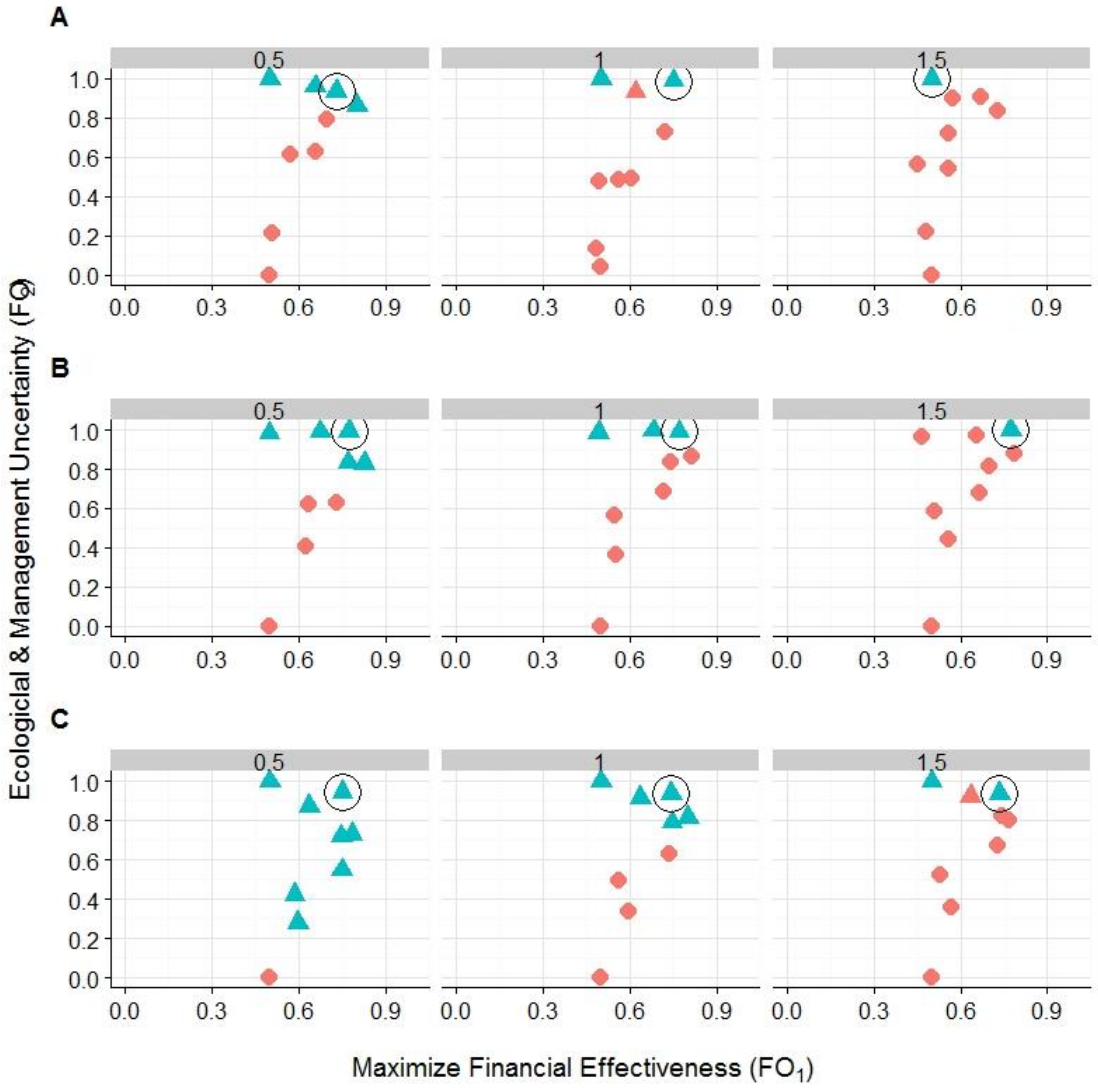

CHAPTER FOUR

NON-LINEAR PATTERNS IN MERCURY BIOACCUMULATION IN AMERICAN ALLIGATORS AS A FUNCTION OF PREDICTED AGE

Abstract

Mercury is a widespread environmental contaminant that readily biomagnifies in wetlands with sulfate-reducing bacteria. Species that feed at the top trophic level within wetlands are predicted to have higher mercury loads compared to species feeding at lower trophic levels and are therefore often used for mercury biomonitoring. However, mechanisms for mercury bioaccumulation in sentinel species are often poorly understood, due to a lack of long-term studies or an inability to differentiate between potentially confounding variables. We examined accumulation patterns of mercury in the whole blood of American alligators (*Alligator mississippiensis*) from a long-term, mark-recapture study (1979–2017) in South Carolina, USA. Using recently-developed growth models and auxiliary information on predicted age at first capture, we were able to differentiate between age- and size-related variation in mercury bioaccumulation, which was previously confounded due to long-held assumptions of indeterminate growth patterns in the species. Contrary to predictions that the oldest or largest individuals are likely to have the highest mercury levels, our best-supported model included interactions between sex and both predicted age and predicted age^2. We found that mercury levels peaked at 30–40 years of age (depending on the sex), and then slowly declined in older individuals. To evaluate the robustness of our findings, we repeated the analysis using

data from a previously published study of mercury in alligators sampled at Merritt Island National Wildlife Refuge in Florida. In contrast to the South Carolina data, the data from Florida contained minimal auxiliary information regarding age. Similarly, the best supported model indicated a quadratic relationship between mercury and body size, a less-precise indicator of age, rather than a linear relationship. These findings highlight how long-term monitoring could be used to differentiate between confounding variables (e.g., age and size) to better elucidate complex relationships between contaminant exposure and demographic factors in sentinel species. Given the rise in popularity of alligator recreational harvest and meat consumption, the use of alligators as a sentinel species has relevant and important applications for both ecosystem- and human-health.

Introduction

Elemental mercury (Hg) is a ubiquitous contaminant that enters the environment through natural atmospheric deposition and as a pollutant from anthropogenic activities (e.g., gold mining, waste incineration, coal-burning power plants) (Hower et al., 2010; Pirrone et al., 2009; Selin, 2010). Following deposition, sulfate-reducing bacteria commonly found in wetland sediments can readily convert Hg to its bioavailable form, methylmercury, a potent neurotoxin that accounts for >95% of the Hg detected in biota (Bank et al., 2005; Compeau, G.C.; Bartha, 1985; Wagemann et al., 1998). Adverse effects of Hg exposure are well-documented in humans and wildlife and include reduced neurological function and immunocompetence, increased embryonic deformities or mortality, and impaired reproductive output (Becker et al., 2017; Bergeron et al., 2011;

Evers et al., 2008; Frederick and Jayasena, 2011; Grippo and Heath, 2003; Wolfe et al., 1998). Methylmercury readily increases in concentration from lower to upper trophic levels (i.e., biomagnification); therefore, apex predators or scavengers are often at increased risk of Hg exposure (Chumchal et al., 2011; Marzio et al., 2018; Snodgrass et al., 2000) and may serve as effective sentinel species for biomonitoring (Sergio et al., 2008). Often, predators have multiple demographic or behavioral traits (e.g., long lifespan, extended parental care, low densities, site fidelity) that make them both sensitive to disturbances (e.g., contaminants) (Benson et al., 2016; Duffy, 2002; Weaver et al., 1996) and amenable to long-term longitudinal monitoring for Hg exposure.

In the context of Hg bioaccumulation in sentinel species, monitoring plans are most effective when designed to identify and differentiate between potentially confounding sources of variation in Hg levels. For example, studies that are limited in temporal scope (<1 year) may be poorly-suited to reduce the uncertainty associated with a chronic environmental stressor such as Hg, particularly in geographic areas with annually-variable or long-term trends in deposition. In the absence of longitudinal sampling of individuals, potentially biologically meaningful relationships between Hg and age or growth rates, as documented in several fish species (Lavigne et al., 2010; Sandheinrich and Drevnick, 2016), cannot be established for species that lack reliable age indicators (e.g., otoliths, plumage patterns). In turn, a limited understanding of growth patterns could also lead to spurious conclusions regarding mercury bioaccumulation as a function of putative or estimated age.

In the southeastern United States, American alligators (*Alligator mississippiensis*; hereafter alligator) are keystone predators that exhibit strong top-down effects on prey community structure and function, and create habitat for other wetland species through the creation of "alligator holes" (Bondavalli and Ulanowicz, 1999; Mazzotti and Brandt, 1994; Nifong and Silliman, 2013). Alligators are an effective sentinel species for Hg biomonitoring because they frequently occupy the top position within wetland food webs (Nifong and Silliman, 2013; Rosenblatt and Heithaus, 2011), are long-lived (Wilkinson et al., 2016), and appear to exhibit long-term site fidelity (A.J. Lawson, P.M. Wilkinson, *unpublished data*). This suite of traits makes them amenable to long-term longitudinal sampling that is reflective of Hg in the surrounding environment (Milnes and Guillette, 2008). Recently, recreational harvest of alligator populations has been implemented throughout most of their range (inset, Fig. 4.1), prompting concerns for human exposure to Hg through the consumption of alligator meat. Therefore, the use of alligators as a sentinel species is relevant for both ecosystem and human health.

Despite the potential utility of alligators for biomonitoring, many studies have reported inconsistent findings with respect to Hg levels as they relate to demographic factors, such as sex or body size (Campbell et al., 2010; Heaton-Jones et al., 1997; Nilsen et al., 2016, 2017b; Rumbold et al., 2002; Yanochko et al., 1997). Recent studies suggest that alligators and other crocodilians exhibit determinate (i.e., asymptotic) rather than indeterminate growth, and continue to reproduce for many years following growth cessation in middle age (Campos et al., 2014; Taylor et al., 2016; Tucker et al., 2006; Wilkinson et al., 2016). For species with determinate growth, age and body size are

confounded in individuals who are near or beyond the average size at growth cessation, in the absence of auxiliary mark-recapture data. In this context, an incorrect presumption of asymptotic (determinate) growth, in which age could be inferred from body size alone, may obscure fine-scale relationships between age and Hg or other interacting variables (e.g., sex, metabolic requirements).

We investigated total mercury (THg) patterns in whole blood of adult and subadult alligators from a population in South Carolina, USA, which supports one of the longest-running crocodilian mark-recapture studies in the world (1979–present). Our objectives were to investigate demographic, individual, and temporal variation in THg bioaccumulation patterns, including previously-unexplored non-linear effects. Whole blood collection is a non-destructive technique that enables longitudinal sampling within individuals, and is also an effective predictor of THg concentrations in both muscle (subject to human consumption) and liver tissues (Moore, 2004; Nilsen et al., 2017b). Additionally, contaminant concentrations in whole blood are linked to mobilization of fat and liver tissues (Jepson et al., 2005; Keller et al., 2014). Therefore, we use the term "bioaccumulation" here, in the context of recent studies that suggest whole blood may be an indicator of THg bioaccumulation in internal tissues for both alligators (Moore, 2004; Nilsen et al., 2017b) and other taxa (Bergeron et al., 2010; Cizdziel et al., 2003; Eagles-Smith et al., 2008).

Alligators exhibit positive allometry, in which changes in jaw structure, musculature, and bite force facilitates consumption of larger prey items (of potentially higher trophic status) throughout growth (Dodson, 1975; Erickson et al., 2003). We

predicted that the relationship between THg bioaccumulation and age in alligators would be nonlinear. We base this prediction on asymptotic growth patterns documented in our study population (Wilkinson et al., 2016), and in subsequent age-related changes in both diet composition (a consequence of positive allometry) and metabolism, as widely documented in other taxa (Elliott et al., 2015 and references therein). We expected to find variation in THg among sexes, potentially due to documented vertical transfer of endogenous THg from females to eggs from our study location (Nilsen et al., 2018) and known differences between male and female reproductive output, growth, movement, and habitat use patterns (Joanen and Mcnease, 1972; Joanen and McNease, 1970; Lawson et al., 2018; Wilkinson et al., 2016). We were also interested in evaluating the applicability of our findings to other alligator studies that lacked auxiliary previous-capture information, so we conducted a replicated, post-hoc analysis on a previously published dataset (Nilsen et al., 2017a) from a shorter-term study, with uncertainty regarding the true age of individuals in the sampled population. Lastly we also examined our results in the context of how age or body size could relate to consumption risk, as quantified by estimated THg muscle content based on whole blood content (Nilsen et al., 2017b).

Materials and Methods

Study area

Our study focused on an alligator population on the north-central coast of South Carolina, USA. We captured alligators on the South and Cat Island portions of the 6033 ha Thomas A. Yawkey Wildlife Center (YWC; 33.217°N, -79.236°W), a state-operated

wildlife management area that has been closed to alligator hunting since the early 1900s. YWC is surrounded by marine (>26 salinity parts per thousand; ppt) and brackish water habitats (5–25 ppt) (Fig. 4.1), in which the mean tidal range is 116 cm (http://www.saltwatertides.com/cgi-local/seatlantic.cgi). Our sampling area within YWC included tidal marsh (2,524 ha), primarily comprised of smooth cordgrass (*Spartina alterniflora*) and black needle rush (*Juncus roemerianus*) and managed impounded wetlands (hereafter impoundments; 1,012 ha). The impoundments contained both emergent vegetation, including smooth cordgrass, tall cordgrass (*S. cynosuroides*), and saltmarsh bulrush (*Scirpus robustus*), as well as submerged vegetation, such as widgeon grass (*Ruppia maritiuma*). Impoundment water levels were typically maintained at 60 cm water depth, with the exception a spring draw-down period lasting approximately 5–6 weeks, to promote seed propagation. Water management practices and rainfall influenced impoundment water salinity, which ranged from 0–35 ppt.

Sample collection

We collected whole blood from alligators captured on YWC from 2010–2017 to examine THg bioaccumulation patterns (hereafter THg study). These individuals were also part of a concurrent, long-term (1979–2017) mark-recapture study on YWC to evaluate alligator growth and demographic patterns. A portion of the individuals in the THg study had been previously encountered by the mark-recapture study (prior to THg study initiation); therefore, we used auxiliary capture information from these individuals to obtain predicted age conditioned on initial capture. Alligators were captured on YWC

intermittently using a combination of modified baited trip-snares (Murphy et al., 1983), walk-through snares (Wilkinson, 1994), snare poles, snatch hooks (Cherkiss et al., 2004), and hand captures (for small alligators only). For each individual, we determined the sex through cloacal examination (Chabreck, 1963) and recorded three standard morphometric measurements (±0.5 cm): total length (TL), snout-vent length (SVL), and tail girth (TG). Individuals were uniquely marked using a combination of toe clipping (1979–1993) (Wilkinson, 1983), tail and caudal scute notching (1979–2017) (Chabreck, 1963; Wilkinson, 1983), metal self-piercing tags applied to the webbing between toes (Conservation Tags 1005-1 (1979–1982) and 1005-681 (2009–2017), National Band & Tag Company) (Jennings et al., 1991), and passive integrated transponder (PIT) tags subcutaneously inserted above the right masseter (GPT12, Biomark, Boise, ID) (Eversole et al., 2014). See Wilkinson et al. (2016) for a detailed description of capture, measurement, and marking techniques. For the THg study, we targeted large subadults (Females: 63.032 cm ≤ SVL < 94.548; Males: 63.398 ≤ SVL < 95.098) and adults (F: ≥ 94.548; M: ≥ 95.098) to increase the likelihood of encountering previously marked individuals. Though exceptions exist, alligators typically reach reproductive maturity at 1.8m TL (Joanen and McNease, 1980; Wilkinson, 1983). We established SVL cutoff values to distinguish between subadults and adults based on predicted SVL at 1.8m TL using sex-specific SVL:TL values from individuals with in-tact tails from our study population (Females: 0.517, Males: 0.520; Wilkinson et al. 2016).

In 2010 we began collecting whole blood from captured alligators to evaluate THg concentrations. Whole blood collection is a non-destructive technique that enables

longitudinal sampling within individuals, and is also an effective predictor of THg concentrations in muscle tissue (Nilsen et al., 2017b), which are subject to human consumption. Immediately following each alligator capture, we collected blood samples via the post-occipital venous sinus using a 6.4 cm sterile 20-gauge needle and a 30 mL syringe (Myburgh et al., 2014). Blood samples were transferred to three 10 mL lithium heparin Vacutainer tubes (BD, Franklin Lakes, NJ) and placed on wet ice in the field before being stored in a -20°C freezer until analysis. Following marking, measurements, and blood collection, all alligators were released at their capture sites. We acquired all necessary alligator sample collection permits from the South Carolina Department of Natural Resources, and the study was approved by the Institutional Animal Care and Use Committees at Clemson University (Permit nos. 2015007, 2016059) and the Medical University of South Carolina (Permit no. 3069).

Whole blood THg laboratory analysis

We used thermal decomposition spectrophotometry, with an automated Direct Mercury Analyzer (DMA-80, Milestone, Inc., Shelton, CT, USA; hereafter DMA) at the Savannah River Ecology Laboratory, University of Georgia (Aiken, SC, USA) to determine the mass fraction of THg in alligator blood samples. We prioritized analyzing (1) longitudinal samples of whole blood from individuals that were captured multiple times within the THg study and (2) samples from individuals that were previously encountered by the mark-recapture study (prior to THg study initiation) so that we could obtain a more accurate predicted age. Blood samples were thawed at room temperature and placed

on a Vortex homogenizer for 30 s, and 1 aliquot (100 μL) was transferred to a nickel weigh boat for analysis in the DMA-80. A portion of the blood samples contained extensive clots that we were unable to homogenize, therefore, we transferred each of the clotted whole blood samples to pre-weighed 15 mL polypropylene centrifuge tubes (VWR, Radnor PA) and freeze-dried them to a constant mass (± 0.1 mg) using a FreeZone lyophilizer (Labconco, Kansas City, MO, USA). We then manually homogenized the freeze-dried (hereafter solid) blood samples using a mortar and pestle before placing 0.01 g of each sample into the nickel weigh boats.

We constructed an external 14-point calibration curve ranging from 0 to 200 ng using the solid Certified Reference Materials (CRM) for trace metals, PACS-3 marine sediment (3.04 ± mg kg^{-1} THg) and TORT-2 lobster hepatopancreas (0.292 ± 0.022 mg kg^{-1} THg) from the Natural Resource Council of Canada (NRC-CNRC; Ontario, Canada). The limit of detection for the curve was 0.302 ng g^{-1}. At the beginning of each day we performed a quality control check that included six instrumental blanks (empty slots within the DMA) interspersed with one PACS-3 and one TORT-2 sample to ensure proper machine functionality and calibration. For quality assurance, whole blood samples were analyzed in batches of ten (approximately) alongside one instrumental blank, two procedural blanks (empty nickel boats), one field blank (thawed Milli-Q Water from lithium-heparin vacutainers filled and frozen in 2011), one standard reference material, and one duplicate of a whole blood sample (Table C1.1). Instrumental and procedural blanks were used to quantify background THg levels within the instrument and weigh

boats, whereas field blanks were used to correct for THg associated with the field sampling procedure.

Blood samples were phase- (liquid vs. solid) and matrix-matched to and reference materials within each run. For liquid samples, we used the National Institute of Standards and Technology (NIST) Standard Reference Material (SRM) 955c levels 3 and 4, Toxic Metals in Caprine Blood, with reference values for total mercury at 17.8 ± 1.6 ng g^{-1} and 33.9 ± 2.1 ng g^{-1}, respectively. For solid samples we used PACS-3, TORT-2, and a NIST SRM 955C level 4 vial that we freeze-dried using the same procedure for the blood samples. We prioritized analyzing liquid samples to replicate the methods of other recent alligator whole blood-based THg studies (e.g., Nilsen et al., 2017b, 2017a, 2016) as closely as possible, and because our matrix-matched SRMs were certified for THg values in liquid phase. We blank corrected all samples in which the instrumental, procedural and/or field blanks were above the detection limit. Additionally, we performed a cleaning procedure that included six machine blanks, two boat blanks, one nickel boat with 0.1 g of all-purpose flour, and one quartz boat containing 0.1 g nitric acid routinely throughout the analytical procedure.

Statistical analysis

Dry to wet weight conversion — To account for sample preparation differences (i.e., use of liquid and solid samples), we used the following formulas from Lusk et al. (2005) to convert the solid sample THg dry weight (*dw*) measurements to THg wet weight (*ww*), both in mg kg^{-1} or parts per million (ppm) units:

$$M = \frac{wm - dm}{wm} * 100 \quad (4.1)$$

$$ww = dw * (1 - \frac{M}{100}) \quad (4.2)$$

We calculated percent moisture content (*M*) of each sample based on the wet mass of the original sample (*wm*) and dried mass of the original sample (*dm*) in g (Eq. 4.1) and used sample *M* and *dw* (measured in mg kg^{-1} by the DMA) to estimate THg wet weight. Moreover, to make our results comparable to other studies, we converted our whole blood THg measurements to estimated muscle THg concentration using a blood to muscle (both mg kg^{-1} *ww*) conversion formula in Fig. 3 of Nilsen et al. (2017b):

$$Muscle = \frac{0.9475 * Blood - 18.701}{1000} \quad (4.3)$$

Method duplicate comparison and sample adjustment — Twenty-three un-clotted whole blood samples were analyzed in both liquid and solid forms (hereafter method duplicates) alongside other phase-matched samples (Table C1.1) to determine potential THg losses from the freeze-drying (lyophilization) process (Litman et al., 1975; Ortiz et al., 2002). The method duplicates (17 females, 6 males) represented all study years except 2015(Table C1.2). Using the converted wet weight (*ww*) THg measurements from the solid samples, we assessed differences in *ww* between paired method duplicates. We identified a single outlier, in which the converted THg *ww* measurement (i.e., the sample

was run as a solid with a converted *dw* to *ww*) was extremely low. The difference between this method duplicate's liquid-run THg *ww* minus its solid-run (converted) THg *ww* was more than 6x the mean difference between paired liquid and solid samples for all method duplicates. We concluded that the method duplicate outlier's solid-run THg value was an anomaly, as opposed to the liquid run sample value, because the liquid sample was run in duplicate during the liquid run and produced consistent THg values. As a result, the outlier's solid run THg value was excluded from all further analyses.

Following outlier removal, THg was significantly higher in liquid samples (mean: 0.142 mg kg^{-1} *ww* ± 0.065 SD) compared to solid samples (0.136 ± 0.069) based on a two-sided paired Wilcox rank-sign test for small sample sizes ($p < 0.001$). The liquid samples averaged 0.006 ± 0.009 mg kg^{-1} *ww* higher than the solids, though three solid method duplicates had higher THg measurements than their liquid counterparts. We squared the difference between paired method duplicates (liquid minus solid THg *ww*) to obtain all positive values, required for Box-Cox transformation. We confirmed that our transformed data followed a normal distribution using Shapiro-Wilks test, and applied two one-way ANOVAs in which difference^2 was modeled as a function of Year or Sex, compared to a null model. Neither term was significant ($p > 0.05$), suggesting no systematic differences could be attributed to the differences between liquid vs. solid samples. Therefore, we added +0.006 mg kg^{-1} to all solid-run sample THg *ww* values. We then averaged all within-run and method duplicates to obtain a single THg value for each unique capture event. We conducted a duplicate analysis in which we applied a solid sample adjustment value that was derived from all method duplicates (+0.007 mg kg^{-1}),

including the outlier, to assess the sensitivity of our results to extreme values and methodological adjustments.

Linear Regression — All statistical analyses were performed in R Version 3.5.0 (R Core Team, 2017). To ensure the data fit the assumptions of linear regression, we assessed it for outliers using boxplots, Cleveland dotcharts, and the 1.5 * interquartile range (IQR) guideline. Though the IQR procedure identified six potential outliers, these data points did not form a consistent pattern based on field, laboratory, or sample variables (e.g., sex, sample age) and their THg values were well within the range of values reported for American alligators (Table 1 in Nilsen et al., 2017a). As the purported outliers were not suggestive of unusual specimens or protocol failure, we retained these values in subsequent analyses. We applied a Box-Cox transformation ($\lambda = 0.384$) to our dataset to meet normality assumptions and to pass the Shapiro-Wilks test.

We examined a suite of covariates in a multi-model linear regression framework to evaluate our hypotheses regarding THg bioaccumulation in alligators. All covariates are continuous unless otherwise stated, with mean values and ranges reported in Table 4.1. We included both Year (categorical) and ordinal date (OD) (day of year) in our analyses to investigate seasonal and annual variation in THg deposition, which has been documented in other studies (Frederick et al., 2004; George and Batzer, 2008; Nilsen et al., 2017a). We included Sex (categorical) and Predicted Age (PA) (described in 2.4.3.1) to evaluate potential demographic differences between individuals, as well as SVL (i.e., body size) which serves as a proxy for age prior to growth cessation. In general, larger individuals are thought to feed on larger-bodied prey items that are more likely to have

higher THg; similarly, if THg intake exceeds offloading, then we expect THg to positively vary with age. We also included body mass index (BMI), as individuals with higher THg loads are more likely to have reduced neuromuscular function, which could affect foraging behaviors and thereby body condition (Nilsen et al., 2017a). We checked for multicollinearity between our continuous covariates using linear regression and Pearson's correlation coefficients. The only correlation we detected was between SVL and PA (r: 0.56), so we did not construct any models that contained both of those terms. The continuous covariates contained no missing values and were z-standardized across years (mean = 0.0, SD = 1.0). Lastly, we also considered models that included Year or individual as a random effect, the latter to account for the nested structure in our dataset (i.e., repeated samples from individuals).

Predicted age and body mass index calculations — In our YWC study population, individuals appear to exhibit determinate (i.e., asymptotic) rather than indeterminate growth (Wilkinson et al. 2016). We used the Baker et al. (1991) form of the Schnute (1981) growth formula to estimate predicted age at first capture for a given SVL using the sex-specific growth parameters for our study population as reported in Wilkinson et al. (2016). Note that the PA estimation formula (Eq. 4.4) in Wilkinson et al. (2016) is incorrect; therefore, we used Eq. 5 in Baker et al. (1991):

$$t_m = \tau_1 - \frac{1}{a} - \ln\{\frac{{y_m}^b - {y_1}^b}{{y_2}^b - {y_1}^b}\left(1 - e^{-a(\tau_2 - \tau_1)}\right)\} \quad (4.4)$$

In which t_m and y_m denote the age and SVL of an individual at marking (i.e., first capture), respectively. The τ_1 and τ_2 terms are fixed values that indicate the minimum and maximum ages observed in a population (both sexes: 0–45), whereas y_1 (both sexes: 12.5 cm) and y_2 (females: 135.0 cm, males: 182.8 cm) denote the SVL at ages τ_1 and τ_2, respectively. The *a* term is the fixed growth rate (females: 0.113 yr^{-1}, males: 0.098 yr^{-1}) and *b* (females: 0.721, males: 0.692) is the dimensionless shape parameter. We assigned the average age at cessation of growth (females: 31, males: 43) for individuals whose y_m was equal to or exceeded the estimated SVL at growth cessation (females: 131.4, males: 182.0) as estimated in identified in Wilkinson et al., (2016). We then used the predicted age at first capture as a basis to estimate predicted age (PA) for all subsequent captures by counting forward in whole years for each subsequent encounter. Additionally, we derived estimates of PA in decimal years that could account for the actual date within a capture year and performed a t-test on model parameters from the whole-years and decimal-years models to determine if they were significantly different.

We also evaluated the relationship between BMI as a predictor of THg. Animals were not weighed during the study; therefore, we opted to use the BMI estimator described by Nilsen et al. (2017a), which relies on the standard morphometric measurements we collected.

$$BMI = \frac{TG}{SVL*2} \quad (4.5)$$

In which: TG denotes tail girth (i.e., circumference) in cm at the cloaca (urogenital slit), and SVL denotes snout-vent length in cm. After assessing BMI covariate values, we opted to model BMI as a continuous covariate, rather than categorical as done by Nilsen et al.,

(2017a) because all but three of our observations fell into the "Normal" BMI category based on the 0.18 BMI cutoff value.

Model Construction and Selection — We began our model-selection process by constructing a set of univariate models that contained each of our covariates, quadratic effects for the continuous covariates (BMI, OD, PA, SVL), the two random effects (Year, Indiv), and an intercept-only (null) model. We also created interactive and additive models to investigate several biologically relevant relationships: Sex * OD, Sex * SVL, Sex * PA, Year * OD, and OD * PA. We were particularly interested in the sex-related covariate interactions as Nilsen et al. (2018) reported that nesting female alligators can vertically transfer their endogenous THg to egg yolk. The Sex * OD interaction allows the mean levels of THg prior to and following nesting activity to vary by sex over the course of the season. Similarly, the Year * OD interaction permits within-season trend in THg to vary annually. Interactions between Sex and the size and age variables, SVL and PA, allow their linear relationship with THg to differ by Sex, which may be expected as male and female alligators in our study population differ in growth rates and age at sexual maturity (Wilkinson et al., 2016). Finally, any differential pattern in the within-season trend in THg that is related to alligator age may be reflected in the OD * PA interaction. Any interactive or quadratic term appearing in a model was accompanied by its lower-order constituent effects as additive terms. Note that models containing random effects were fit with restricted maximum likelihood (REML) and deviance values are not directly comparable to non-REML fit models.

We used Akaike's information criterion adjusted for small sample size (AICc) to identify the most parsimonious models using the *MuMIn* package in R (Bartoń, 2018). Following the initial model construction phase (*n*=23 models), we performed AICc model selection and created three additional models that combined the covariate effects contained in competitive models (i.e., within 4 ΔAICc units of the best-supported) (Burnham and Anderson, 2002) to determine the best-supported model overall. We evaluated covariate effect significance within individual models based on whether or not the coefficient's 85% confidence intervals overlapped zero (Arnold, 2010).

Post-hoc re-analysis of Merritt Island National Wildlife Refuge THg study

We conducted a post-hoc re-analysis of Nilsen et al.'s (2017a) data collected at Merritt Island National Wildlife Refuge (MINWR) in eastern-central Florida (inset, Fig. 4.1) from 2007–2014 (see Nilsen et al., 2017a for details on study site, sample collection, and laboratory methods). We were particularly interested in exploring effects that were not evaluated by Nilsen et al. (2017a), including predicted age and quadratic relationships for the covariate effects described in this paper. Like the YWC population, a mark-recapture study was initiated at MINWR in 2006, prior to the Nilsen et al. (2017a) THg study. To estimate predicted age, we obtained additional data on SVL at first capture for the MINWR alligators (R.H. Lowers, *unpublished data*), and applied the growth model developed for our study population (Wilkinson et al., 2016) as described in Section 2.4.2, as no growth model currently exists for Florida alligators. We excluded four outliers that were removed in the original study, and applied a Box-Cox transformation ($\lambda = 0.02$) to

the remaining MINWR data, which passed the Shapiro-Wilks test for normality upon transformation. We then followed the same procedure for covariate formatting (e.g., continuous vs. categorical) and standardization, model construction, and model selection as applied to the YWC data. Note that BMI was modeled as a categorical covariate by Nilsen et al. (2017a), whereas here we treated it as continuous for comparison purposes. Lastly, we decided not to conduct a pooled analysis that included both YWC and MINWR individuals due to differences in mark-recapture study sampling period (OD in Table 4.1) and duration that would have caused confounding issues between site and the predicted age covariate.

Results

Quality assurance/quality control

The limit of detection (LOD) for our DMA analyses was 0.302 μg kg^{-1}, based on 3*SD of all procedural blanks (n=57) used in 11 runs (Table C1.1). The mean THg value for our analytical blanks was 0.075 ± 0.101 SD μg kg^{-1}, and all but three of our samples were below the LOD, therefore were did not blank-correct our samples. All means hereafter reported ± unless stated otherwise. We computed mean percent recovery (SRM sample THg divided by the SRM certified value expressed as a percentage) for each SRM type (Table C1.3) and across SRM samples within a run (Table C1.4). The mean percent recovery was highest for SRM 955c level 3 (117.8% ± 8.9; 108.4, 136.7), followed by SRM 955c level 4 (117.2% ± 8.2; 103.6, 132.1), TORT-3 (100.9% ± 2.0; 98.9, 103.5), and PACS-2 (90.2% ± 6.2; 98.9, 103.5). The absolute difference between the mean Hg

SRM value for each standard and it's certified THg value was less than 2.5*certified THg SD for all standards. The overall mean recovery percentage across runs (n=11) was 110.7% ± 8.2, whereas run 11 had the lowest percent recovery (98.9% ± 19.3) and run 4 had the highest (127.4% ± 13.1) (Table C1.4).

A potential explanation for the high percent recovery for both SRM 955c level 3 and run 4 is that it was the final session in which we used our single vial of this standard. While we followed NIST's recommendation that a vial not be used if less than one-third on the original blood volume remained, due to potential evaporative losses that could increase the THg concentration, it is possible that evaporative losses occurred before the volume threshold was reached. We also note that the mean percent recovery is also fairly high for SRM 955c level 4 (Table C1.3). However, the SRM 955 level 4's certified values are in *ww*, whereas the mean sample value we calculated in Table C1.4 includes eight samples that were run as solids (runs 8–11 in Table C1.1), meaning that they were not phase-matched— which is why we also included phase-matched standards (TORT-3, PACS-2) for all of the solid runs. When the non-phase matched samples are excluded, the SRM 955c level 4 mean value drops to 111.2% ± 5.3 (Table C1.3).

Tom Yawkey Wildlife Center

Summary statistics — We analyzed 218 whole blood samples for THg (Table C1.1), which included 30 within-run and 23 method duplicates, associated with 165 unique capture events from 113 individual alligators (67 Females, 46 Males) captured at YWC from 2010–2017 (Table 4.1). Based on SVL cutoff values, adults comprised the

majority of our capture events (n=159; F: 105, M: 54) compared to subadults (n=6; F: 2, M: 4). Our sample included 37 individuals (27 F, 10 M) that were recaptured during the THg study period, with a mean of 864 ± 653 days between recapture events (F: 957 ± 706, M: 552 ± 269). Similarly, 38 individuals (27 F, 11 M) were initially encountered by the YWC long-term mark-recapture study prior to their first blood-sampling event for this study. Based on sample summary statistics (Table 4.1), females in our sample population appeared to be older and smaller than males, with a mean predicted age of 31 ± 13 years (range: 8–66) and SVL ranging from 78.6 to 150.5 cm (mean: 127.26 ± 11.58), whereas males averaged 23 ± 13 (range: 8–59) years of age, and ranged from 85.0 to 191.8 SVL (mean: 141.69 ± 30.05). Mean BMI (0.22 ± 0.02) did not differ between sexes, and only two females and one male were categorized as having "Low" BMI (i.e., BMI < 0.18 as specified by Nilsen et al. 2017a). Lastly, we generally captured females later in the year (mean ordinal date: 157 ± 41) than males (139 ± 64), though the range for ordinal date of capture was the same for both (56–271). The preponderance of females captured later in the year is a result of a research focus on alligator nesting ecology at YWC from 2009–2017 (P.M. Wilkinson, *unpublished data*). Over this period, both sexes were captured for general mark-capture purposes each year during April and May, while females tended to be captured during June and July (nesting season).

Model selection results — After converting the solid samples from *dw* to *ww* (mean percent moisture: 85.32 ± 3.37) and adding the methodological adjustment (+0.006 mg kg^{-1}) to the converted *ww*, and then averaging within-run and method duplicates, THg whole blood averaged 0.16 ± 0.05 mg kg^{-1} *ww* for our study population (Females: 0.15 ±

0.05, Males: 0.16 ± 0.07). All mercury values hereafter are reported in THg mg kg^{-1} *ww* unless otherwise stated. Estimated muscle THg averaged 0.13 ± 0.04 (F: 0.13 ± 0.04, M: 0.13 ± 0.06), and ranged from 0.02 to 0.32. Of the 26 regression models we constructed (Table 4.2), two were considered competitive (ΔAICc < 2.0) (Burnham and Anderson, 2002) and overlapped in covariate support (Table 4.2). Our best-supported model contained 0.46 of the model weight (w_i) and included an interaction of Sex with both PA and PA^2 (Fig. 4.2a). The relationship between age and THg in whole blood of alligators was quadratic peaking at approximately 40 years in both males and females; the slopes and maximum points differed, however, between sexes (Fig. 4.2a). Based on 85% CIs we detected significant covariate effects for PA (β_{PA} = 0.15 ± 0.08 SE; 85% CI: 0.03, 0.26), PA^2 (-0.15 ± 0.07; -0.26, -0.04), Sex * PA (0.26 ± 0.13; 0.07, 0.46), and Sex * PA^2 (-0.33 ± 0.14; -0.54, -0.12).

Our second best-supported model (ΔAICc = 0.47; w_i = 0.37) also contained significant PA (0.19 ± 0.05 SE; 0.11, 0.27) and PA^2 (-0.20 ± 0.05; -0.28, -0.12) terms, but lacked sex effects in either additive or interactive form (Fig. 4.2b). We detected no statistically significant differences between the beta coefficients in the predicted age derived from whole-years models (reported here) vs. decimal-years ($p > 0.05$). Lastly, our duplicate analysis that used the adjustment value derived from all method duplicate differences (including the outlier) produced identical model rankings and therefore is not discussed further.

Merritt Island National Wildlife Refuge

Summary statistics— Our post-hoc re-analysis of Nilsen et al.'s (2017a) data included THg measurements associated with 189 unique capture events from 169 individual alligators (72 females, 97 males) captured at the Merritt Island National Wildlife Refuge (MINWR) from 2007–2014 (Table 4.1). Like YWC, adults comprised the majority of our capture events (n=177; F: 70, M: 107), compared to subadults (n=12; F: 8, M: 4). The MINWR data included 19 individuals (6 F, 13 Males) that were recaptured during the study, with a mean of 693 ± 607 days between recapture events (F: 716 ± 610, M: 683 ± 629). Additionally, 18 individuals (4 F, 14 M) were previously encountered by the MINWR mark-recapture study prior to the first blood-sampling event for Nilsen et al. (2017a).

Based on the estimated mean predicted age derived from the first-capture event information (R.H. Lowers, *unpublished data*) and the Wilkinson et al. (2016) growth model, individuals in the MINWR study averaged ≥ 20 ± 7 years of age (F: 19 ± 6, M: 21± 7). The MINWR study sampled individuals over a broader range of ordinal dates (MINWR: 5–365, YWC: 56–271), though individuals were of similar body condition (BMI) and size (SVL) compared to the YWC population (Table 4.1). Additional MINWR mean covariate values and sex-specific comparisons, previously published by Nilsen et al. (2017a), are listed in Table 4.1.

Model Selection Results — The mean for THg in whole blood for the MINWR alligators (Overall: 0.18 ± 0.09, Females: 0.18 ± 0.09, Males: 0.19 ± 0.09; Nilsen et al., 2017a) appeared similar to the YWC study population. In the initial model construction phase, we constructed 23 linear regression models in an AICc model selection

framework. All covariate terms contained in the competitive models (ΔAICc $\leq$ 4.0) were already combined in existing models, therefore, we did not construct additional models as done for YWC. The best-supported model received an overwhelming majority of the model weight (w_i = 0.85, Table 4.3) and contained significant effects of SVL (β_{SVL} = 2.03 ± 0.35 SE; 85% CI: 1.52, 2.54) and SVL^2 (-1.95 ± 0.07; -2.46, -1.44) with large effect sizes. The second best-supported model was not competitive based on its ΔAICc score (Burnham and Anderson, 2002), and only received 0.15 of the model weight, though it overlapped in covariate support with the most parsimonious model (Table 3).

Discussion

Total mercury concentrations in whole blood

Our study is among the most comprehensive assessments of total mercury (THg) bioaccumulation patterns in crocodilians to date and is the first to differentiate between size- and age-driven sources of variation in THg in adult alligators. Due to the temporal breadth of the YWC study (2010–2017), we analyzed whole blood samples of varying age and quality that required multiple processing methods and analytical adjustments. Previous studies have reported mixed results of storage time on THg concentrations in whole blood. Varian-Ramos et al. (2011) analyzed frozen whole blood samples at multiple time points over a three-year period and detected an average 6% increase in THg concentrations. However, storage time explained less than 11% of an instantaneous, rather than progressive, increase in THg over time (Varian-Ramos et al., 2011). In contrast, Sommer et al. (2016) reported that multiple Hg species in whole blood remain

stable for at least one year if stored below 23°C. All YWC samples were analyzed in February and April 2018 (Table C1.1); therefore, including Year as a covariate in regression models could potentially capture temporal variation of Hg in the environment, sample age (freezer storage time), or both. Though none of our regression models that contained Year were competitive (Table 4.2), we acknowledge that both freezer storage time and environmental factors may be confounded. South Carolina does not have a long-term monitoring network for environmental THg. It is theoretically possible, therefore, that THg may have increased over time in our stored samples (as observed in Varian-Ramos et al., 2011), while concomitantly environmental THg may have decreased. Such a phenomena could produce a null effect of time similar to what we observed.

The whole blood THg values reported here for the YWC population in coastal South Carolina appear similar to a concurrent study of nesting females in the same population (0.17 ± 0.063 SD mg kg^{-1} *ww*) (Nilsen et al., 2018), as well as several sites in Florida, including MINWR (Nilsen et al., 2017a), Lake Lochloosa (0.20 ± 0.08), Lake Trafford (0.18 ± 0.07), and the St. Johns River (0.13 ± 0.06) (Nilsen et al., 2016). In contrast, THg in our samples appears to be considerably lower compared to samples from adult alligators in Florida occupying Water Conservation Areas 2A (0.41 ± 0.22) and 3A (0.53 ± 0.42) near Everglades National Park (Nilsen et al., 2016), and compared to Par Pond at the Savannah River Site in South Carolina (0.32, converted from *dw* to *ww* using methodological adjustment and percent moisture reported here, SD not reported) (Jagoe et al., 1998). Both Everglades and the Savannah River Site (approximately 233 km. inland from YWC, Fig. 4.

1) have an established history of Hg pollution from natural and anthropogenic sources (Brisbin et al., 1996; Frederick et al., 2004; Rumbold et al., 2008; Yanochko et al., 1997). Local Hg input may also explain why the findings of Jagoe et al. (1998) contrast with South Carolina's increasing Hg gradient from the Blue Ridge/Piedmont physiographic region to the coastal plain (Guentzel 2009), which is reflected in fish species and is primarily driven by the percentage of wetland area within each watershed (Glover et al., 2010).

Demographic factors in THg patterns

We detected three consistent, general patterns in THg concentrations in alligator whole blood in the YWC and MINWR populations (Tables 4.2, 4.3). Specifically, (1) potential but inconsistently-supported differences between THg bioaccumulation and sex; (2) a relationship between THg and age-based indicators (i.e., predicted age estimated from growth models and mark-recapture records at YWC, and snout-vent length (which is a reliable indicator of age prior to growth cessation) at MINWR; Figure 3); and (3) that age-related patterns in THg were best described by quadratic terms. We discuss each in turn.

The model sets from both YWC and MINWR included support for potential differences among sexes in THg bioaccumulation, though the strength of evidence differed between the two populations (Tables 4.2, 4.3). Though our study detected sex differences in THg, many studies in alligators (Burger et al., 2000; Campbell et al., 2010; Rumbold et al., 2002; Yanochko et al., 1997) and other crocodilians (Eggins et al., 2015;

Schneider et al., 2012; Vieira et al., 2011) have not. Sex-specific differences in behaviors that likely influence THg exposure (e.g., diet, movement, and habitat use; (Joanen and Mcnease, 1972; Joanen and McNease, 1970; Lawson et al., 2018) are well established. However, it remains unclear what, if any, local environmental, habitat, or demographic variables may promote or homogenize behavioral differences among sexes. As such, sex-specific differences in THg could be driven by complex spatiotemporal variation in alligator behavior, which could explain the lack of a consistent pattern regarding sex and THg across all studies.

The two best-supported models from YWC included predicted age, although predicted age did not appear in the most competitive model from MINWR (Tables 4.2, 4.3). We suggest that the mixed support for the predicted age covariate at MINWR compared to YWC is likely due to three factors: (1) differences in mark-recapture study length duration (YWC: 39 years; MINWR: 9 years) which would limit the potential age ranges that could be observed; (2) the limited number of individuals with auxiliary first capture data prior to the THg studies (YWC: 38; MINWR: 18); and (3) the use of a South Carolina-based growth model (Wilkinson et al. 2016) to derive predicted age estimates for MINWR alligators. Though latitudinal differences in temperature can create variation in the length of growing season for alligators, YWC growth rates are similar to those observed in coastal Louisiana, which has a similar latitude to that of MINWR (Jacobsen and Kushlan, 1989; Joanen and McNease, 1971; Wilkinson et al., 2016). While predicted age derived from a growth formula is a more direct indicator of "true" age, size may serve as an effective proxy in individuals that are still growing. In a post-hoc assessment,

only 1% of observations in the MINWR dataset had reached the mean sex-specific size at cessation of growth (F: 131.4, M: 182.0) (Wilkinson et al., 2016), compared to YWC (27.2%). Therefore, in settings like MINWR in which sampled animals have not ceased growing, we posit that SVL may be an effective proxy for true age. We also acknowledge, however, that using the YWC growth model may have introduced uncertainty in MINWR predicted age estimates and that size at cessation of growth may differ between the two populations.

Both model sets indicated strong support for quadratic patterns in THg bioaccumulation with age (Tables 4.2, 4.3). In the YWC population, THg increases prior to the onset of reproductive maturity at 15.8 years for females and 11.6 years for males (corresponding to 1.8 m TL) (Joanen and McNease, 1980; Wilkinson et al., 2016), and peaks at 43 (female) and 38 (male) years of age (Fig. 4.2), before declining. The decrease in THg that we observed in the oldest individuals (Fig. 4.2) contrasts with studies in fish that have reported strictly linear, positive relationships between mercury and age (as determined by otolith analysis) (Chumchal and Hambright, 2009; Lavigne et al., 2010). Multiple avian studies have documented no age-related effects in adult individuals of known-age (Becker et al., 2002; Burger et al., 1994; Furness et al., 1990; Thompson et al., 1991). We assert that the age-related decline in THg is not an artifact of our study design for several reasons. First, we determined that predicted age associated with each sample was not a function of capture year (i.e., we were not encountering older individuals in later study years). Therefore, more recent samples, for which storage time was shorter, were not characterized by lower THg values nor were they associated with

older individuals. Second, it is unlikely that our results reflect a survivorship bias in our data, in which individuals with higher THg levels had higher mortality rates, leaving only individuals with lower THg available for encounter at the oldest ages. The maximum whole blood THg value we measured (0.35 mg kg^{-1} *ww*) is substantially lower compared to values observed in the Everglades (1.33–1.56) (Nilsen et al., 2016), and our maximum estimate of THg in muscle (0.32 mg kg^{-1} *ww*) is less than the World Health Organization's fish consumption advisory value (0.50 mg kg^{-1} *ww*) (WHO, 1990). Lastly, there appears to be only a single potential case of mercury-induced mortality in a wild alligator, in which the individual had muscle THg levels (3.48 mg kg^{-1} *ww*) 27 times higher than the estimated YWC mean, and also surpassed all known lethality levels observed in dosing studies in other reptiles and amphibians (Brisbin et al., 1998; Hall, 1980; Wolfe and Norman, 1998).

Predicted Age as an Indicator of THg in Crocodilians

Traditionally, growth patterns in reptiles have been universally described as indeterminate (i.e., no growth cessation) (Charnov et al., 2001; Congdon et al., 2013; Kozlowski, 1996), however, there is increasing consensus that some species within reptile taxa exhibit determinate (i.e., asymptotic) growth, including lizards (Congdon et al., 2001), turtles (Congdon et al., 2001), and crocodilians (Campos et al., 2014; Taylor et al., 2016; Tucker et al., 2006; Wilkinson et al., 2016; Woodward et al., 2011). While size could serve as an appropriate proxy for age in species with indeterminate growth, reliance on size as an indicator of age in determinate growth species is particularly problematic

for individuals that are near or have growth cessation (i.e., terminal size). In this context, it is not surprising that the majority of studies in both alligators and other crocodilian species have either detected a weakly positive (Nilsen et al., 2017a; Schneider et al., 2012; but see Eggins et al., 2015) or non-existent relationship between size/age and mercury (Campbell et al., 2010; Rainwater et al., 2007; Rumbold et al., 2002), or reported an inconsistent relationship that differed in effect size depending on the tissue sampled or study site (Jagoe et al., 1998; Yanochko et al., 1997).

Concomitant with long-held assumptions of indeterminate growth, existing alligator studies have only explored linear relationships between mercury and age proxies, reflecting an assumption of mercury bioaccumulation throughout an individual's lifespan. Increases in mercury are to be expected for growing individuals and are supported by our results. During the growth phase, juveniles and young adults feed at lower trophic levels compared to adults (Hanson et al., 2015; Nifong et al., 2015; Santos et al., 2018) and are therefore expected to have lower THg than older, larger individuals. However, it is unclear how bioaccumulation patterns may change following growth cessation, given the dearth of studies that have evaluated known- or minimum-age patterns in behaviors that could affect mercury bioaccumulation (e.g., diet, movement, etc.).

Our study indicates that THg begins to decline in individuals around the age of expected growth cessation (Fig. 4.2a), and here we provide two general hypotheses to explain this pattern: (1) alligators become more efficient at shedding or offloading mercury after reaching middle age, or (2) older alligators are exposed to or intake less mercury. Regarding the first point, female alligators can mobilize and deposit stored

mercury in developing eggs during vitellogenesis (maternal transfer), thereby reducing mercury body burdens in the former following oviposition (Nilsen et al., 2018). However, if this were the primary mechanism underlying the non-linear pattern we observed, then THg would begin to decrease at the onset of sexual maturity which occurs at ca. 16 years of age (Fig. 4.2) (Joanen and McNease, 1980; Wilkinson et al., 2016). In contrast, the relationship we detected suggests that THg concentrations continue to increase for many years following the onset of sexual maturity. Additionally, though both sexes excrete mercury in keratinized tissues such as their skin and claws, it is unclear how the speed or efficiency of this process relates to age (Burger et al., 2000; Jagoe et al., 1998).

Alternatively, the patterns we observed may be due to reduced mercury exposure and accumulation in older individuals that are either exposed to or consume less mercury compared to younger individuals. Differences in exposure among age classes would require that the oldest and youngest adults/old subadults inhabit areas with lower mercury bioavailability compared to areas inhabited by middle-aged individuals. Although spatial segregation of adult size classes has been documented in Nile crocodiles (*Crocodylus niloticus*) (Hutton, 1989), we suggest this is unlikely for alligators in our study area where extensive population surveys and capture efforts in fixed locations have demonstrated considerable spatial overlap among adult size classes (A. Lawson, P. Wilkinson, *unpublished data*). Additionally, large alligators (> 2.73m TL) are generally the most cannibalistic and consume both juveniles and young adults (1.22–2.12) (Rootes and Chabreck 1993), further suggesting a spatial overlap among age classes.

Lower mercury levels in the oldest individuals could also reflect reduced mercury intake from either age-related shifts in diet, where food items were characterized by different mercury loads, or from an age-related change in the amount of food consumed. While age-related differences in diet between adult and juvenile alligators are well-established through stable isotope and stomach content analyses (Delany et al., 1999; Nifong et al., 2015; Santos et al., 2018), fine-scale, size-related variation within adults or longitudinal patterns within individuals remain relatively unexamined. In saltwater crocodiles (*C. porosus*), Hanson et al. (2015) detected a quadratic relationship between body size and trophic position (as indicated by $\delta^{15}N$), with medium-sized individuals foraging upon a larger proportion of prey items from higher trophic levels compared to the smallest and largest individuals. Moreover, Hanson et al., (2015) did not detect evidence of spatial segregation among size classes, suggesting that individuals were feeding in the same areas. Similarly, in Yacare caimans (*Caiman yacare*), Rivera et al. (2016) reported that large adult caimans had significantly lower THg content than seven common fish prey species, despite being a top predator. However, like THg, long-term, longitudinal studies would provide a means by which to evaluate age-related diet patterns within adults and other age classes.

Reduced mercury intake as a consequence of reduced food consumption could also occur due to senescence. Though age-related declines in metabolism are well-documented across wildlife taxa (Elliott et al., 2015 and references therein), such patterns have yet to be investigated in reptiles. The quadratic relationship we detected suggests that the cessation of growth (31 years for females, 43 years for males, vertical dashed

lines in Fig. 4.2a) coincides with the onset of the decline in THg. In the YWC alligator population, mark-recapture data indicate that females continue to reproduce for at least twenty years following the cessation of growth (Wilkinson et al. 2016). Therefore, while maternal transfer of THg does not explain the patterns we observed in younger, smaller adults, this could act as a depuration mechanism in older females, particularly those that have ceased growing. We further acknowledge that variation in THg levels in early life stages not evaluated by this study (e.g., hatchlings) could affect individual growth rates or trajectories and bias estimates of predicted age. However, multiple studies focused on fish indicate strong support for biodilution, in which mercury accumulation is determined by individual growth rates, rather than initial mercury concentrations determining eventual growth rates, and faster-growing individuals accumulated mercury at lower rates than slower-growing individuals (Lavigne et al., 2010; Sandheinrich and Drevnick, 2016). Though further studies are needed to determine if biodilution effects are present in alligator populations, in this context it is unlikely that variation in early-life Hg exposure biased our estimates of predicted age.

Implications for Mercury Biomonitoring

We acknowledge that the use of predicted age to predict THg content in whole blood and muscle of alligators is potentially problematic for several reasons and warrants additional study if this relationship is to be used to inform guidelines regarding consumption of alligator meat. First the use of predicted age is a considerable violation of the required assumption in linear regression that covariates are measured without error, as it is a value

output from a predictive model, i.e. the Baker et al. (1991) formula. Thus, the error for predicted age is likely to be is positively related to SVL at first capture (i.e., a larger prediction error for individuals at or near the average size at growth cessation), resulting in a non-constant variance that may induce some bias into our regression coefficients. Nonetheless, despite this issue we posit that the general quadratic pattern of THg of age is robust for two main reasons. First, though SVL was likely measured imperfectly in the field, it does not include a directional bias associated with the predicted age covariate and also received consistent support for both study populations (YWC and MINWR; Tables 4.2, 4.3). Second, the MINWR population had a much smaller proportion of individuals that had passed the average size at growth cessation, thus, reducing potential bias in the covariate for that population. However, given the caveats just described, we suggest that if the relationship between age/size and THg were to be used to inform consumption guidelines, additional studies limited to known-age individuals would be necessary to explore potential risks regarding the use of predicted, rather than known-age, as it relates to THg bioaccumulation.

Conclusion

Mercury is a ubiquitous contaminant that is biomagnified within wetland food webs. We detected a previously undescribed pattern of THg in blood samples from two alligator populations, in which THg peaks at middle age approximately coinciding with the cessation of growth. Therefore, our data suggest that regulatory agencies interested in minimizing risk from consumption of alligators may consider developing additional

studies to further examine this relationship. While this pattern contrasts with previous assumptions of increasing THg throughout an individual's lifetime, we posit that the observed reduction in THg is likely due to age-related changes in foraging behaviors (e.g., reduced food intake due to senescence or selection of lower trophic level prey by older alligators) following the cessation of growth, though further study is needed to differentiate between these two mechanisms. This study highlights the means by which long-term, longitudinal monitoring studies could be used to differentiate between potential confounding effects of time, age, and size in sentinel species, the latter two of which are particularly important for long-lived reptiles.

Acknowledgements

We thank members of the Guillette Lab, the South Carolina Department of Natural Resources (SCDNR), and the many other individuals who assisted with alligator captures and sample collection at the Tom Yawkey Wildlife Center (YWC) and Merritt Island National Wildlife Refuge. We also thank Jamie Dozier, manager of YWC, for his support of alligator research on the property; Angela Lindell for her laboratory training and guidance; and John Bowden, Matthew Hale, Stacey Lance, Benjamin Parrott, and Josh Zajdel for their assistance providing samples and laboratory materials.

We honor the memories of our coauthors, Drs. Kate W. McFadden and Louis J. Guillette Jr., both driven, innovative scientists with an innate curiosity about the natural world and a passion for interdisciplinary collaboration. The SCDNR and the United States Geological Survey funded this research. Authors declare no conflict of interest.

Any use of trade, firm, or product names is for descriptive purposes only and does not imply endorsement by the U.S. Government. This paper represents Technical Contribution Number 6688 of the Clemson University Experiment Station.

Literature Cited

Arnold, T.W., 2010. Uninformative Parameters and Model Selection Using Akaike's Information Criterion. J. Wildl. Manage. 74, 1175–1178. https://doi.org/10.2193/2009-367

Baker, Timothy T.; Lafferty, R.; Quinn, T.J., 1991. A General Growth Model for Mark Recapture Data. Fish. Res. 11, 257–281.

Bank, M.S., Loftin, C.S., Jung, R.E., 2005. Mercury bioaccumulation in northern two-lined salamanders from streams in the northeastern United States. Ecotoxicology 14, 181–191. https://doi.org/10.1007/s10646-004-6268-8

Bartoń, K., 2018. MuMIn: Multi-model inference. R package version 1.42.1.

Becker, D.J., Chumchal, M.M., Bentz, A.B., Platt, S.G., Czirják, G., Rainwater, T.R., Altizer, S., Streicker, D.G., 2017. Predictors and immunological correlates of sublethal mercury exposure in vampire bats. R. Soc. Open Sci. 4. https://doi.org/10.1098/rsos.170073

Becker, P.H., Gonzàlez-Solìs, J., Behrends, B., Croxall, J., 2002. Feather mercury levels in seabirds at South Georgia: Influence of trophic position, sex and age. Mar. Ecol. Prog. Ser. 243, 261–269. https://doi.org/10.3354/meps243261

Benson, J.F., Mahoney, P.J., Sikich, J.A., Serieys, L.E.K., Pollinger, J.P., Ernest, H.B., Riley, S.P.D., 2016. Interactions between demography, genetics, and landscape connectivity increase extinction probability for a small population of large carnivores in a major metropolitan area. Proc. R. Soc. B Biol. Sci. 283. https://doi.org/10.1098/rspb.2016.0957

Bergeron, C.M., Bodinof, C.M., Unrine, J.M., Hopkins, W.A., 2010. MERCURY ACCUMULATION ALONG A CONTAMINATION GRADIENT AND NONDESTRUCTIVE INDICES OF BIOACCUMULATION IN AMPHIBIANS. Environ. Toxicol. Chem. 29, 980–988. https://doi.org/10.1002/etc.121

Bergeron, C.M., Hopkins, W.A., Todd, B.D., Hepner, M.J., Unrine, J.M., 2011. Interactive effects of maternal and dietary mercury exposure have latent and lethal consequences for amphibian larvae. Environ. Sci. Technol. 45, 3781–3787. https://doi.org/10.1021/es104210a

Bondavalli, C., Ulanowicz, R.E., 1999. Unexpected effects of predators upon their prey: The case of the american alligator. Ecosystems 2, 49–63. https://doi.org/10.1007/s100219900057

Brisbin, I.L., Gaines, K.F., Jagoe, C.H., Consolie, P.A., 1996. Population studies of American alligators inhabiting a reservoir: responses to long-term drawdown and subsequent refill. Proc. 13th Work. Meet. Crocodile Spec. Gr. 446–477.

Brisbin, L.I.J., Jagoe, C.H., Gaines, K.F., Gadboldi, J.C., 1998. Environmental contaminats as concern for the conservation biology of crocodilians. Proc. 14th Work. Meet. Crocodile Spec. Gr. Species Surviv. Comm. IUCN 155–173.

Burger, J., Gochfeld, M., Rooney, A.A., Orlando, E.F., Woodward, A.R., Guillette, L.J., 2000. Metals and metalloids in tissues of American alligators in three Florida lakes. Arch. Environ. Contam. Toxicol. 38, 501–508. https://doi.org/10.1007/s002449910066

Burger, J., Nisbet, M.C., Gochfeld, M., 1994. Heavy metal and selenium levels in feathers of known-aged common terns (Sterna hirundo). Arch. Environ. Contam. Toxicol. 26, 351–355.

Burnham, K.P., Anderson, D.R., 2002. Model selection and multimodel inference – a practical information-theoretic approach, Second Ed. ed. Springer US.

Campbell, J.W., Waters, M.N., Tarter, A., Jackson, J., 2010. Heavy Metal and Selenium Concentrations in Liver Tissue From Wild American Alligator (Alligator Mississippiensis) Livers Near Charleston, South Carolina. J. Wildl. Dis. 46, 1234–1241. https://doi.org/10.7589/0090-3558-46.4.1234

Campos, Z., Mouraõ, G., Coutinho, M., Magnusson, W.E., 2014. Growth of caiman crocodilus yacare in the brazilian pantanal. PLoS One 9, 1–5. https://doi.org/10.1371/journal.pone.0089363

Chabreck, R.H., 1963. Methods of capturing, marking, and sexing alligators. Proc. Ann. Conf. Southeast. Assoc. Game Fish Comm. 17, 47–50.

Charnov, E.L., Turner, T.F., Winemiller, K.O., 2001. Reproductive constraints and the evolution of life histories with indeterminate growth. Proc. Natl. Acad. Sci. 98,

9460–9464. https://doi.org/10.1073/pnas.161294498

Cherkiss, M.S., Fling, H.E., Mazzotti, F.J., Rice, K.G., 2004. Counting and capturing crocodilians. Gainesville, Florida.

Chumchal, Matthew M Hambright, K.D., 2009. Ecological Factors Regulating Mercury Contamination of Fish From Caddo Lake, Texas, USA. Environ. Toxicol. Chem. 28, 962–972.

Chumchal, M.M., Rainwater, T.R., Osborn, S.C., Roberts, A.P., Abel, M.T., Cobb, G.P., Smith, P.N., Bailey, F.C., 2011. Mercury speciation and biomagnification in the food web of Caddo Lake, Texas and Louisiana, USA, a subtropical freshwater ecosystem. Environ. Toxicol. Chem. 30, 1153–1162. https://doi.org/10.1002/etc.477

Cizdziel, J., Hinners, T., Cross, C., Pollard, J., 2003. Distribution of mercury in the tissues of five species of freshwater fish from Lake Mead , USA. https://doi.org/10.1039/b307641p

Compeau, G.C.; Bartha, R., 1985. Sulfate-reducing bacteria: principal methylators of mercury in anoxic estuarine sediment. Appl. Environ. Microbiol. 50, 498–502.

Congdon, J.D., Gibbons, J.W., Brooks, R.J., Rollinson, N., Tsaliagos, R.N., 2013. Indeterminate growth in long-lived freshwater turtles as a component of individual fitness. Evol. Ecol. 27, 445–459. https://doi.org/10.1007/s10682-012-9595-x

Congdon, J.D., Nagle, R.D., Kinney, O.M., Van Loben Sels, R.C., 2001. Hypotheses of aging in a long-lived vertebrate, Blanding's turtle (Emydoidea blandingii). Exp. Gerontol. 36, 813–827. https://doi.org/10.1016/S0531-5565(00)00242-4

Delany, M.F., Linda, S.B., Moore, C.B., 1999. Diet and condition of American alligators in 4 Florida lakes. Proc. Annu. Conf. Southeast Assoc. Fish Wildl. Agencies 53, 375–389.

Dodson, P., 1975. Functional and ecological significnce of relative growth in Alligator. J. Zool. London 175, 315–355.

Duffy, J.E., 2002. Biodiversity and ecosystem function: The consumer connection. Oikos 99, 201–219. https://doi.org/10.1034/j.1600-0706.2002.990201.x

Eagles-Smith, C.A., Ackerman, J.T., Adelsbach, T.L., Takekawa, J.Y., Miles, A.K., Keister, R.A., 2008. MERCURY CORRELATIONS AMONG SIX TISSUES FOR FOUR WATERBIRD SPECIES BREEDING IN SAN FRANCISCO BAY , CALIFORNIA , USA. Environ. Toxicol. Chem. 27, 2136–2153.

Eggins, S., Schneider, L., Krikowa, F., Vogt, R.C., Silveira, R. Da, Maher, W., 2015. Mercury concentrations in different tissues of turtle and caiman species from the Rio Purus, Amazonas, Brazil. Environ. Toxicol. Chem. 34, 2771–2781. https://doi.org/10.1002/etc.3151

Elliott, K.H., Hare, J.F., Le Vaillant, M., Gaston, A.J., Ropert-Coudert, Y., Anderson, W.G., 2015. Ageing gracefully: Physiology but not behaviour declines with age in a diving seabird. Funct. Ecol. 29, 219–228. https://doi.org/10.1111/1365-2435.12316

Erickson, G.M., Lappin, A.K., Vliet, K.A., 2003. The ontogeny of bite-force performance in American alligator (Alligator mississippiensis). J. Zool. 260, 317–327. https://doi.org/10.1017/S0952836903003819

Evers, D.C., Savoy, L.J., Desorbo, C.R., Yates, D.E., Hanson, W., Taylor, K.M., Siegel, L.S., Cooley, J.H., Bank, M.S., Major, A., Munney, K., Mower, B.F., Vogel, H.S., Schoch, N., Pokras, M., Goodale, M.W., Fair, J., 2008. Adverse effects from environmental mercury loads on breeding common loons. Ecotoxicology 17, 69–81. https://doi.org/10.1007/s10646-007-0168-7

Eversole, C.B., Henke, S.E., Ballard, B.M., Powell, R.L., 2014. Duration of marking tags on American Alligators (Alligator mississippiensis). Herpetol. Rev. 45, 223–226.

Frederick, P., Jayasena, N., 2011. Altered pairing behaviour and reproductive success in white ibises exposed to environmentally relevant concentrations of methylmercury. Proc. R. Soc. B Biol. Sci. 278, 1851–1857. https://doi.org/10.1098/rspb.2010.2189

Frederick, P.C., Hylton, B., Heath Julie, A., Spalding Marilyn, G., 2004. A historical record of mercury contamination in southern florida (USA) as inferred from avian feather tissue. Environ. Toxicol. Chem. 23, 1474–1478. https://doi.org/10.1897/03-403

Furness, R.W., Lewis, S.A., Mills, J.A., Unit, A.O., Zealand, N., 1990. Mercury levels in the plumage of red-billed gulls Larus novaehollandiae scopulinus of known sex and age. Environ. Pollut. 63, 33–39.

George, B.M., Batzer, D., 2008. Spatial and temporal variations of mercury levels in Okefenokee invertebrates: Southeast Georgia. Environ. Pollut. 152, 484–490. https://doi.org/10.1016/j.envpol.2007.04.030

Glover, J.B., Domino, M.E., Altman, K.C., Dillman, J.W., Castleberry, W.S., Eidson, J.P., Mattocks, M., 2010. Mercury in South Carolina Fishes, USA. Ecotoxicology 19, 781–795. https://doi.org/10.1007/s10646-009-0455-6

Grippo, M.A., Heath, A.G., 2003. The effect of mercury on the feeding behavior of fathead minnows (Pimephales promelas). Ecotoxicol. Environ. Saf. 55, 187–198. https://doi.org/10.1016/S0147-6513(02)00071-4

Hall, R.J., 1980. Effects of Environrnental Contaminants on Reptiles: A Review. U.S. Fish and Wildlife Service Special Report No. 228. Washington, DC.

Hanson, J.O., Salisbury, S.W., Campbell, H.A., Dwyer, R.G., Jardine, T.D., Franklin, C.E., 2015. Feeding across the food web: The interaction between diet, movement and body size in estuarine crocodiles (Crocodylus porosus). Austral Ecol. 40, 275–286. https://doi.org/10.1111/aec.12212

Heaton-Jones, T.G., Homer, B.L., Heaton-Jones, D.L., Sundlof, Stephen, F., 1997. Mercury Distribution in American Alligators (Alligator mississippiensis) in Florida. J. Zoo Wildl. Med. 28, 62–70.

Hower, J.C., Senior, C.L., Suuberg, E.M., Hurt, R.H., Wilcox, J.L., Olson, E.S., 2010. Mercury capture by native fly ash carbons in coal-fired power plants. Prog. Energy Combust. Sci. 36, 510–529. https://doi.org/10.1016/j.pecs.2009.12.003

Hutton, J., 1989. Movements , Home Range , Dispersal and the Separation of Size Classes in Nile Crocodiles Jonathan Hutton Movements , Home Range , Dispersal and the Separation of Size Classes in Nile Crocodiles1. Am. Zool. 29, 1033–1049.

Jacobsen, T., Kushlan, J.A., 1989. Growth Dynamics in the American Alligator (Alligator-Mississippiensis). J. Zool. 219, 309–328.

Jagoe, C., Arnold-Hill, B., Yanochko, G., Winger, P., Brisbin Jr, I., 1998. Mercury in alligators (Alligator mississippiensis) in the south eastern United States. Sci. Total Environ. 213, 255–262.

Jennings, M.L., David, D.N., Portier, K.M., 1991. Effect of Marking Techniques on Growth and Survivorship of Hatchling Alligators. Wildl. Soc. Bull. 19, 204–207.

Jepson, P.D., Bennett, P.M., Deaville, R., Allchin, C.R., Baker, J.R., Law, R.J., 2005. Relationships between polychlorinated biphenyls and health status in harbor porpoises (Phocoena phocoena) stranded in the United Kingdom. Environ. Toxicol. Chem. 24, 238–248. https://doi.org/10.1897/03-663.1

Joanen, T., Mcnease, L., 1972. A Telemetric Study of Adult Male Alligators on Rockefeller Refuge, Louisiana 26, 252–275.

Joanen, T., McNease, L., 1980. Reproductive biology of the American alligator in southwest Louisiana, in: Murphy, J.B., Collins, J.T. (Eds.), Reproductive Biology

and Diseases of Captive Reptiles. Contributions to Herpetology, Society for the Study of Amphibians and Reptiles, Lawrence, Kansas, USA, pp. 153–159.

Joanen, T., McNease, L., 1971. Propagation of the American alligator in captivity. Proc SE Assoc Game Fish Comm 25, 106–116.

Joanen, T., McNease, L., 1970. A telemetric study of nesting female alligators on rockefeller refuge, Louisiana. Annu. Conf. Southeast. Assoc. Fish Wildl. Agencies 24, 175–193.

Keller, J.M., Balazs, G.H., Nilsen, F., Rice, M., Work, T.M., Jensen, B.A., 2014. Investigating the Potential Role of Persistent Organic Pollutants in Hawaiian Green Sea Turtle Fibropapillomatosis. Environ. Sci. Technol. 48, 7807–7816. https://doi.org/10.1021/es5014054

Kozlowski, J., 1996. Optimal allocation of resource explains interspecif life-history patters in animals with indeterminate growth. Proc. R. Soc. London B 263, 359–366.

Lavigne, M., Lucotte, M., Paquet, S., 2010. Relationship between Mercury Concentration and Growth Rates for Walleyes, Northern Pike, and Lake Trout from Quebec Lakes. North Am. J. Fish. Manag. 30, 1221–1237. https://doi.org/10.1577/M08-065.1

Lawson, A.J., Strickland, B.A., Rosenblatt, A.E., 2018. Patterns, drivers and effects of alligator movement behavior and habitat use, in: Henke, S.E., Eversole, C.B. (Eds.), American Alligators: Habitats, Behaviors, and Threats. Nova Science Publishers, Hauppauge, NY, USA, pp. 47–77.

Litman, R., Flnston, H.L., Williams, E.T., 1975. Evaluation of Sample Pretreatments for Mercury Determination. Anal. Chem. 47, 2364–2369. https://doi.org/10.1021/ac60364a026

Lusk, J.D., Rich, E., Bristol, R.S., 2005. Methylmercury and Other Environmental Contaminants in Water and Fish Collected from Four Recreational Fishing Lakes on the Navajo Nation, 2004. Albuquerque, New Mexico.

Marzio, A. Di, Gómez-ramírez, P., Barbar, F., Lambertucci, S.A., García-fernández, A.J., Martínez-lópez, E., 2018. Mercury in the feathers of bird scavengers from two areas of Patagonia (Argentina) under the influence of different anthropogenic activities : a preliminary study. Environ. Sci. Pollut. Res. 25, 13906–13915.

Mazzotti, F.J., Brandt, L.A., 1994. Ecology of the American alligator in a seasonally fluctuating environment, in: Everglades: The Ecosystem and Its Restoration. pp. 485–505.

Milnes, M.R., Guillette, L.J., 2008. Alligator Tales: New Lessons about Environmental Contaminants from a Sentinel Species. Bioscience 58, 1027–1036. https://doi.org/10.1641/B581106

Moore, L.A.N.N., 2004. Distribution of Mercury in the American Alligator (Alligator. University of Georgia.

Murphy, T., Wilkinson, P., Coker, J., Hudson, M., 1983. The alligator trip snare: a live capture method. Columbia, South Carolina.

Myburgh, J.G., Kirberger, R.M., Steyl, J.C.A., Soley, J.T., Booyse, D.G., Huchzermeyer, F.W., Lowers, R.H., Guillette Jr, L.J., 2014. The post-occipital spinal venous sinus of the Nile crocodile (<i>Crocodylus niloticus</i>): Its anatomy and use for blood sample collection and intravenous infusions. J. S. Afr. Vet. Assoc. 85, 1–10. https://doi.org/10.4102/jsava.v85i1.965

Nifong, J.C., Layman, C.A., Silliman, B.R., 2015. Size, sex and individual-level behaviour drive intrapopulation variation in cross-ecosystem foraging of a top-predator. J. Anim. Ecol. 84, 35–48. https://doi.org/10.1111/1365-2656.12306

Nifong, J.C., Silliman, B.R., 2013. Impacts of a large-bodied, apex predator (Alligator mississippiensis Daudin 1801) on salt marsh food webs. J. Exp. Mar. Bio. Ecol. 440, 185–191. https://doi.org/10.1016/j.jembe.2013.01.002

Nilsen, F.M., Dorsey, J.E., Lowers, R.H., Guillette, L.J., Long, S.E., Bowden, J.A., Schock, T.B., 2017a. Evaluating mercury concentrations and body condition in American alligators (Alligator mississippiensis) at Merritt Island National Wildlife Refuge (MINWR), Florida. Sci. Total Environ. 607–608, 1056–1064. https://doi.org/10.1016/j.scitotenv.2017.07.073

Nilsen, F.M., Kassim, B.L., Delaney, J.P., Lange, T.R., Brunell, A.M., Guillette, L.J., Long, S.E., Schock, T.B., 2017b. Trace element biodistribution in the American alligator (Alligator mississippiensis). Chemosphere 181, 343–351. https://doi.org/10.1016/j.chemosphere.2017.04.102

Nilsen, F.M., Parrott, B.B., Bowden, J.A., Kassim, B.L., Somerville, S.E., Bryan, T.A., Bryan, C.E., Lange, T.R., Delaney, J.P., Brunell, A.M., Long, S.E., Guillette, L.J., 2016. Global DNA methylation loss associated with mercury contamination and aging in the American alligator (Alligator mississippiensis). Sci. Total Environ. 545–546, 389–397. https://doi.org/10.1016/j.scitotenv.2015.12.059

Nilsen, F.M., Parrott, B.B., Rainwater, T.R., Brunell, A.M., Bowden, J.A., Guillette, L.J.J., Long, S.E., Schock, T.B., 2018. Maternal Transfer of Mercury in American

alligators (Alligator mississippiensis). Ecotoxicol. Environ. Saf. In Review.

Organization, W.H., 1990. Environmental Health Criteria no. 101. Geneva, Switzerland.

Ortiz, A.I.C., Albarrán, Y.M., Rica, C.C., 2002. Evaluation of different sample pre-treatment and extraction procedures for mercury speciation in fish samples. J. Anal. At. Spectrom. 17, 1595–1601. https://doi.org/10.1039/b207334j

Pirrone, N., Cinnirella, S., Feng, X., Finkelman, R.B., Friedli, H.R., Leaner, J., Mason, R., Mukherjee, A.B., Stracher, G., Streets, D.G., Telmer, K., 2009. Global mercury emissions to the atmosphere from natural and anthropogenic sources. Mercur. Fate Transp. Glob. Atmos. Emiss. Meas. Model. 3–49. https://doi.org/10.1007/978-0-387-93958-2_1

Rainwater, T.R., Wu, T.H., Finger, A.G., Cañas, J.E., Yu, L., Reynolds, K.D., Coimbatore, G., Barr, B., Platt, S.G., Cobb, G.P., Anderson, T.A., McMurry, S.T., 2007. Metals and organochlorine pesticides in caudal scutes of crocodiles from Belize and Costa Rica. Sci. Total Environ. 373, 146–156. https://doi.org/10.1016/j.scitotenv.2006.11.010

Rivera, S.J., Pacheco, L.F., Achá, D., Molina, C.I., Miranda-Chumacero, G., 2016. Low total mercury in Caiman yacare (Alligatoridae) as compared to carnivorous, and non-carnivorous fish consumed by Amazonian indigenous communities. Environ. Pollut. 218, 366–371. https://doi.org/10.1016/j.envpol.2016.07.013

Rosenblatt, A.E., Heithaus, M.R., 2011. Does variation in movement tactics and trophic interactions among American alligators create habitat linkages? J. Anim. Ecol. 80, 786–798. https://doi.org/10.1111/j.1365-2656.2011.01830.x

Rumbold, D.G., Fink, L.E., Laine, K.A., Niemczyk, S.L., Chandrasekhar, T., Wankel, S.D., Kendall, C., 2002. Levels of mercury in alligators (Alligator mississippiensis) collected along a transect through the Florida Everglades. Sci. Total Environ. 297, 239–252. https://doi.org/10.1016/S0048-9697(02)00132-8

Rumbold, D.G., Lange, T.R., Axelrad, D.M., Atkeson, T.D., 2008. Ecological risk of methylmercury in Everglades National Park, Florida, USA. Ecotoxicology 17, 632–641. https://doi.org/10.1007/s10646-008-0234-9

Sandheinrich, M.B., Drevnick, P.E., 2016. Relationship among mercury concentration, growth rate, and condition of northern pike: A tautology resolved? Environ. Toxicol. Chem. 35, 2910–2915. https://doi.org/10.1002/etc.3521

Santos, X., Navarro, S., Campos, J.C., Sanpera, C., Brito, J.C., 2018. Stable isotopes

uncover trophic ecology of the West African crocodile (Crocodylus suchus). J. Arid Environ. 148, 6–13. https://doi.org/10.1016/j.jaridenv.2017.09.008

Schneider, L., Peleja, R.P., Kluczkovski, A., Freire, G.M., Marioni, B., Vogt, R.C., Da Silveira, R., 2012. Mercury concentration in the spectacled caiman and black caiman (Alligatoridae) of the Amazon: Implications for human health. Arch. Environ. Contam. Toxicol. 63, 270–279. https://doi.org/10.1007/s00244-012-9768-1

Schnute, J., 1981. A Versatile Growth Model with Statistically Stable Parameters. Can. J. Fish. Aquat. Sci. 38, 1128–1140. https://doi.org/10.1139/f81-153

Selin, N.E., 2010. Global Biogeochemical Cycling of Mercury: A Review. Ssrn. https://doi.org/10.1146/annurev.environ.051308.084314

Sergio, F., Caro, T., Brown, D., Clucas, B., Hunter, J., Ketchum, J., McHugh, K., Hiraldo, F., 2008. Top Predators as Conservation Tools: Ecological Rationale, Assumptions, and Efficacy. Annu. Rev. Ecol. Evol. Syst. 39, 1–19. https://doi.org/10.1146/annurev.ecolsys.39.110707.173545

Snodgrass, J.W., Jagoe, C.H., Bryan, Jr., A.L., Brant, H.A., Burger, J., 2000. Effects of trophic status and wetland morphology, hydroperiod, and water chemistry on mercury concentrations in fish. Can. J. Fish. Aquat. Sci. 57, 171–180. https://doi.org/10.1139/cjfas-57-1-171

Sommer, Y.L., Ward, C.D., Pan, Y., Caldwell, K.L., Jones, R.L., 2016. Long-term stability of inorganic, methyl and ethyl mercury in whole blood: Effects of storage temperature and time. J. Anal. Toxicol. 40, 222–228. https://doi.org/10.1093/jat/bkw007

Taylor, P., Li, F., Holland, A., Martin, M., Rosenblatt, A.E., 2016. Growth rates of black caiman (Melanosuchus Niger) in the Rupununi region of Guyana. Amphib. Reptil. 37, 9–14. https://doi.org/10.1163/15685381-00003024

Team, R.C., 2017. R: A language and environment for statistical computing.

Thompson, D.R., Hamer, K.C., Furness, R.W., 1991. Mercury Accumulation in Great Skuas Catharacta skua of Known Age and Sex, and Its Effects Upon Breeding and Survival. J. Appl. Ecol. 28, 672–684.

Tucker, A.D., Limpus, C.J., McDonald, K.R., McCallum, H.I., 2006. Growth dynamics of freshwater crocodiles (Crocodylus johnstoni) in the Lynd River, Queensland. Aust. J. Zool. 54, 409–415. https://doi.org/10.1071/ZO06099

Varian-Ramos, C.W., Condon, A.M., Hallinger, K.K., Carlson-Drexler, K.A., Cristol,

D.A., 2011. Stability of mercury concentrations in frozen avian blood samples. Bull. Environ. Contam. Toxicol. 86, 159–162. https://doi.org/10.1007/s00128-010-0164-0

Vieira, L.M., Nunes, V.D.S., Amaral, M.C.D.A., Oliveira, A.C., Hauser-Davis, R.A., Campos, R.C., 2011. Mercury and methyl mercury ratios in caimans (Caiman crocodilus yacare) from the Pantanal area, Brazil. J. Environ. Monit. 13, 280–287. https://doi.org/10.1039/c0em00561d

Wagemann, R., Trebacz, E., Boila, G., Lockhart, W.L., 1998. Methylmercury and total mercury in tissues of arctic marine mammals. Sci. Total Environ. 218, 19–31. https://doi.org/10.1016/S0048-9697(98)00192-2

Weaver, J.L., Paquet, P.C., Ruggiero, L.F., 1996. Society for Conservation Biology Resilience and Conservation of Large Carnivores in the Rocky Mountains. Conserv. Biol. 10, 964–976.

Wilkinson, P.M., 1994. A walk-through snare design for the live capture of alligators, in: Proceedings of the 12th Working Meeting of the Crocodile Specialist Group, Volume 2. IUCN–The World Conservation Union, Gland, Switzerland, pp. 74–75.

Wilkinson, P.M., 1983. Nesting ecology of the American alligator in coastal South Carolina. Study Completion Report. Columbia, South Carolina.

Wilkinson, P.M., Rainwater, T.R., Woodward, A.R., Leone, E.H., Carter, C., 2016. Determinate Growth and Reproductive Lifespan in the American Alligator (Alligator mississippiensis): Evidence from Long-term Recaptures. Copeia 104, 843–852. https://doi.org/10.1643/CH-16-430

Wolfe, M., Norman, D., 1998. Effects of waterborne mercury on terrestrial wildlife at Clear Lake: Evaluation and testing of a predictive model. Environ. Toxicol. Chem. 17, 214–227. https://doi.org/10.1897/1551-5028(1998)017<0214:EOWMOT>2.3.CO;2

Wolfe, M.F., Scwarzback, S., Sulaiman, R.A., 1998. Effects of mercury on wildlife: A comprehensive review, Environ. Toxicol. Chem 17146160, 146–160.

Woodward, H.N., Horner, J.R., Farlow, J.O., 2011. Osteohistological Evidence for Determinate Growth in the American Alligator. J. Herpetol. 45, 339–342. https://doi.org/10.1670/10-274.1

Yanochko, G.M., Jagoe, C.H., Brisbin, I.L., 1997. Tissue mercury concentrations in alligators (Alligator mississippiensis) from the Florida Everglades and the Savannah River Site, South Carolina. Arch Env. Contam Toxicol 32, 323–328.

Table 4.1. Sample summary and covariate comparisons for alligator whole blood samples from the Tom Yawkey Wildlife Center in South Carolina (2010–2017) and the Merritt Island National Wildlife Refuge in Florida (2007–2014). The whole numbers in the first two fields represent summary totals, whereas sample means ± standard deviations with range values in parentheses are given below them.

	Tom Yawkey Wildlife Center			Merritt Island National Wildlife Refuge		
	Females	Males	Overall	Females	Males	Overall
Unique Individuals	67	46	113	72	97	169[a]
# Maximum Blood Sampling Events						
1	40	36	76	66	84	150
2	16	8	24	6	12	18
3	9	2	11	0	1	1
4	2	0	2	0	0	0
Mean Days Between Blood Samples	957 ± 706 (7–2256)	552 ± 269 (285–1127)	864 ± 653 (7–2256)	716 ± 610 (106–1730)	683 ± 629 (21–1877)	693 ± 607 (21–1877)
Ordinal Date	157 ± 41 (56–271)	139 ± 64 (56–271)	150 ± 51 (56–271)	177 ± 103 (9–365)	181 ± 114 (5–365)	180 ± 109 (5–365)
Predicted Age[b]	31 ± 13 (8–66)	23 ± 13 (8–59)	28 ± 14 (8–66)	19 ± 6 (10–31)	21 ± 7 (8–43)	20 ± 7 (8–43)
Snout-Vent Length (cm)	127.26 ± 11.58 (78.60–150.50)	141.69 ± 30.05 (85.00–191.80)	132.33 ± 21.17 (78.60–191.80)	114.75 ± 12.00 (87.00–135.00)	145.24 ± 20.92 (88.50–187.20)	132.65 ± 23.27 (87.0–187.2)
Body Mass Index[c]	0.22 ± 0.02 (0.15–0.26)	0.22 ± 0.02 (0.16–0.26)	0.22 ± 0.02 (0.15–0.26)	0.21 ± 0.02 (0.15–0.25)	0.21 ± 0.02 (0.14–0.26)	0.21 ± 0.02 (0.14–0.26)

[a]MINWR summary statistics and covariate means exclude four outlier samples identified by Nilsen et al. (2017a).

[b]Predicted age derived using sex-specific growth parameters from Wilkinson et al. (2016) in Eq. 5 in Baker et al. (1991).

[c]Body mass index derived using Eq. 1 in Nilsen et al. (2017a)

Table 4.2. Linear regression models representing hypotheses about total mercury (THg) bioaccumulation patterns in whole blood of American alligators captured on the Tom Yawkey Wildlife Center coastal South Carolina from 2010–2017. Only models within ≤ 20 ΔAICc units of the best-supported model are listed here, full list in Supplementary Material (Table C1.5).

Model[a]	Number parameters	Dev.[b]	ΔAICc	w_i
Sex * PA + Sex * PA^2	7	4.46	0.00	0.46
PA + PA^2	4	4.65	0.47	0.37
Sex * SVL + Sex * SVL^2	7	4.56	3.67	0.07
~Indiv.	3	*	4.19	0.06
BMI	3	4.96	9.03	0.01
OD	3	4.96	9.14	0.00
SVL + SVL^2	4	4.90	9.15	0.00
Intercept	2	5.03	9.26	0.00
SVL	3	4.96	9.27	0.00
~Indiv. + PA + PA^2	5	*	9.33	0.00
BMI + BMI^2	4	4.94	10.50	0.00
PA	3	5.02	11.01	0.00
OD + OD^2	4	4.96	11.11	0.00
Sex * SVL	5	4.89	11.13	0.00
Sex + OD	4	4.96	11.22	0.00
Sex	3	5.03	11.33	0.00
PA* OD	5	4.95	12.91	0.00
Sex + PA	4	5.02	13.11	0.00
Sex * OD	5	4.96	13.30	0.00
Sex * PA	5	5.00	14.58	0.00
Year	9	4.76	15.36	0.00
Year * OD	17	4.28	16.89	0.00
Sex * OD + Sex * OD^2	7	4.95	17.42	0.00
~Year	3	*	17.72	0.00

[a]Model selection notation (following Burnham and Anderson 2002) presents models according to the highest-order effects contained, with all lower-order constituent effects

included as additive effects; a superscript ^{2} denotes a quadratic effect, a + sign indicates an additive effect between two variables, a * denotes an interaction, whereas a ~ indicates a random effect. Year (categorical) = annual variation, PA = predicted age of the individual at sampling based on estimated predicted age at first capture using the Wilkinson et al. (2016) growth formula for our study population; SVL = snout-vent length in cm at capture; Indiv. = individual alligator modeled as a random intercept; BMI = body mass index (Nilsen et al., 2017a) at capture; OD = ordinal date or day of year. The continuous covariates contained no missing values and were z-standardized across years (mean = 0.0, SD = 1.0).

[b]Models containing random effects were fit with restricted maximum likelihood (REML) and deviance values are not directly comparable to non-REML fit models.

Table 4.3. Linear regression models representing hypotheses about total mercury (THg) bioaccumulation patterns in the whole blood of American alligators captured on the Merritt Island National Wildlife Refuge in eastern Florida from 2007–2014. Only models within ≤ 20 ΔAICc units of the best-supported model are listed here, full list in Supplementary Material (Table C1.6).

Model[a]	Number parameters	Dev.[b]	ΔAICc	w_i
SVL + SVL^2	4	34.06	0.00	0.85
Sex * SVL + Sex * SVL^2	7	33.54	3.52	0.15
PA + PA^2	4	36.78	14.56	0.00
Sex * PA + Sex * PA^2	7	35.82	15.93	0.00
Sex * SVL	5	37.10	18.28	0.00

[a]Model selection notation (following Burnham and Anderson 2002) presents models according to the highest-order effects contained, with all lower-order constituent effects included as additive effects; a superscript ^{2} denotes a quadratic effect, a + sign indicates an additive effect between two variables, a * denotes an interaction. PA = predicted age of the individual at sampling based on estimated predicted age at first capture using the Wilkinson et al. (2016) growth formula for our study population; SVL = snout-vent length in cm at capture; The continuous covariates contained no missing values and were z-standardized across years (mean = 0.0, SD = 1.0).

Figure 4.1.A map of the Tom Yawkey Wildlife Center (YWC) in coastal South Carolina, USA, which has been closed to hunting for over 100 years. American alligator (*Alligator mississippiensis*) whole blood samples were collected on Cat and South Islands (denoted by the bold dashed line) within YWC from 2010–2017. YWC is comprised of 1,012 ha impounded fresh and brackish water wetlands (dark gray areas within YWC), surrounded by a series of dikes and dirt roads (thin black lines). The inset (lower right) shows the alligator's distribution and our two study sites: YWC (black star) and the Merritt Island National Wildlife Refuge (MINWR; black square), described in detail in Nilsen et al. (2017a). Alligator distribution layer provided by CrocBITE.org.

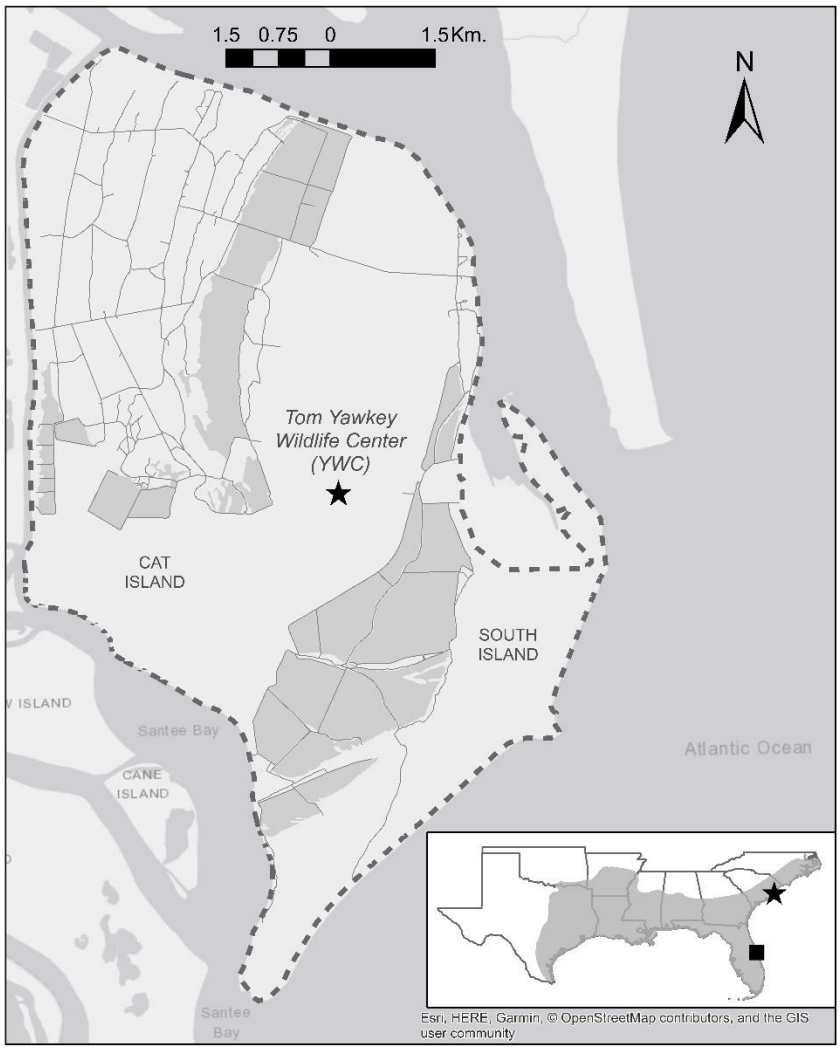

Figure 4.2. Predicted total mercury (THg) mg kg^{-1} ww in American alligator whole blood samples from the Tom Yawkey Wildlife Center, South Carolina (2010–2017). Predicted values are represented by the solid lines and the shaded areas represent the 95% confidence intervals. Panel (a.) shows the predictions from the best-supported linear regression model in our model set (Table 4.2), which contained Sex x Predicted Age (PA) and Sex x PA^2 covariate terms. Females are represented by the red lines and the males in blue. The vertical dashed lines represent the sex-specific age at cessation of growth derived by Wilkinson et al. (2016). Panel (b.) depicts predicted THg from the second best-supported model (Table 4.2) that only contained PA and PA^2 terms, with no sex interaction. For both models, the PA estimates were based on the estimated predicted age at first capture, including potential encounters prior to this study (1979–2009), using the growth formula for our study population by Wilkinson et al. (2016).

a)

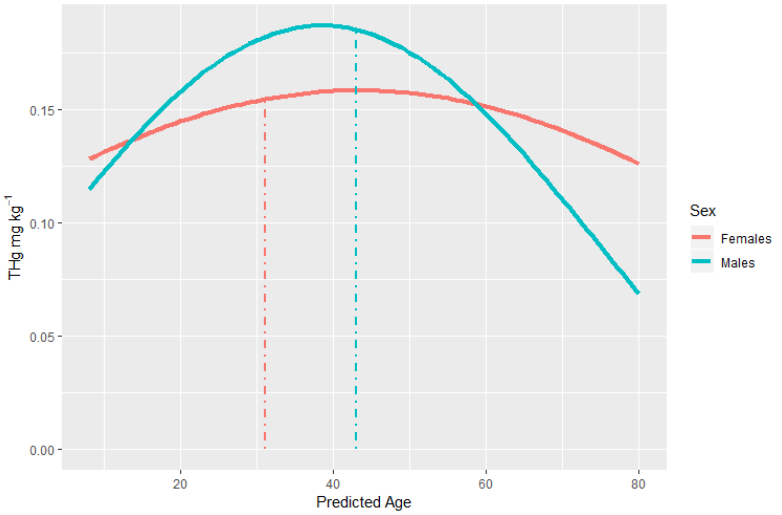

b)

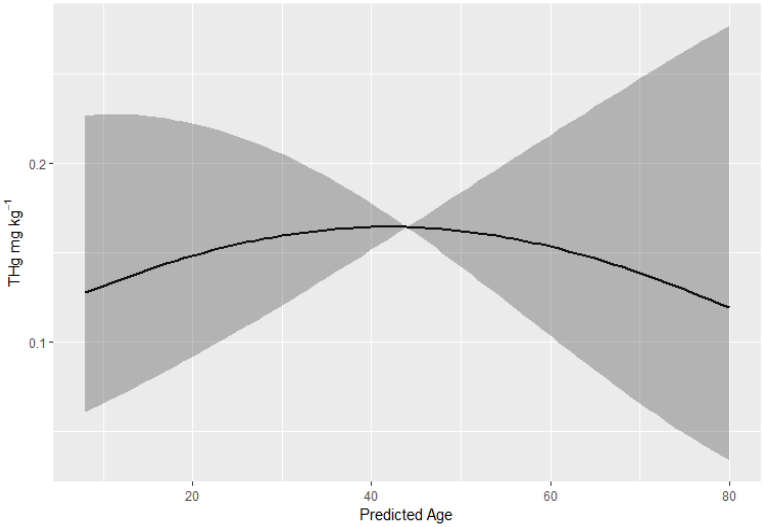

Figure 4.3. Predicted total mercury (THg) mg kg^{-1} ww in alligator whole blood samples from Merritt Island National Wildlife Refuge, Florida (2007–2014) with 95% confidence intervals in the shaded areas. Predicted values in are derived from the best-supported linear regression model in our model set (Table 3), which contained snout-vent length (SVL) and SVL^2 covariate terms.

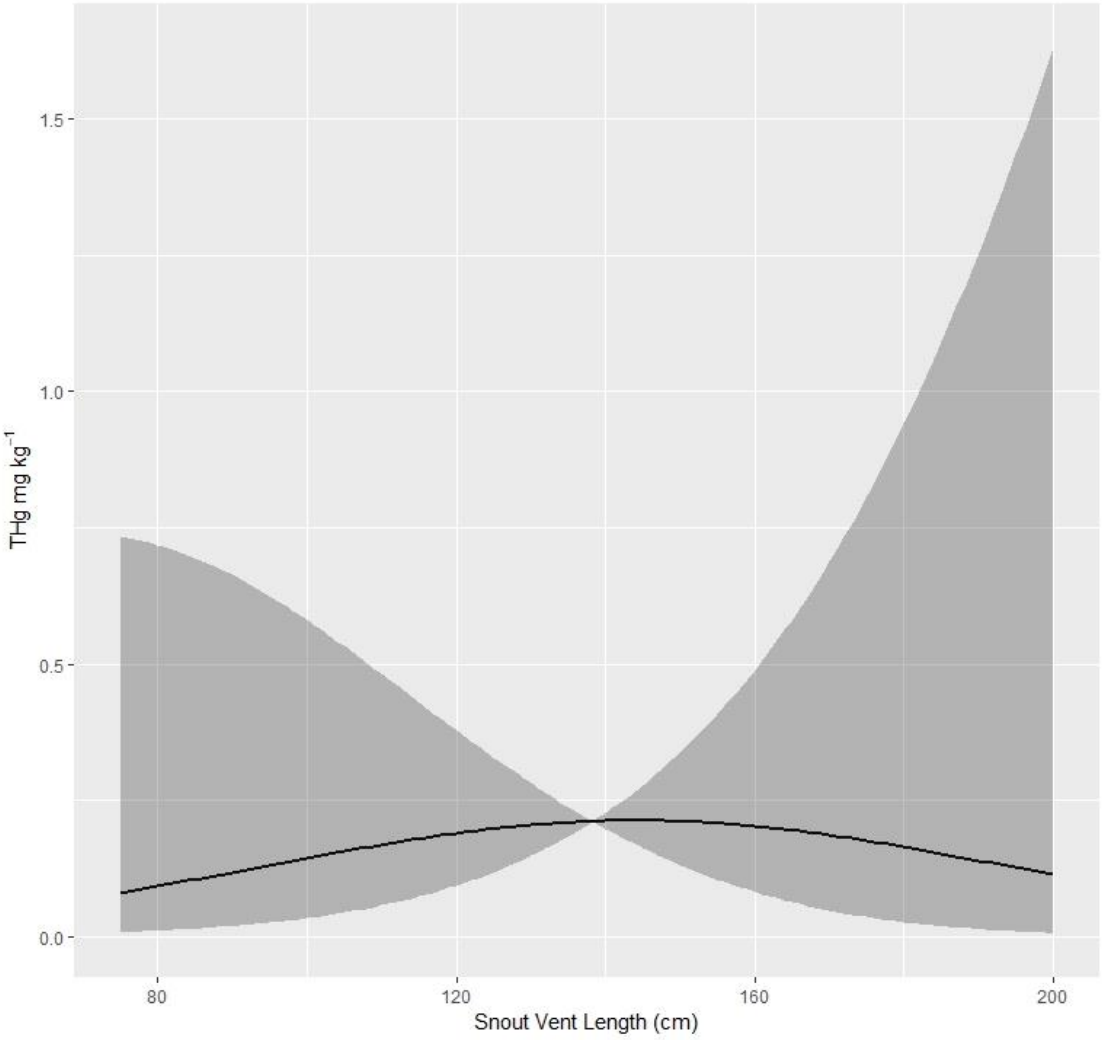

APPENDICES

APPENDIX A1

Integrated Population Model Data Summaries

Table A1.1. Summary of mark-recapture data of American alligator (*Alligator mississippiensis*) from the Tom Yawkey Wildlife Center, South Carolina, USA, for the entire study period (1979–2017; left) and from 1993–2017 (right). Dashes (–) indicate zeroes. Mean days between recapture events show the sample mean ± standard deviations with range values in parentheses given below, and excludes within-year recaptures. Capture events by state *j* (Table 2.1) reflect the total number of captures for each observable state: size class ($j \leq 6$) or dead recoveries ($j=7$).

	1979–2017			1993–2017		
	Females	Males	Unknown	Females	Males	Unknown
Unique Indiv.	275	282	282	250	215	20
Indiv. Max. Capture Events						
1	200	213	282	189	181	20
2	47	54	–	40	26	–
3	11	10	–	10	6	–
4	10	2	–	7	–	–
5	5	3	–	3	2	–
6	1	–	–	1	–	–
7	1	–	–	–	–	–
Mean Days	3213 ± 3059	2468 ± 3089	–	2691 ± 2566	2438 ± 2573	–

Betw. Recaptures	(207–12,351)	(204–12,973)	–	(267–8566)	(285–8337)	–
Capture Events by State (*j*)						
1	4	1	257	–	–	–
2	57	42	25	55	38	20
3	20	50	–	16	34	–
4	168	95	–	140	50	–
5	152	90	–	133	60	–
6	–	84	–	–	70	–
7[a]	4	12	–	4	9	–

[a]Includes five alligators (1 female, 4 males) legally taken by the public harvest program since 2008

Table A1.2. Annual summary of an American alligator (*Alligator mississippiensis*) mark-recapture study at the Tom Yawkey Wildlife Center, South Carolina, USA (1979–2017), broken down by sex. No data were collected during 1983–1992, 1994–2004, and 2008.

	Female	Male	Unknown[a]	Total		Female	Male	Total		Female	Male	Total
1979	5	7	0	12	2006	5	12	17	2012	13	2	15
1980	10	30	171	211	2007	4	5	9	2013	19	20	39
1981	24	37	91	152	2008[b]	0	1	1	2014	22	9	31
1982	18	36	0	54	2009	14	0	14	2015	20	11	31
1993	129	99	20	248	2010	17	0	17	2016	44	31	75
2005	5	10	0	15	2011	33	42	75	2017	19	11	30

[a]No individuals of unknown sex were encountered after 1993

[b]Data point from a public alligator harvest-recovery in Georgetown County

Table A1.3. Summary of annual nightlight surveys of American alligator (*Alligator mississippiensis*) conducted at two river sites (Great Pee Dee and Waccamaw Rivers – GPD; South Santee River – SAN; Fig. 2.1) in South Carolina from 2011–2016 (no data collected in 2012). Ordinal date reflects the day-of-year the survey was initiated; survey start and end are in 24-hour time format. Water level is the river's height as recorded by two USGS stream gauges located near each survey route (Fig. 2.1), whereas water temperature was recorded by a hand-held YSI salinity meter using a 1m probe at 2.3 km intervals during each survey. If water temperature was not recorded during the survey due to equipment malfunction, we used the temperature recording from the route's designated stream gauge. The first six columns within the alligator observations section, at right, show size class-specific (*j*) observations (Table 2.1), whereas age.im and age.ad refer to alligators that could be assigned to the immature or adult age classes, respectively, whereas unknown (Unk) observations were for observations in which neither size nor age could be determined. The overall mean (±SD) size-classification (sum of size class observations divided by total observations) and age-aggregation (sum of size class-specific, age.im, and age.ad observations divided by the total) rates across all surveys at both sites are shown at the bottom.

Survey Site	Year	Ordinal Date	Survey Start	Survey End	Water Level (ft.)	Water Temp. (°C)	*Alligator Observations*									
							j=1	2	3	4	5	6	Age.im	Age.ad	Unk.	Total
GPD	2011	228	20:30	0:14	17.49	29.98[a]	0	3	6	5	9	3	0	0	25	51
	2013	224	21:15	1:30	16.69	28.20	0	1	4	5	8	2	0	0	37	57
	2014	174	20:51	23:25	16.98	28.55	0	0	1	11	2	2	0	0	14	30
	2015	161	21:23	0:14	13.85	26.40	0	2	5	7	4	1	4	4	54	81
	2016	133	23:14	1:49	16.94	22.85	0	5	4	4	1	0	5	3	28	50
SAN	2011	229	21:12	23:30	23.69	[b]	0	4	6	15	17	1	0	0	27	70
	2013	225	3:05	4:50	21.06	29.40	0	0	2	2	3	4	0	0	20	31
	2014	175	1:15	3:48	21.59	27.65	6	2	7	6	3	1	0	1	48	74

2015	173	21:21	23:24	21.84	32.15	17	2	2	5	4	1	18	6	87	142
2016	217	20:56	21:43	24.15	29.90	0	1	5	1	0	0	1	0	52	60

Size-classification rate: 35 ± 5% Age-aggregation rate: 40 ± 13%

---

[a]Water temperature data collected from a USGS stream gauge on the Waccamaw River (Fig. 2.1)

[b]Water temperature not available from survey recording or North Santee River stream gauge (Fig. 2.1)

Table A1.4. Summary of alligator harvest data on public lands by size class (Table 2.1) for American alligator (*Alligator mississippiensis*) in Georgetown County (GXN), South Carolina, USA (Fig. 2.1). Harvest regulations permit the take of alligators over 1.2 m total length (TL; distance from snout to tail tip), therefore, totals for size classes not exposed to harvest (j<3) are not shown. TL values are self-reported by hunters and does not adjust for alligators that are missing portions of their tail. The average total length (m) of harvested alligators in GXN ($\overline{TL}$) each year is show in the far right column. Only data that overlapped with the nightlight counts (2011–2016) were used in the IPM.

Year	Statewide Quota	*Alligator harvest by size class (j)*					
		j=3	4	5	6	Total	$\overline{TL}$
2008	1,000	2	11	23	22	58	2.80
2009	1,000	3	27	41	24	95	2.74
2010	1,200	3	33	35	29	100	2.74
2011	1,200	3	34	47	29	113	2.65
2012	1,200	0	24	53	35	112	2.74
2013	1,200	7	41	50	16	114	2.53
2014	1,000	4	34	24	18	80	2.56
2015	1,000	6	20	25	13	64	2.53
2016	1,000	2	31	31	21	85	2.65

APPENDIX A2

Auxiliary Data and Sensitivity Analysis

Auxiliary data description

We used breeding and nesting productivity data from multiple studies conducted in coastal South Carolina from 1980–1982 (Wilkinson, 1983) to parameterize our models. To determine the annual proportion of adult females that nested (*BP* in Figs. 3.2, 3.3, Eq. 3.7), adult female alligators were captured on YWC each spring, before the onset of nesting, and fitted with a VHF radio transmitter (n=29; n=4 tracked >1 nesting season). The marked females were tracked multiple times per week for two months to determine if their area of activity included a nest site. In spring 1982, two blood samples were collected from each adult female captured (n=37) on YWC; one directly from the heart and another from the jugular vein. The blood samples were kept on ice and later centrifuged to separate the blood plasma, which was then assayed to quantify calcium (Ca) levels (Lance et al., 1983), an indicator of vitellogenesis. The two methods produced similar estimates for the proportion of breeding females, as 25% of the nesting cycles monitored by the telemetry component (after adjusting for radio failure) and 29.7% of the plasma samples suggested nesting, for an overall estimate of 27.5% when pooling the two methods (Wilkinson, 1983). The nests monitored in the telemetry study, as well as additional nests in GXN located via helicopter surveys over the same time period were used to determine apparent nest success rate. Of 117 monitored nests, 82 (70.1%) were successful (i.e., at least one egg hatched) (Wilkinson, 1983) (*NS* in Figs. 3.2. 3.3, Eq. 3.5). Here we use the term *apparent nest success* because the nests used to derive NS

included two detection methods (tracking nesting females and helicopter flights), neither of which adjusted for potential biases such as nests being undetected or that successful nests survive longer and are therefore more likely to be detected. We pooled clutch sizes observed by the Wilkinson (1983) study and more recent nest monitoring (2009–2017) efforts at YWC (P.M. Wilkinson, unpubl. data) to determine an average clutch size of 45 eggs (Fig. 2.2, *CL* in Fig. 2.3, Eq. 3.7).

Similarly, we used information on sex ratio (female proportion; FP_j) derived from previous studies or from expert opinion to parameterize our models. Rhodes and Lang (1996) reported 72% of hatchlings from 23 nests originally located on the Cape portion of Santee Coastal Reserve (the launch site for the South Santee River nightlight survey) in 1994 were female. Data from an experimental harvest (1989–1990) and live captures (Table 7 in Woodward, 1996) of alligators in Orange Lake, Florida, provided estimates of percent female for the juvenile (37%; live captures only in Woodward et al., 1992), subadult (47%), and small adult (47%; referred to as "Reproductive" in Woodward, 1996) size classes. Lastly, we consulted multiple experts to parameterize the female percentage in the large adult (35%) and bull size classes (0%; A.J. Lawson and P.M. Wilkinson, unpubl. data). A summary of the auxiliary data provided in Table A2.1.

Sensitivity Analysis

We conducted a sensitivity analysis to evaluate the effect of the extrinsic variables on our model output. For computing efficiency, we used a simplified version of the IPM (hereafter simplified model) for all sensitivity analyses. The simplified model only

included count data from the combined Great Pee Dee and Waccamaw River survey route (GPD); therefore, the sensitivity analysis did not include any site effects. Additionally, we did not incorporate the harvest data into the abundance state process (i.e., no harvest adjustment in Eq. 3.8–9). Lastly, the three count-detection parameters (*p.d*, *p.a*, *p.c*) were constrained to be equal across size classes, and we did not include any covariate effects or their selection terms.

To assess the sensitivity of our results to the extrinsic variable means, we conducted a perturbation analysis in which we compared outputs from a model with the variables fixed to their mean values (i.e., baseline; Table A2.1) to a set of models in which each of the productivity variables (with the exception of *CL*) and the female proportions were perturbed ±1% in isolation (i.e., only one of the seven variables was increased or decreased in each of the model runs). We used non-informative wide priors for all parameters and ran three chains with a 3,000-iteration adaptive phase, followed by 80,000 iterations with the first 10,000 discarded as burn-in, and a thinning rate of 30. All analyses were completed using the *jagsUI* (Kellner, 2015) package in program R (Team, 2017).

To evaluate the IPM's sensitivity to the perturbations, we calculated the percent change between the baseline and perturbation outputs for each parameter, and converted to absolute value. For simplicity, here we focus on the sensitivity of structural parameters (apparent survival, mark-recapture detection probabilities, recovery probability, and count-based detection probabilities) to the perturbation analysis (Table A2.2). In general, φ_j, $p.m_{.5}$, *p.a*, and *p.c* were less sensitive to perturbation compared to *r*, *p.d*, and $p.m_j$

(with the exception of large adults), based on examining the most sensitive parameter for each perturbation (Table A2.2). Across perturbation scenarios, *p.d* was the most sensitive parameter on average, followed by $p.m._3$, and *r*. Reducing FP_3 prompted the greatest percent change across parameters, followed by increasing FP_4, and reducing FP_2. The largest overall percent change we observed was 5.5% in *p.d* in the low FP_3 scenario.

It is difficult to place the results of our sensitivity analysis in the context of other IPM studies. Based on sample sizes (Table A2.1), some of our auxiliary variables had more uncertainty associated with them than others. Therefore, it is promising that there did not appear to be a relationship between parameter sensitivity, as quantified by scenario mean (Table A2.2), and auxiliary variable parametric uncertainty. For example, FP_5 was based on expert-opinion and therefore has the most parametric uncertainty, yet the mean percent change across parameters for both FP_5 perturbation scenarios (±1%) was relatively moderate: 0.007 (range: 0.003–0.013). Similarly, FP_4 also has relatively more parametric uncertainty based on sample size, though the high (increase) scenario induced a much greater percent change (0.012) compared to the low (decrease) scenario (0.006).

Given the relatively large percent changes that occurred in some of our parameters under different perturbation scenarios, we elected to incorporate further parametric uncertainty into the main analysis by sampling each auxiliary variable (except clutch size) from a beta distribution. Except in one case, we used a methods of moment approach to derive parameters of the beta distributions based on sample means and variances reported in the associated studies. For the large adult female proportion (FP_5),

we based the mean estimate on expert opinion (A.J. Lawson personal observation). Using the mean estimate $(\widehat{SR_5})$ and a coefficient of variation of m = 20%, we computed a standard error:

$$\sigma_{SR_5} = \sqrt{\widehat{SR_5} - (1 - \widehat{SR_5})} * m/100$$

and the corresponding beta parameters by method of moments.

Table A2.1. Summary of extrinsic variables for an American alligator (*Alligator mississippiensis*) integrated population model. Each variable's mean values ± standard deviation are given in the far right column, and the numbers in parentheses below are a 1% decrease ("low") and increase ("high") of the mean value, as used in a sensitivity analysis.

Variable Name	Description	Source	Sample Size	Mean (±SD)
FP_1	Proportion of females in the Hatchling (j=1) size class	Rhodes and Lang 1996	778	0.72 ± 0.02 (0.713, 0.727)
FP_2	Proportion of females in the Juvenile (j=2) size class	Woodward 1996, Appendix A, Table 7	928	0.37 ± 0.02 (0.366, 0.374)
FP_3	Proportion of females in the Subadult (j=3) size class	Woodward 1996, Appendix A, Table 7	463	0.47 ± 0.02 (0.465, 0.475)
FP_4	Proportion of females in the Small Adult (j=4) size class	Woodward 1996, Appendix A, Table 7	53	0.47 ± 0.07 (0.465, 0.475)
FP_5	Proportion of females in the Large Adult (j=5) size class	A.J. Lawson pers. obsv.	–	0.35 ± 0.10[a] (0.346, 0.354)
BP	Proportion of females in the small adult and large that breed each year	Wilkinson 1983	69	0.275 ± 0.05 (0.272, 0.278)
NS	Proportion of nests in which one egg successfully hatched	Wilkinson 1983	117	0.7 ± 0.04 (0.693, 0.707)
CL	Clutch size; the average number of eggs per nest at YWC based on long-term nest monitoring (1979–2017)	P.M. Wilkinson pers comm., Wilkinson 1983	400	45[b]

[a]Standard deviation estimated using an estimated 0.20 coefficient of variation based on the mean estimate

[b]Clutch size was modeled as a fixed variable in the integrated population model.

Table A2.2. Output from a sensitivity analysis of an integrated population model (IPM) for American alligators (*Alligator mississippiensis*) in coastal South Carolina. Each column represents a perturbation scenario in which a single extrinsic variable— size class-specific female proportion (FP_j), breeding probability (*BP*), or nest success (*NS*)— was decreased by 1% ("low") or increased by 1% ("high") relative to the baseline value (Table A2.1). The parameter column contains structural parameters from the IPM: size class-specific survival (φ_j), mark-recapture probability ($p.m_j$), recovery probability (r), detection probability ($p.d$), aggregation probability ($p.a$), and classification probability ($p.c$). The numerical values are the absolute value of the percent change in each parameter relative to its baseline value, for each perturbation scenario. The bolded values in each column indicate the parameter that was most sensitive to each perturbation (i.e., had the largest percent change). Overall and scenario-specific means represent the mean percent changes (in absolute value units) across columns and rows, respectively.

	FP_1		FP_2		FP_3		FP_4		FP_5		*BP*		*NS*		Overall
Param.	Low	High	Low	High	Low	High	Low	High	Low	High	Low	High	Low	High	Mean
φ_1	0.001	0.016	0.003	0.015	0.018	0.002	0.016	0.038	0.012	0.015	0.001	0.007	0.010	0.010	0.012
φ_2	0.000	0.001	0.001	0.002	0.001	0.003	0.004	0.010	0.002	0.007	0.002	0.002	0.005	0.005	0.003
φ_3	0.002	0.002	0.001	0.000	0.002	0.001	0.001	0.001	0.000	0.002	0.001	0.000	0.002	0.000	0.001
φ_4	0.001	0.001	0.001	0.001	0.001	0.001	0.001	0.002	0.000	0.001	0.002	0.000	0.000	0.002	0.001
φ_5	0.000	0.002	0.001	0.000	0.001	0.001	0.001	0.002	0.001	0.001	0.000	0.001	0.000	0.001	0.001
φ_6	0.001	0.006	0.011	0.003	0.015	0.002	0.002	0.006	0.009	0.006	0.000	0.002	0.010	0.002	0.006
$p.m_3$	**0.011**	0.003	0.021	**0.026**	0.002	0.028	**0.027**	0.018	**0.022**	0.013	0.026	**0.031**	0.020	0.004	0.018
$p.m_4$	0.007	0.000	0.002	0.002	0.002	0.003	0.000	0.007	0.003	0.002	0.003	0.001	0.005	0.003	0.003
$p.m_5$	0.001	0.006	0.002	0.002	0.002	0.004	0.002	0.009	0.002	0.006	0.005	0.002	0.003	0.008	0.004
$p.m_6$	0.004	0.018	0.027	0.009	0.036	0.007	0.006	0.016	**0.022**	0.015	0.000	0.008	**0.025**	0.007	0.014
r	0.002	0.028	0.014	0.002	0.054	0.019	0.009	**0.042**	0.004	**0.017**	0.003	0.002	0.008	0.014	0.016

p.d	0.003	**0.038**	**0.029**	0.008	**0.055**	**0.028**	0.017	0.013	0.013	0.009	**0.035**	0.011	0.002	**0.019**	**0.020**
p.a	0.000	0.001	0.000	0.001	0.000	0.001	0.001	0.000	0.000	0.001	0.001	0.000	0.000	0.001	0.001
p.c	0.000	0.000	0.000	0.001	0.000	0.000	0.001	0.000	0.000	0.000	0.000	0.000	0.000	0.001	0.000
Scen. Mean	0.003	0.009	0.008	0.005	0.013	0.007	0.006	0.012	0.007	0.007	0.006	0.005	0.006	0.005	

APPENDIX A3

Model Output Comparison

Table A3.1. American alligator (*Alligator mississippiensis*) model parameter estimates from three integrated population models (IPM): Global 1993 (G93), Reduced 1993 (R93), and Reduced 1979 (R79). The multistate mark-recapture section includes survival (φ) probabilities, mark-recapture detection probabilities (*p.m*) parameters (size class-specific βs), and recovery probability (*r*). The state-space count model section includes intercept (β^{x}) and size class linear trend terms ($\beta^{x.T}$) for detection probabilities *p.a*, *p.a*, and *p.c*, respectively. The last section includes coefficients (β) and indicator variables (ω ;Hooten and Hobbs, 2015) for each covariate. Capture effort (CE) was included in the *p.m* model, whereas water level (WL) and water temperature (WT) were included with *p.d*. Covariate indicator variable terms were fixed to one for the R93 and R79 models, as indicated by the asterisk.

	Global 1993		Reduced 1993		Reduced 1979	
Parameter	Mean ± SD (95% CRI)	$\hat{R}$[a]	Mean ± SD (95% CRI)	$\hat{R}$	Mean ± SD (95% CRI)	$\hat{R}$
Multistate mark-recapture parameters						
φ_1[b]	0.16 ± 0.04 (0.1, 0.25)	1.03	0.16 ± 0.04 (0.08, 0.25)	1.01	0.15 ± 0.04 (0.08, 0.24)	1.01
φ_2	0.61 ± 0.11 (0.38, 0.82)	1.00	0.64 ± 0.12 (0.4, 0.85)	1.03	0.67 ± 0.1 (0.47, 0.85)	1.00
φ_3	0.89 ± 0.06 (0.77, 0.98)	1.00	0.88 ± 0.06 (0.76, 0.98)	1.00	0.86 ± 0.05 (0.75, 0.94)	1.00
φ_4	0.96 ± 0.02 (0.92, 0.99)	1.00	0.96 ± 0.02 (0.92, 0.99)	1.01	0.94 ± 0.02 (0.91, 0.97)	1.00
φ_5	0.93 ± 0.02 (0.89, 0.96)	1.00	0.93 ± 0.02 (0.89, 0.96)	1.02	0.95 ± 0.01 (0.92, 0.97)	1.00
φ_6	0.92 ± 0.03 (0.86, 0.96)	1.00	0.92 ± 0.02 (0.87, 0.97)	1.03	0.93 ± 0.02 (0.9, 0.96)	1.00
β_3	-3.34 ± 0.93	1.00	-3.31 ± 0.93	1.00	-2.36 ± 0.6	1.00

	(-5.32, -1.66)		(-5.25, -1.63)		(-3.6, -1.25)	
β_4	-2.6 ± 0.21 (-3.02, -2.2)	1.00	-2.6 ± 0.21 (-3.02, -2.19)	1.00	-2.06 ± 0.18 (-2.42, -1.72)	1.00
β_5	-2.18 ± 0.17 (-2.51, -1.86)	1.00	-2.18 ± 0.17 (-2.51, -1.86)	1.00	-1.99 ± 0.14 (-2.27, -1.73)	1.00
β_6	-2.47 ± 0.29 (-3.04, -1.91)	1.00	-2.5 ± 0.29 (-3.07, -1.93)	1.02	-2.39 ± 0.24 (-2.86, -1.93)	1.00
r	0.14 ± 0.04 (0.08, 0.23)	1.00	0.14 ± 0.04 (0.08, 0.23)	1.00	0.15 ± 0.03 (0.09, 0.22)	1.00
	State-space count model					
β^d	-2.33 ± 0.3 (-2.89, -1.69)	1.00	-3.08 ± 1.29 (-5.59, -1.7)	3.17	-2.32 ± 0.29 (-2.89, -1.72)	1.02
$\beta^{d.T}$	-0.3 ± 0.08 (-0.47, -0.15)	1.02	-0.05 ± 0.39 (-0.47, 0.67)	3.31	-0.29 ± 0.1 (-0.5, -0.09)	1.05
β^a	-3.54 ± 0.39 (-4.31, -2.79)	1.00	-1.53 ± 3.29 (-4.28, 4.94)	3.28	-2.89 ± 0.41 (-3.65, -2.05)	1.01
$\beta^{a.T}$	1.38 ± 0.23 (0.97, 1.84)	1.01	0.73 ± 1.06 (-1.2, 1.83)	3.25	1.07 ± 0.23 (0.61, 1.52)	1.00
β^c	0.47 ± 0.39 (-0.28, 1.25)	1.00	0.46 ± 0.4 (-0.31, 1.26)	1.00	-0.26 ± 0.36 (-0.95, 0.45)	1.00
$\beta^{c.T}$	0.35 ± 0.11 (0.12, 0.58)	1.00	0.35 ± 0.12 (0.12, 0.59)	1.00	0.64 ± 0.13 (0.4, 0.9)	1.00
	Covariates					
β^{CE}	0.36 ± 0.09 (0.18, 0.54)	1.00	0.37 ± 0.09 (0.19, 0.54)	1.00	0.59 ± 0.08 (0.43, 0.75)	1.00
β^{WL}	-0.15 ± 0.09 (-0.29, 0.03)	1.00	-0.2 ± 0.07 (-0.34, -0.08)	1.29	-0.18 ± 0.06 (-0.3, -0.06)	1.00
β^{WT}	0.41 ± 0.04 (0.32, 0.5)	1.00	0.41 ± 0.05 (0.32, 0.5)	1.00	0.41 ± 0.04 (0.32, 0.49)	1.00

ω_{CE}	1.0 ± 0.06 (1.0, 1.0)	1.02	*	*
ω_{WL}	0.81 ± 0.39 (0.0, 1.0)	1.00	*	*
ω_{WT}	1.0 ± 0.0 (1.0, 1.0)	NA[c]	*	*

[a]Gelman-Rubin diagnostic statistic (Gelman et al., 2004) in which $\hat{R} < 1.15$ indicates convergence.

[b]Numerical subscripts indicate size class (Table 2.1)

[c]The extremely high probability of inclusion precluded estimation of an $\hat{R}$ value.

Table A3.2. Covariate selection output from the American alligator (*Alligator mississippiensis*) Global 1993 integrated population model. Each row (model) reflects a unique combination of three covariates (capture effort, water level, and water temperatures), in which 1 indicates covariate inclusion and 0 reflects exclusion. The model weight reflects the proportion of iterations in which the model's particular covariate combination was included in the IPM.

Model	Weight	Capture Effort	Water Level	Water Temp.
m_1	0.00	0	0	0
m_2	0.00	1	0	0
m_3	0.00	0	1	0
m_4	0.00	1	1	0
m_5	0.00	0	0	1
m_6	0.19	1	0	1
m_7	0.00	0	1	1
m_8	0.81	1	1	1

APPENDIX A4

Population Growth Analysis

Table A4.1. Population growth rates of American alligators (*Alligator mississippiensis*) in coastal South Carolina derived from Lefkovitch matrices (λ^L), and changes in abundance estimates (λ^N). For each of the three models, we used the individual samples (n=4,000 per chain) within the MCMC chains (n=3) of the size class-specific apparent survival (φ_j) posterior distributions to generate a distribution of λ^L values based on the intrinsic population growth rate of the Lefkovitch projection matrix. Similarly, we used the MCMC chain samples for the total abundance estimates for the first and final years of the study (Eq. 2.11) to derive an overall measure of population growth (λ^N) on the Great Pee Dee and Waccamaw River (GPD) and South Santee River (SAN) survey sites (Fig. 2.1). The values in parentheses below the means ± SD represent the 95% CRI range, in addition to the total number and proportion of samples that produced an increasing population growth rate (λ>1).

	Site	Model	Mean ± SD	No. Samples $\lambda > 1.0$	Proportion
λ^L	–	G93	0.93 ± 0.01 (0.91, 0.96)	0	0.00
		R93	0.93 ± 0.01 (0.92, 0.97)	1	0.00
		R79	0.93 ± 0.01 (0.92, 0.96)	0	0.00
λ^N	GPD	G93	0.71 ± 0.10 (0.64, 0.93)	98	0.01
		R93	0.67 ± 0.09 (0.61, 0.86)	10	0.00
		R79	0.68 ± 0.08 (0.63, 0.86)	10	0.00
	SAN	G93	0.94 ± 0.13 (0.85, 1.23)	3559	0.30
		R93	0.93 ± 0.10 (0.80, 1.15)	2633	0.22
		R79	0.89 ± 0.12 (0.85, 1.15)	2164	0.18

Figure A4.1. Histogram of intrinsic population growth rates (λ^L) for American alligators (*Alligator mississippiensis*) in coastal South Carolina derived from the posterior distributions of size class-specific apparent survival rates applied to a six-stage (size class) Lefkovitch projection matrix. Each gray panel reflects one of three integrated population models, with the solid vertical line indicating the mean of the λ^L distribution whereas the dashed line denotes asymptotic population growth (λ^L=1) for reference. The red values indicate a declining growth rate (λ^L<1.0), whereas blue bars (R93 model only) indicate a population increase.

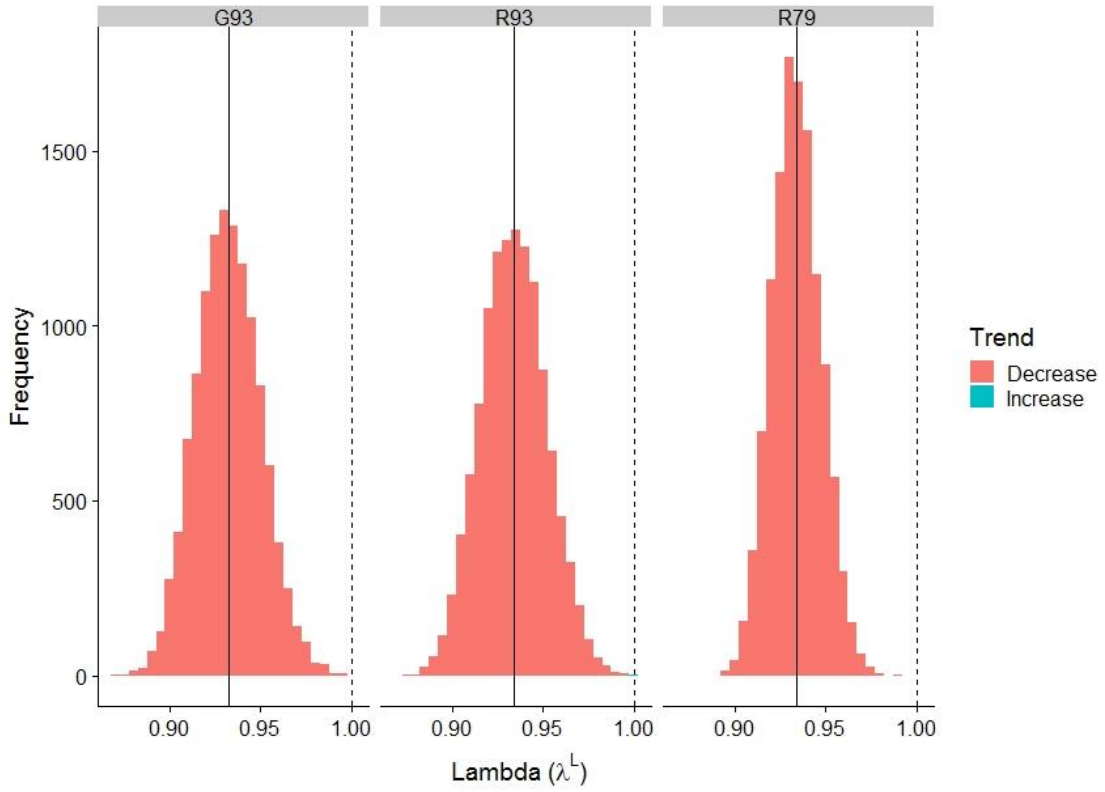

Figure A4.2. Histogram of intrinsic population growth rates (λ^N) for American alligators (*Alligator mississippiensis*) in coastal South Carolina derived from the posterior distributions of total abundance estimates from the initial and final years of the study. The top row shows λ^N for the Great Pee Dee and Waccamaw River (GPD) survey site and the South Santee River (SAN) is shown at bottom, whereas each of the columns indicates a different integrated population model, of increasing parametric certainty. The solid vertical line indicating the mean of the λ^N distribution whereas the dashed line denotes asymptotic population growth (λ^N=1) for reference. The red bars indicate a declining growth rate (λ^N<1.0), whereas blue bars (R93 model only) indicate a population increase.

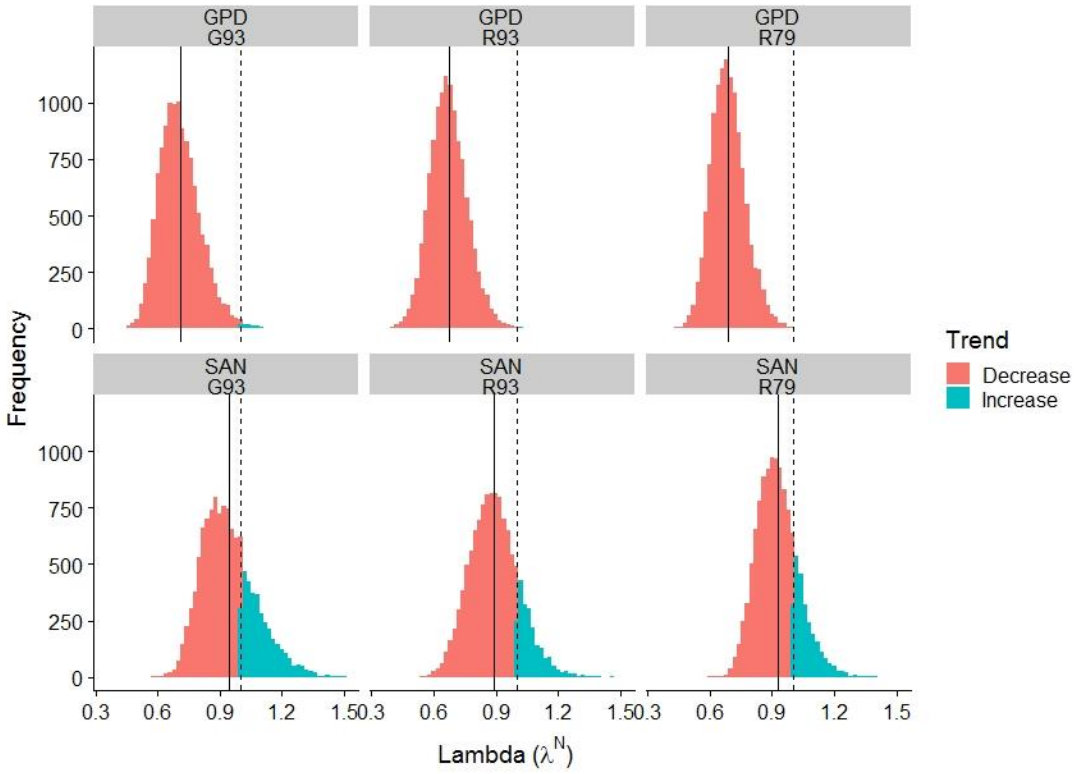

APPENDIX B1.

Lefkovitch Matrix Elasticity Analysis

Table B1.1. Elasticity values from Lefkovitch matrices containing American alligator (*Alligator mississippiensis*) stage-specific (*j*; Table 3.2) growth (G_j), retention (P_j), and fecundity (F_j) parameters. Matrix **L′** contained apparent survival probabilities estimated in Chapter 2, whereas **L** increased the stage-specific survival probabilities within the G_j and P_j equations (Eqs. 3.1, 3.2) for stages 3–5 by 4% (Table 3.2) in order to maintain stable population growth under the maximum harvest rate (Table 3.1) in a perfect information scenario. Lefkovitch matrix elements not listed here (e.g., P_6) had elasticity values of 0.

	Retention				*Growth*				*Fecundity*	
	P_2	P_3	P_4	P_5	G_1	G_2	G_3	G_4	F_4	F_5
L'	0.070	0.153	**0.317**	0.169	0.066	0.066	0.066	0.028	0.038	0.028
L	0.063	0.151	**0.323**	0.183	0.063	0.063	0.063	0.028	0.035	0.028

Table B1.2. Stage class life table summary for American alligators (*Alligator mississippiensis*) in South Carolina, USA. We constructed a six-stage Lefkovitch population projection matrix, using parameters from the primary literature, and performed additional calculations when necessary. All values contained in the table were used in the simulation with the exception of survival probabilities in parentheses, which that were increased by 4% to the bolded terms, to attain a positive population growth rate for simulation. The stable stage distributions (right eigenvector) for both projection matrices (**L** and **L′**) are shown; and Harvest proportion refers to the stage class distribution of harvested alligators. Sources are from South Carolina unless otherwise stated, and are reported in the footnotes.

Stage class (j)	Name	Total length range (cm)	Female proportion $FP_j \pm$ SD[a]	Survival prob. $\varphi_j \pm$ SD[b]	Transition prob. $\psi_{j,j+1} \pm$ SD[c]	Fecundity	Stable stage dist. (**L′**)	Stable stage dist. (**L**)	Harvest proportion
1	Hatchlings	≤30	0.72 ± 0.02	0.16 ± 0.04	1.00		0.53	0.54	0.00
2	Juveniles	31–121	0.37 ± 0.02	0.61 ± 0.11	0.17 ± 0.01		0.18	0.18	0.00
3	Subadults	122–182	0.47 ± 0.02	**0.96** (0.89 ± 0.06)	0.22 ± 0.04		0.06	0.06	0.04
4	Small Adults	183–243	0.47 ± 0.07	**0.99** (0.96 ± 0.02)	0.15 ± 0.05	4.07	0.07	0.08	0.30
5	Large Adults	244–304	0.35 ± 0.10	**0.96** (0.93 ± 0.02)	0.08 ± 0.05	3.03	0.07	0.08	0.40
6	Bulls	≥305	0.00	0.92 ± 0.03	0.00		0.08	0.06	0.26
Productivity Terms[d]:		*NS* = 0.70	*BP* = 0.275	*CL* = 45					
							0.53		

[a]Hatchlings: Rhodes and Lang 1996; Juveniles–Large Adults: Woodward 1996 (Florida)

[b]Chapter 2

[c]Calculated weighted mean of sex-specific growth probabilities in Chapter 1 for each transition using the female proportion. Sex-specific growth probability estimates originally derived from Wilkinson et al. (2016)

[d]Calculated from public alligator harvest records for Georgetown County, South Carolina 2008–2017 (SCDNR 2017)

[f]Nest success (*NS*), breeding probability (*BP*), and clutch size (*CL*) from Wilkinson (1983), multiplied by FP_j (Woodward 1996) for stage-specific fecundity

APPENDIX C1.

Mercury Supplementary Material

Table C1.1. Summary of Direct Mercury Analyzer (DMA) runs to analyze total mercury (THg) adult American alligator (*Alligator mississippiensis*) whole blood collected at the Tom Yawkey Wildlife Center, South Carolina (2010–2017). Date indicates the calendar date that the DMA machine run was initiated, whereas Sample PHase refers to whether the alligator whole blood was in liquid (L) or solid (S; lyophilized) form. We used three types of blanks for quality assurance purposes—Instrumental refers to empty slots within the DMA machine (i.e., no weigh boat added); Procedural blanks were empty nickel weigh boats; whereas Field blanks were filled with thawed Milli-Q Water that was stored in a lithium-heparinized vacutainer since the 2011 field season. We used at least two types of Reference Materials within each run, depending on the Sample Form. For liquid runs (1–7) we used the National Institute of Standards and Technology (NIST) Standard Reference Material (SRM) 955c levels 3 and 4, Toxic Metals in Caprine Blood, with reference values for total mercury at 17.8 ± 1.6 ng g^{-1} and 33.9 ± 2.1 ng g^{-1}, respectively. For our solid-only DMA runs (8–11), we used a freeze-dried NIST SRM 955C level 4 vial, as well as Certified Reference Materials (CRM) for trace metals, PACS-2 marine sediment (3.04 ± mg kg^{-1} THg) and TORT-3 lobster hepatopancreas (0.292 ± 0.022 mg kg^{-1} THg) from the Natural Resource Council of Canada (NRC-CNRC; Ontario, Canada). Unique Blood Samples refers to the number of unique capture events within a particular run, whereas Blood Reps. is the number of unique samples that that had a duplicate within the run, whereas Total is the sum of all Blanks, Reference Materials, Unique Blood Samples, and Blood Replicates. Detection Limit is the lowest amount of THg that can be distinguished from the absence of THg in a sample.

Run	Date	Sample Phase	*Blank Samples*			*Reference Materials*				Unique Blood Samples	Blood Reps.	Total	Detect. Limit (μg kg^{-1})[b]
			Instru-mental	Proced-ural	Field	955c Lvl. 3	955c Lvl. 4[a]	PACS-2	TORT-3				
1	2/20/2018	L	4	6	2	2				20	3	37	0.0342
2	2/21/2018	L	5	5	0	2				17	5	34	0.0893
3	2/21/2018	L	4	5	0	2				22	4	37	0.0893
4	2/22/2018	L	4	5	0	2				19	3	33	0.0893

5	2/23/2018	L	5	5	0	2			18	4	34	0.4080
6	4/2/2018	L	4	4	0	2			9	1	20	0.3990
7	4/3/2018	L	4	4	0	1			11	2	22	0.6190
8	4/4/2018	S	10	5	0	2	1	2	15	2	35	0.3420
9	4/4/2018	S	8	5	0	2	1	2	20	2	40	0.3420
10	4/5/2018	S	8	5	0	2	1	2	20	2	40	0.0689
11	4/5/2018	S	8	5	0	2	1	2	19	3	40	0.0689

[a]The 955c Level 4 reference material was run as a liquid for runs 5–7 and as a solid for 8–11

[b]The mean detection limit across all runs is 0.302 μg kg^{-1}

Table C1.2. List all of the un-clotted American alligator blood samples run in both their liquid and solid (lyophilized) forms (hereafter method duplicates) from the Tom Yawkey Wildlife Center, South Carolina. Year and Ordinal Date (day of year) indicate the whole blood sample's collection date. Liquid and Solid indicate the total mercury (THg) concentration in the sample in milligrams per kilogram (mg kg^{-1}), whereas Difference is the Liquid minus the Solid concentration. A single outlier (indicated by the *) was excluded from the mean Difference calculation for solid sample adjustment (0.006 ± 0.009 SD mg kg^{-1}). The solid THg measurement for this sample was also excluded from all further analyses because the liquid form was run in duplicate and produced consistent THg measurements.

Alligator ID	Sex	Year	Ordinal Date	Liquid (mg kg^{-1})	Solid (mg kg^{-1})	Difference
366	Female	2011	172	0.2315	0.2216	0.0099
45	Female	2011	179	0.0551	0.0431	0.0120
422	Female	2011	189	0.1440	0.1408	0.0031
25	Female	2012	174	0.1573	0.1341	0.0232
438	Female	2012	180	0.1067	0.0972	0.0094
519	Female	2013	173	0.1253	0.1172	0.0081
367	Female	2013	178	0.0806	0.0765	0.0041
521	Female	2013	179	0.1154	0.1154	-0.0001
364	Female	2013	181	0.3313	0.2870	*0.0443
518	Male	2013	163	0.1594	0.1560	0.0034
15	Male	2013	187	0.0486	0.0442	0.0044
8	Female	2014	172	0.1660	0.1620	0.0040
365	Female	2014	176	0.2340	0.2252	0.0088
232	Female	2014	177	0.1624	0.1637	-0.0013
534	Female	2014	178	0.1403	0.1369	0.0033
404	Male	2014	93	0.1445	0.1211	0.0234
531	Male	2014	181	0.3397	0.3604	-0.0207
462	Female	2016	176	0.1888	0.1812	0.0075
54	Female	2016	180	0.1293	0.1260	0.0033
435	Female	2016	181	0.1446	0.1240	0.0206
194	Female	2016	183	0.0895	0.0853	0.0042
880	Male	2017	175	0.1047	0.1017	0.0031
879	Male	2017	175	0.0733	0.0697	0.0036

Table C1.3. Summary of reference material total mercury (THg) values analyzed alongside American alligator (*Alligator mississippiensis*) whole blood samples from South Carolina (2010–2017). All analyses were conducted using a (DMA-80, Milestone, Inc., Shelton, CT, USA; hereafter DMA) at the Savannah River Ecology Laboratory, University of Georgia (Aiken, SC, USA). Run refers to the specific sample batch or session on the DMA— see Table C1.1 for additional details of each run— whereas Boat Position refers to the sequence which (maximum=40) the sample was analyzed within a run. Alligator whole blood samples were phase-matched (liquid vs. solid) to reference samples in each run. For the liquid runs (1–7) we used the National Institute of Standards and Technology (NIST) Standard Reference Material (SRM) 955c levels 3 and 4, Toxic Metals in Caprine (goat) Blood, with reference values for total mercury at 0.017.8 ± 0.0016 mg kg^{-1} and 0.0339 ± 0.0021 mg kg^{-1}, respectively. For the solid runs (8–11) we used solid (phase-matched) Certified Reference Materials (CRM) for trace metals, PACS-2 marine sediment (3.04 ± 0.20 mg kg^{-1} THg), TORT-3 lobster hepatopancreas (0.292 ± 0.022 mg kg^{-1} THg) from the Natural Resource Council of Canada (NRC-CNRC; Ontario, Canada), as well as a freeze-dried vial of NIST SRM 955c level 4. Both the solid (freeze-dried) NIST SRM 955c level 4 and alligator whole blood samples in runs 8–11 were freeze-dried to a constant mass (± 0.1 mg) using a FreeZone lyophilizer (Labconco, Kansas City, MO, USA).

The Sample THg (mg kg^{-1}) column reflects the THg density estimate in phase-matched units (i.e., if the certified THg value is reported in *dw* then the Sample THg column directly to the right is also in *dw*). As such, this table shows the converted *ww* THg measurements (Section 2.4.1) for freeze-dried 955c L4 samples (runs 8–11) with the methodological adjustment applied (Section 2.4.2). Lastly, the Percent Recovery column is the Certified THg divided by the Sample THg, then multiplied by 100 to convert to a percentage form. Percent recovery values over 100% indicate that the THg content measured by the DMA exceeded the certified value.

At the bottom, we provide mean Sample THg (± SD) and Percent Recovery broken down by each standard. The 955c L4 certified values are reported in *ww*, whereas the solid run samples for this standard were measured in *dw* and then converted to *ww*. We acknowledge that the phase-mismatch during DMA analysis introduces some uncertainty regarding the reliability of percent recovery estimates as an indicator of quality control. Therefore, we reported both the overall (i.e., all runs) and liquid-run only (runs 5–7) mean Sample THg and Percent Recovery values for the 955c L4 standard.

Run	Boat Position	Standard Name	Matrix Type	Certified THg (mg kg^{-1})	Sample THg (mg kg^{-1})[a]	Percent Recovery
1	4	955c L3	Caprine Blood	0.0178 ± 0.0016 *ww*	0.0193	108.4%
1	21	955c L3	Caprine Blood		0.0207	116.2%
2	4	955c L3	Caprine Blood		0.0194	109.0%
2	20	955c L3	Caprine Blood		0.0203	114.2%
3	4	955c L3	Caprine Blood		0.0214	120.4%
3	19	955c L3	Caprine Blood		0.0214	120.4%
4	4	955c L3	Caprine Blood		0.0210	118.1%
4	19	955c L3	Caprine Blood		0.0243	136.7%
5	4	955c L4	Caprine Blood	0.0339 ± 0.0021 *ww*	0.0378	111.4%
5	20	955c L4	Caprine Blood		0.0393	116.0%
6	5	955c L4	Caprine Blood		0.0369	108.8%
6	16	955c L4	Caprine Blood		0.0394	116.3%
7	5	955c L4	Caprine Blood		0.0351	121.3%
8	23	955c L4	Caprine Blood		0.0374	110.3%
8	33	955c L4	Caprine Blood		0.0396	116.9%
9	22	955c L4	Caprine Blood		0.0390	114.9%
9	38	955c L4	Caprine Blood		0.0393	116.1%
10	22	955c L4	Caprine Blood		0.0423	124.8%
10	38	955c L4	Caprine Blood		0.0417	123.0%
11	22	955c L4	Caprine Blood		0.0440	129.8%
11	38	955c L4	Caprine Blood		0.0448	132.1%
8	19	PACS-2	Marine Sediment	3.0400 ± 0.2000 *dw*	2.6025	85.6%
9	18	PACS-2	Marine Sediment		2.6170	86.1%
10	18	PACS-2	Marine Sediment		3.0068	98.9%
11	18	PACS-2	Marine Sediment		2.7460	90.3%

8	17	TORT-3	Lobster Hepatopancreas	0.2920 ± 0.0220 *dw*	0.3022	103.5%
8	31	TORT-3	Lobster Hepatopancreas		0.2983	102.2%
9	16	TORT-3	Lobster Hepatopancreas		0.3017	103.3%
9	36	TORT-3	Lobster Hepatopancreas		0.2888	98.9%
10	16	TORT-3	Lobster Hepatopancreas		0.3012	103.2%
10	36	TORT-3	Lobster Hepatopancreas		0.2937	100.6%
11	16	TORT-3	Lobster Hepatopancreas		0.2902	99.4%
11	36	TORT-3	Lobster Hepatopancreas		0.2889	98.9%

Overall 955c L3	0.0210	± 0.0016	117.8% ± 8.9%
Overall 955c L4	0.0397	± 0.0028	117.2% ± 8.2%
Liquid-only 955c L4	0.0384	± 0.0012	111.2% ± 5.3%
Overall PACS-2	2.7431	± 0.1873	90.2% ± 6.2%
Overall TORT-3	0.2956	± 0.0059	100.9% ± 2.0%

[a]THg values in this column correspond to the units used in the Certified THg directly to the left. This applies to the 955c L4 Caprine Samples used in DMA Runs 8–11, which were freeze-dried and analyzed as solids, resulting in *dw* units, which were then converted to *ww* with the solid-sample adjustment (+0.006 mg kg^{-1}).

Table C1.4. Reference material total mercury (THg) percent capture values, summarized by sample batch (Run), analyzed alongside American alligator (*Alligator mississippiensis*) whole blood samples from South Carolina (2010–2017). All analyses were conducted using a (DMA-80, Milestone, Inc., Shelton, CT, USA; hereafter DMA) at the Savannah River Ecology Laboratory, University of Georgia (Aiken, SC, USA). Run refers to a specific sample batch (session) on the DMA— see Table C1.1 for additional details of each run. The number of standard samples is the number of individual reference material samples (not the number of reference material types) within a run. The mean percent recovery column is the average percentage of THg measured by the DMA, relative to the certified reference material value.

Run	No. Standard Samples	Mean Percent Recovery (± SD)
1	2	112.3% ± 5.4%
2	2	111.6% ± 3.6%
3	2	120.4% ± 0.0%
4	2	127.4% ± 13.1%
5	2	113.6% ± 3.2%
6	2	112.5% ± 5.2%
7	1	103.6% ± NA
8	5	103.7% ± 11.7%
9	5	103.8% ± 12.3%
10	5	110.1% ± 12.7%
11	5	98.9% ± 19.4%

Table C1.5. Linear regression models representing hypotheses about total mercury (THg) bioaccumulation patterns in whole blood of American alligators (*Alligator mississippiensis*) captured on the Tom Yawkey Wildlife Center in coastal South Carolina from 2010–2017.

Model[a]	Number of parameters	Dev.[b]	ΔAICc	w_i
Sex * PA + Sex * PA^2	7	4.46	0.00	0.46
PA + PA^2	4	4.65	0.47	0.37
Sex * SVL + Sex * SVL^2	7	4.56	3.67	0.07
~Indiv.	3	*	4.19	0.06
BMI	3	4.96	9.03	0.01
OD	3	4.96	9.14	0.00
SVL + SVL^2	4	4.90	9.15	0.00
Intercept	2	5.03	9.26	0.00
SVL	3	4.96	9.27	0.00
~Indiv. + PA + PA^2	5	*	9.33	0.00
BMI + BMI^2	4	4.94	10.50	0.00
PA	3	5.02	11.01	0.00
OD + OD^2	4	4.96	11.11	0.00
Sex * SVL	5	4.89	11.13	0.00
Sex + OD	4	4.96	11.22	0.00
Sex	3	5.03	11.33	0.00
PA* OD	5	4.95	12.91	0.00
Sex + PA	4	5.02	13.11	0.00
Sex * OD	5	4.96	13.30	0.00
Sex * PA	5	5.00	14.58	0.00
Year	9	4.76	15.36	0.00
Year * OD	17	4.28	16.89	0.00
Sex * OD + Sex * OD^2	7	4.95	17.42	0.00
~Year	3	*	17.72	0.00
~Indiv. + Sex * PA + Sex * PA^2	8	*	22.07	0.00
~Indiv. + Sex * SVL + Sex * SVL^2	8	*	22.16	0.00

[a]Model selection notation (following Burnham and Anderson 2002) presents models according to the highest-order effects contained, with all lower-order constituent effects included as additive effects; a superscript ^{2} denotes a quadratic effect, a + sign indicates an additive effect between two variables, a * denotes an interaction, whereas a ~ indicates a random effect. Year (categorical) = annual variation, PA = predicted age of the individual at sampling based on estimated predicted age at first capture using the Wilkinson et al. (2016) growth formula for our study population; SVL = snout-vent length in cm at capture; Indiv. = individual alligator modeled as a random intercept; BMI = body mass index (Nilsen et al., 2017a) at capture; OD = ordinal date or day of year. The continuous covariates contained no missing values and were z-standardized across years (mean = 0.0, SD = 1.0).

[b]Models containing random effects were fit with restricted maximum likelihood (REML) and deviance values are not directly comparable to non-REML fit models.

Table C1.6. Linear regression models representing hypotheses about total mercury (THg) bioaccumulation patterns in the whole blood of American alligators (*Alligator mississippiensis*) captured on the Merritt Island National Wildlife Refuge in eastern Florida from 2007–2014.

Model[a]	Number of parameters	Dev.[b]	ΔAICc	w_i
SVL + SVL^2	4	34.06	0.00	0.85
Sex * SVL + Sex * SVL^2	7	33.54	3.52	0.15
PA + PA^2	4	36.78	14.56	0.00
Sex * PA + Sex * PA^2	7	35.82	15.93	0.00
Sex * SVL	5	37.10	18.28	0.00
Sex * PA	5	37.85	22.06	0.00
BMI + BMI^2	4	38.46	22.98	0.00
PA * OD	5	38.08	23.21	0.00
OD + OD^2	4	38.80	24.67	0.00
BMI	3	39.44	25.68	0.00
SVL	3	39.58	26.3	0.00
PA	3	39.69	26.87	0.00
OD	3	39.98	28.23	0.00
Year * OD	17	33.88	28.39	0.00
PA + OD	4	39.67	28.83	0.00
Sex + OD	4	39.88	29.82	0.00
Sex * OD + Sex * OD^2	7	38.75	30.78	0.00
~Indiv.	3	*	31.05	0.00
Intercept	2	41.04	31.11	0.00
Sex * OD	5	39.87	31.91	0.00
Year	9	38.22	32.59	0.00
Sex	3	40.95	32.76	0.00
~Year	3	*	36.43	0.00

[a]Model selection notation (following Burnham and Anderson 2002) presents models according to the highest-order effects contained, with all lower-order constituent effects included as additive effects; (Year) denotes annual variation (categorical), a superscript ^{2} denotes a quadratic effect, a + sign indicates an additive effect between two variables, a *

denotes an interaction, whereas a ~ indicates a random effect. PA = predicted age of the individual at sampling based on estimated predicted age at first capture using the Wilkinson et al. (2016) growth formula for our study population; SVL = snout-vent length in cm at capture; Indiv. = individual modeled as a random intercept; BMI = body mass index (Nilsen et al., 2017a) at capture; OD = ordinal date or day of year. The continuous covariates contained no missing values and were z-standardized across years (mean = 0.0, SD = 1.0).

[b]Models containing random effects were fit with restricted maximum likelihood (REML) and deviance values are not directly comparable to non-REML fit models.